UNIVERSITY OF TASMANIA

DEPARTMENT OF PHYSICS

THE OPTICAL PROBLEMS OF THE RITCHEY-CHRETIEN ASTRONOMICAL TELESCOPE

by

M.L.N.Vyakaranam, M.Sc. (Tech)

Thesis submitted for the

Degree of Master of Science

September 1969

The Optical Problems of the Ritchey-Chretien Astronomical Telescope

by M.L.N. VYAKARANAM

ABSTRACT

The optical design principles of the two-mirror Ritchey-Chretien telescope objective system are developed systematically, starting from fundamentals. The third-order aberration coefficients of Buchdahl are derived for such a system and based on these coefficients, expressions for the first of the extra-axial curvature coefficients of the mirrors which provide aplanatic condition at the Cassegrain focus are derived.

A numerical example (proposed Anglo-Australian 150-inch telescope) is considered to illustrate the principles. Third-order correction to achieve aplanatism is found to be inadequate when spot diagram analysis is made. The expressions for the fifth-order spherical aberration coefficient, μ_1, and linear coma coefficients, μ_2, μ_3 for the two-mirror system are then derived and are used to achieve aplanatic condition to fifth-order. When this is applied to the numerical example, the performance of the system is found to be extremely good. The profiles of the mirrors of the seventh-order aplanatic system are found to be scarcely distinguishable from those of the fifth-order aplanatic system. The mirrors are then considered as two hyperboloids, based on third-order aberrations, and it is noticed that the curvature coefficients of these mirrors and the performance of such a system is not far removed from that of the fifth-order aplanatic system, justifying the popular view. A consideration of the aberration balance technique has brought the hyperboloid system still closer to the fifth-order system.

The design principles of two types of secondary focus correctors to eliminate the residual astigmatism and field curvature of the aplanatic system are outlined. These are an aspheric plate with field flattener and a Rosin type doublet. The principles are successfully adopted to develop these correctors for the numerical example. With the former type of corrector, it is noticed that best correction can be achieved if the Ritchey-Chretien mirror constants are slightly changed. Rosin type corrector is associated with colour problems.

Expressions for the prime focus aberrations are derived and the design principles of single plate and three-plate correctors to correct these aberrations are discussed. Two-plate correctors provide no practicable arrangement. The single plate corrector provides a small useful field, whereas the three-plate corrector offers more useful field. With these correctors in place, the prime focus largely suffers from higher order aberrations.

The conclusions are mostly derived from the numerical example. However, they are valid for a wide range of parameters.

DECLARATION STATEMENT

I, M.L.N.Vyakaranam, hereby declare that, except as stated therein, the Thesis contains no material which has been accepted for the award of any other degree or diploma in any University, and that, to the best of my knowledge and belief, the thesis contains no copy or paraphrase of material previously published or written by another person, except when due reference is made in the text of the thesis.

V. M. L. Narasimham

M.L.N. VYAKARANAM

ACKNOWLEDGEMENTS

I wish to thank my Supervisor, Dr. F.D. Cruickshank, for suggesting the study of "The optical problems of the Ritchey-Chretien astronomical telescope", and for his many valuable comments and helpful discussions.

I thank Professor P.S. Gill, Director, Central Scientific Instruments Organisation, Chandigarh, for having provided me with the opportunity of having advanced training in optical design in the University of Tasmania, under the supervision of Dr. Cruickshank. I thank the Director General, UNESCO for the award of the Fellowship.

I wish to express my sincere thanks to Mrs. B.J. Brown for plotting the spot diagrams, to Mrs. J. Scott and Mrs. R. Francey for the typing work, Mrs. E.W. Williams for the drawing work, and to the staff of the Computer Centre.

CONTENTS

ABSTRACT

The optical design principles of the two-mirror Ritchey-Chretien telescope objective system are developed systematically, starting from fundamentals. The third-order aberration coefficients of Buchdahl are derived for such a system and based on these coefficients, expressions for the first of the extra-axial curvature coefficients of the mirrors which provide aplanatic condition at the Cassegrain focus are derived.

A numerical example (proposed Anglo-Australian 150-inch telescope) is considered to illustrate the principles. Third-order correction to achieve aplanatism is found to be inadequate when spot diagram analysis is made. The expressions for the fifth-order spherical aberration coefficient, μ_1, and linear coma coefficients, μ_2, μ_3 for the two-mirror system are then derived and are used to achieve aplanatic condition to fifth-order. When this is applied to the numerical example, the performance of the system is found to be extremely good. The profiles of the mirrors of the seventh-order aplanatic system are found to be scarcely distinguishable from those of the fifth-order aplanatic system. The mirrors are then considered as two hyperboloids, based on third-order aberrations, and it is noticed that the curvature coefficients of these mirrors and the performance of such a system is not far removed from that of the fifth-order aplanatic system, justifying the popular view. A consideration of the aberration balance technique has brought the hyperboloid system still closer to the fifth-order system.

The design principles of two types of secondary focus correctors to eliminate the residual astigmatism and field curvature of the aplanatic system are outlined. These are an aspheric plate with field flattener and a Rosin type doublet. The principles are successfully adopted to develop these correctors for the numerical example. With the former type of corrector, it is noticed that best correction can

be achieved if the Ritchey-Chretien mirror constants are slightly changed. Rosin type corrector is associated with colour problems.

Expressions for the prime focus aberrations are derived and the design principles of single plate and three-plate correctors to correct these aberrations are discussed. Two-plate correctors provide no practicable arrangement. The single plate corrector provides a small useful field, whereas the three-plate corrector offers more useful field. With these correctors in place, the prime focus largely suffers from higher order aberrations.

The conclusions are mostly derived from the numerical example. However, they are valid for a wide range of parameters.

CHAPTER I.

1.1 INTRODUCTION

Reflecting and refracting telescope objectives have been in existence for many years. Because of the chromatic effects associated with the refracting objective, in the earlier days reflecting objectives were preferred, despite the difficulties in figuring the mirrors. Following the invention of the achromatic object glass and because of the difficulties in casting and figuring specula, the refractor for a time, almost completely superseded the reflector. Many practical men seem to think that the refractor has entirely superseded the reflector and that all attempts to improve the reflecting instrument are useless. Larger and larger refracting objectives were made and with the completion of the 36 inch (1888) and the 40 inch (1897) refractors, toward the end of the nineteenth century, no larger objectives have ever been made.

At the time when this development was taking place, the strong proponents of the reflecting objective continued the research to overcome the difficulties associated with the speculum metal and arrived at the silver on glass mirror. Perhaps the 47 inch reflector made in 1860 was the last large telescope using speculum metal for the mirrors. The achievement of the silver on glass mirror, began to bring the reflecting telescope back into favour in the seventies and eighties of the last century.

Newton was the first to overcome the difficulty associated will all systems employing a concave mirror, of obtaining an accessible focal plane, by inserting a plane reflector into the beam of converging light, so that the image is formed outside the incoming light rays, and as a rule lies in a plane which is parallel to the axis of the mirrors. The first telescope of this kind was made by Newton in 1668. A paraboloid mirror must be employed to obtain a stigmatic axial image. The fact that a parabolic mirror produces off-axial comatic imagery,

together with the circumstance that large relative apertures are employed, makes the usable field very small. Another important method of obtaining an accessible focal plane is the cassegrain arrangement, where a convex secondary mirror mounted in the convergent beam returns the image along the axis of the system. In a large astronomical telescope, such an arrangement is often an alternative to the Newtonian arrangement. Different mirrors may be used to obtain a variety of focal lengths. The classical form of this telescope consists of a paraboloid primary mirror and an hyperboloid secondary mirror. In this way spherical aberration correction was achieved but the coma of the system was found to be more than that of a Newtonian paraboloid mirror alone. The petzval sum of the system reduces as a result of the use of the convex secondary mirror. These classical shapes of the primary and secondary mirrors of the cassegrain system are altered to make the system free from spherical aberration and coma. K. Schwarzschild (1905) considered a class of telescope objectives consisting of two aspheric mirrors, and showed that such a system can be made aplanatic. Two telescopes of this type were later constructed, one with an aperture of 24 inches at the University of Indiana, and another with a 12 inch aperture at Brown University. Schwarzschild's analysis was essentially meant for obtaining aplanatic Gregorian focus. Chretien (1922) later gave mathematically exact formulae for the profiles of the mirrors which provide aplanatic images at the cassegrain focus. The mirrors were figured and tested by Ritchey and such systems are therefore often referred to as Ritchey-Chretien telescopes.

Even though, theoretically, solutions for aplanatic objectives were developed, it appears that until recently, no serious view was taken to construct such a telescope system. Much recent development has been done by D.H. Schulte (1963), using spot diagram methods. He observes that the Ritchey-Chretien system

employs a near-hyperboloid primary and secondary, both departing farther from the base sphere than either of their counterparts in the cassegrain system. The resultant improvement in the images due to the removal of the coma term is shown in Figure 1. of his paper. The latest demands set for the field size and the correction of the extra-axial aberrations cannot be realised with the traditional cassegrain and Newtonian types. It appears from the figures given in the literature that the cassegrain system working at f/8 provides a field of 5 minutes only, whereas, the same paraboloic primary mirror alone working at f/3 covers a field of 0.6 minutes. The extra-axial aberration which limits the field size is mainly coma and as a result of this, aplanatic systems are adopted for the telescopes constructed or planned recently. The 84 inch Kitt Peak telescope constructed in 1964 was the first large telescope of this form to be made. The advantage obtained by using the aplanatic system is at the sacrifice of the axially stigmatic images of the traditional cassegrain system at the prime focus.

Wynne (1968) gave equations for the profiles of the mirrors which provide aplanatic condition to third order. He has avoided giving the equations for the third order aberration coefficients, which may be a necessity if residual values for the third order spherical aberration and coma are to be prescribed to balance the higher order aberrations. He limited his analysis to third order and apparently failed to show the advantages offered by analysing the mirrors to provide aplanatism to a higher order. It appears from the literature that there seems to have been no discussion in between the third order aberrations and the mathematically exact formulae of Chretien. It also seems that no limits are given in the literature concerning the extent of physically realisable aplanatism at the cassegrain focus, in the sense that, whether the profiles of the mirrors for a particular order of aplanatism are distinguishable from those of the preceding order of aplanatism.

Since the secondary focus of the Ritchey-Chretien system suffers from astigmatism and field curvature, secondary focus correctors are required, if the field size for good imagery is to be improved. Due to this fact several field correctors consisting of spherical surfaces only, Rosin (1966), Kohler (1966), Wynne (1965,68); and aspherical surfaces, Gascoigne (1965), Schulte (1966) have been proposed. Kohler suggested that a negative lens located at a suitable distance from the focus is capable of correcting the astigmatism and field curvature of the Ritchey-Chretien system. Such a lens may not be a useful proposition as it introduces considerable transverse colour. Wynne (1965) had proposed a two lens corrector which provides a useful field of about 50 minutes. Excepting for few remarks, his paper does not disclose the essential principles underlying the design of the corrector.

Rosin pointed out that the two lens corrector system may be used to correct astigmatism and petzval sum, and colour of the system. As the lenses consist of aplanatic and concentric surfaces they do not introduce any third order spherical aberration or coma, but have a substantial effect on astigmatism and petzval curvature. With such a corrector system either longitudinal or transverse chromatic aberration may be corrected. Gascoigne has suggested that an aspheric plate placed a short distance in front of the focus may be used to correct the astigmatism of the Ritchey-Chretien system. As such an aspheric plate introduces small spherical aberration and coma, he pointed out that the asphericities of the Ritchey-Chretien mirrors and the plate may be chosen simultaneously to correct spherical aberration, coma and astigmatism. Based on such a principle, Schulte developed an anastigmatic objective with very encouraging results. He used a field flattening lens to remove the petzval curvature of the system. This type of correction no longer makes the two mirror system produce aplanatic images at the cassegrain focus, when the correcting system is removed.

The Ritchey-Chretien primary focus suffers considerably from all the monochromatic aberrations. Therefore, if the primary focus is to be used, prime focus correctors are needed even to obtain good imagery on the axis. Gascoigne (1965), Wynne (1965,68), Ross (1935), Kohler (1968), Meinel (1953) and Schulte (1966) have all proposed prime focus corrector systems consisting of either spherical surfaces or aspherical surfaces or both. Gascoigne noted that a single aspheric plate may be used to correct both spherical aberration and coma by a proper choice of the location of the plate and its asphericity. Kohler, following an earlier suggestion by Meinel, used a three plate corrector together with a field flattening lens to correct the prime focus aberrations. The asphericities of the plates may be chosen to correct the spherical aberration, coma and astigmatism, while the paraxial powers of the plates and field flattener correct field curvature and colour. With such a corrector a useful field of one degree may be achieved. Ross designed a doublet corrector for the prime focus of a paraboloid mirror. Wynne's elegant two lens and three lens prime focus correctors are derived mostly from the original Ross doublet. With the doublet corrector, he used the separations, powers and shapes as the parameters to control the monochromatic and chromatic aberrations. With such a corrector system higher order aberrations limit the size of the useful field. He apparently overcame this difficulty by adding one more lens to the system. As a result of this addition he found that the monochromatic aberrations are distributed over the three elements, and, as a result of this the individual curvatures will be small, resulting in small higher order chromatic and monochromatic aberrations. With Wynne's triplet corrector one could achieve almost the same performance as that of Kohler's four element corrector.

An attempt is made in the succeeding chapters to analyse the Ritchey-Chretien aplanatic objective system by making use of Buchdahl's aberration coefficients. Equations are given which provide aplanatic secondary focus to fifth order. The seventh order aplanatism is also discussed. As can be seen later such an aplanatism may not be physically distinguishable from the fifth order aplanatism. An analysis of hyperboloid mirrors is also made. The merits and demerits of the secondary focus correctors of the Gascoigne and Rosin type and the prime focus correctors of the Gascoigne and Meinel type are investigated. The usefulness of the various equations developed is shown by way of a numerical example. Spot diagrams, wherever necessary are provided.

1.2 ASPHERIC SURFACES.

Buchdahl (1954) and Cruickshank (1968) have given various ways of specifying aspheric surfaces of revolution. Each method of definition has a particular advantage. The standard and most usual way of specifying an aspheric surface is by its profile equation, given by

$$x = \sum_{n=1}^{\infty} \theta_n (y^2 + z^2)^n \qquad (1.1)$$

In the meridional plane ($z = 0$), we have

$$x = \theta_1 y^2 + \theta_2 y^4 + \theta_3 y^6 + \theta_4 y^8 + \ldots\ldots \qquad (1.2)$$

where, the values of the coefficients θ_n characterise the surface.

Buchdahl particularly introduced the idea of the extra-axial curvatures which simply represent the curvature of the profile of the surface at any point (x,y) on the profile by a power series in y. This kind of specification is mostly used in the aberration coefficients analysis for aspheric surfaces.

By way of equation, we may write

$$\Gamma = c_0 + 3c_1 y^2 + 5c_2 y^4 + 7c_3 y^6 + \ldots\ldots \qquad (1.3)$$

where c_0, c_1, c_2 .... are defined as the curvature coefficients, in particular, c_0 is defined as the axial curvature of the surface corresponding to the polar tangent sphere, and c_1, c_2, ... c_n are defined as the extra-axial curvature coefficients. The aspheric surface may be defined through either of these coefficients, e_n or c_n. As they define the same surface, a relationship between these coefficients exists and may be obtained by changing equations (1.2) and (1.3) into a common form and then comparing the coefficients of the powers of y.

From calculus, we have

$$\Gamma = \frac{d^2x/dy^2}{\{1 + (dx/dy)^2\}^{3/2}}$$

which after integration with respect to y becomes

$$\int \Gamma \, dy = \frac{dx/dy}{\{1 + (dx/dy)^2\}^{1/2}} = \dot{x}\left(1 - \frac{\dot{x}^2}{2} + \frac{3}{8}\dot{x}^4 - \frac{5}{16}\dot{x}^6 + \ldots.\right) \qquad (1.4)$$

Where, $\dot{x} = dx/dy$

Equation (1.3) after integration with respect to y becomes

$$\int \Gamma \, dy = c_0 y + c_1 y^3 + c_2 y^5 + \ldots\ldots \qquad (1.5)$$

From equation (1.3), after differentiation, we get

$$\dot{x} = 2e_1 y + 4e_2 y^3 + 6e_3 y^5 + 8e_4 y^7 + \ldots\ldots \qquad (1.6)$$

Combining equations (1.4) and (1.6) and then comparing the coefficients of the different powers of y in this equation and those of equation (1.5) we get

$$
\left.
\begin{aligned}
\theta_1 &= \frac{c_0}{2} \\
\theta_2 &= \frac{1}{8}\,(2c_1 + c_0^3) \\
\theta_3 &= \frac{1}{48}\,(8c_2 + 12c_0^2 c_1 + 3c_0^5) \\
\theta_4 &= \frac{1}{128}\,(16c_3 + 24c_0^2 + 30c_0^4 c_1 + 24c_0 c_1^2 + 5c_0^7) \\
\theta_5 &= \frac{1}{160}\,(16c_4 + 24c_0^2 c_3 + 30c_0^4 c_2 + 60c_0^3 c_1^2 + \\
&\qquad + 8c_1^3 + 48c_0 c_1 c_2 + 35c_0^6 c_1 + \tfrac{35}{8} c_0^9)
\end{aligned}
\right\} \qquad (1.7)
$$

A third method of specification, mostly useful for ray tracing through the system, is by the introduction of phi-values, which are the coefficients characterising the departure of the surface of revolution from the spherical form. This may be written in the form of an equation (for the profile of the surface, z = 0) as

$$2x - c_0(x^2 + y^2) = \varphi_0 y^2 + \varphi_1 y^4 + \varphi_2 y^6 + \ldots\ldots \qquad (1.8)$$

Expressing the left hand side of equation (1.8) in terms of a power series of y by using equation (1.2), and then comparing the coefficients of the powers of y along with equations (1.7), we obtain

$$
\left.
\begin{aligned}
\varphi_0 &= 0 \\
\varphi_1 &= \frac{c_1}{2} \\
\varphi_2 &= \frac{1}{6}\,(2c_2 + 3c_0^2 \varphi_1) \\
\varphi_3 &= \frac{1}{8}\,\{2c_3 + 5c_0(c_0\varphi_2 + c_1\varphi_1)\} \\
\varphi_4 &= \frac{1}{160}\,(32c_4 + 112c_0^2\varphi_3 + 248c_0 c_1 \varphi_2 - 27c_0^3 c_1^2 + 16c_1^3)
\end{aligned}
\right\} \qquad (1.9)
$$

1.3 CONICOIDS.

In the previous section, we have shown different methods of specifying an aspheric surface. A conicoid is usually specified by its eccentricity and the axial curvature, and then all other curvature coefficients are defined. It may, therefore, be a necessity to provide relations between the curvature coefficients and the axial curvature and eccentricity. The equation of the profile of a conicoid may be written as

$$x = \frac{c_0 y^2}{2} + \frac{P c_0^3 y^4}{8} + \frac{P^2 c_0^5 y^6}{16} + \frac{5}{128} P^3 c_0^7 y^8 + \\ + \frac{7}{256} P^4 c_0^9 y^{10} + \ldots\ldots \qquad (1.10)$$

where $P = 1 - e^2$, e being the eccentricity.

Comparing the coefficients of the powers of y in equations (1.10) and (1.2) and then using equations (1.7) we obtain

$$\left.\begin{aligned} q_1 &= -\frac{1}{2} e^2 c_0^3 \\ c_2 &= \frac{3}{8} e^4 c_0^5 \\ c_3 &= -\frac{5}{16} e^6 c_0^7 \\ c_4 &= \frac{35}{128} e^8 c_0^9 \\ &\ldots\ldots\ldots\ldots\ldots \end{aligned}\right\} \qquad (1.11)$$

Hence, the equations (1.11) determine the curvature coefficients of a conicoid, once c_0 and e of the surface are specified.

1.4 RAY TRACE SCHEME.

Buchdahl (1954), Ford (1966) and Cruickshank (1968) have described the theory of the marginal ray trace scheme suitable for systems consisting of aspheric surfaces. In this scheme an aspheric surface is completely defined

by its axial curvature and the phi-values, as defined earlier. The surface may be specified by as many phi-values as is necessary. As the aberration coefficients are computed up to seventh order only, which involve the axial curvature and the first of the three extra-axial curvatures, we therefore specify the surface by its first three aspheric constants (phi-values) and as far as our ray trace scheme is concerned all the remaining aspheric constants are considered as zero. Thus the designer has under his control the axial curvature and the first three extra-axial curvatures of an aspheric surface as c_n, $n>4$ are predetermined by the condition that φ_n $(n>3)$ are zero. The preceding statements fail in the case of a conicoid, as the curvature coefficients are predetermined by the axial curvature and the eccentricity. Unless the systems work at a very low aperture and field so that the ninth and higher order aberrations are negligible, the deductions that will be made from the marginal ray traces, where φ_1, φ_2, φ_3 only are given may not be the true deductions. It appears that Ford has overlooked such a case. For this reason expressions are given for φ_4 and φ_5 also.

The ray trace scheme makes use of the $\overline{OT}$ coordinates for the specification of the incident rays. The advantage of these coordinates is that all the rays in the pencil of light from one object point may be specified in turn by changing only the values of S_y and S_z. Choosing the meridional plane as the x - y coordinate plane, the initial coordinates are written as

$$S_y = \rho\cos\theta \qquad T_y = Hy_1/l_{01}$$

$$S_z = \rho\sin\theta \qquad T_z = 0$$

where (ρ,θ) are the coordinates of the point of intersection of the ray in the first polar tangent plane with reference to the coordinates of the intersection point of the principal ray as origin and the y-axis as initial line. The tracing of two formal paraxial rays, namely the a-ray with initial coordinates

$(y_1 = 1,\ v_1 = 1/l_{01})$; and the b-ray with initial coordinates $\{y_1 = pv_1,\ v_1 = 1/(1 - p/l_{01})\}$ where, l_{01} is the distance of the object plane, and p is the distance of the entrance pupil, both measured from the vertex of the first polar tangent plane, give the values of the paracanonical paraxial coefficients, y_{aj}, v_{aj}, y_{bj}, v_{bj} for the system which are ultimately used for the computation of the canonical variables Y, Z, V, W of the ray. The path of an actual ray after refraction or reflection at a surface, will, in general, differ from the ideal ray (paraxial ray) path. Hence, the difference between the coordinates (Y, Z, V, W) of the intersection points at any plane between the ideal ray and the actual ray is used as a measure of the aberration of the ray produced by the surfaces through which the ray has travelled. This principle is used as the main basis for finding the actual aberration of the ray or the intersection point of the actual ray in the paraxial image plane or in any other neighbouring plane. An actual computation scheme, (Ford, 1966), with the results for one particular trace is shown in Table I. For our present telescope objective system the primary mirror acts as the stop of the system and therefore the entrance pupil coincides with the first polar tangent plane. The object lies at infinity. Therefore the initial paracanonical coordinates and the initial particular paracanonical $(\bar{O}\bar{I})$-coordinates, are identically equal. That is, $S_y = Y_1$, $S_z = Z_1$, $T_y = \bar{H}$, and $T_z = 0$. Table I explains clearly the actual process of computation.

The evaluation of the quality of the image is ultimately assessed by producing a spot diagram. To obtain this we need to divide the entrance pupil into a number of small equal areas and then trace a ray from the object point through the centre of each of the small areas. The intersection points of each ray in the selected image plane are then plotted. This produces the spot diagram. The spot diagram illustrates the appearance of the image of a point

object with a fair degree of accuracy. For this purpose, a programme is written in the Algol 60 programming language for the Elliott 503 computer. The programme is suitable for systems consisting of spherical and non-spherical surfaces of revolution. All the displacements will be computed in the paraxial image plane of the e-line. The entrance pupil is divided into small equal areas on the basis of the rectangular grid system. As the rays on each side of the meridional plane are mirror images, only the rays incident on one side of the meridional plane are traced through the system for the extra-axial object points. For axial object points the rays incident in one quadrant of the entrance pupil only are traced as the rays of the other quadrants are mirror images.

TABLE I. Process of finding spherical aberration present in the modified hyperboloid aplanat by marginal ray trace.

Surface Data			1	1	1	2	2	2
	c_0		-1.2			-2.1024735		
	c_1		1.0134987			39.592933		
	c_2		-1.2839744			-1118.3972		
	c_3		1.8073699			35102.009		
$c_1/2$	φ_1		0.50674933			19.796466		
$(2c_2 + 3c_0^2\varphi_1)/6$	φ_2		-0.06313195			-329.04496		
$\{2c_3+5c_0(c_0\varphi_2+c_1\varphi_1)\}/8$	φ_3		0.00959778			6836.4845		
	d		-0.27794118			0.0		
	N'		-1.0			1.0		
	k		-1.0			-1.0		
Paraxial data								
$*t_1 - dt_2$	y_a	t_1	1.0			0.33294117		0.33294117
$*\{(1-k)c_0t_1+kt_2\}$	v_a	t_2	0.0			-2.4		1.0
$*t_3 - dt_4$	y_b	t_3	0.0			-0.27794118		-0.27794118
$*\{(1-k)c_0t_3+kt_4\}$	v_b	t_4	1.0			-1.0		2.1687279
Ray trace								
$*(t_5-t_{45})$	$(S_y+\delta)$	t_5	0.0625			0.06285329		0.06262203
$*(t_6-t_{46})$	$(S_z+\delta)$	t_6	0.0			0.0		0.0
$*(t_7+t_{43})$	$(T_y+\delta)$	t_7	0.0			-0.00007356		-0.00000003
$*(t_8+t_{44})$	$(T_z+\delta)$	t_8	0.0			0.0		0.0

Note: An * before or after a symbol indicates quantities from the preceding or following surface.

$t_1 t_5+t_3 t_7$	Y	t_9	0.0625	0.02094689		0.02084946
$t_1 t_6+t_3 t_8$	Z	t_{10}	0.0	0.0		0.0
$t_2 t_5+t_4 t_7$	V	t_{11}	0.0	-0.15077434		0.06262197
$t_2 t_6+t_4 t_8$	W	t_{12}	0.0	0.0		0.0
$t_9^2 + t_{10}^2$	ξ	t_{13}	0.00390625	0.00043877		
$t_9 t_{11}+t_{10} t_{12}$	η	t_{14}	0.0	-0.00315825		
$t_{11}^2+t_{12}^2$	ζ	t_{15}	0.0	0.02273290		
$t_{15}+1$	P_2	t_{16}	1.0	1.02273290		
$c_0 t_{14}-t_{15}$	P_1	t_{17}	0.0	-0.01609296		
$c_0^2 t_{13}-2t_{17}-t_{16}$	P_0	t_{18}	-0.994375	-0.98860784		
$t_{17} -t_{16} t_{18}$		t_{19}	0.994375	1.01123074		
$(\sqrt{t_{19}}-t_{17})/t_{16}$	P_0	t_{20}	0.99718353	0.99903615		
$(1-t_{20})/c_0$	x_0	t_{21}	-0.00337976	-0.00202647		
go to iteration if aspheric surface						
iteration: $t_{21}(t_{21} t_{15}-2t_{14})+t_{13}$	χ	t_{22}	0.00390625	0.00390625	0.00390625	0.00042606	0.00043591	0.00043589
$\Sigma\varphi_n t_{22}^{n+1}$	$\varphi(\chi)$	t_{23}	0.00000773	0.00000773	0.00000773	0.00000356	0.00000373	0.00000373
$\Sigma(n+1)\varphi_n t_{22}^{n}$	φ	t_{24}	0.00395610	0.00395610	0.00395610	0.01668977	0.01707138	0.01707060
$t_{24}+c_0$		t_{25}	-1.19604390	-1.19604390	-1.19604390	-1.19604390	-2.08578373	-2.08540290
$c_0(t_{21}^2+t_{22})-2t_{21}+t_{23}$	$f(x)$	t_{26}	0.00206605	-0.00000130	0.0	0.00315208	-0.00000532	
$2\{(t_{15}t_{21}-t_{14})(t_{25}+c_0 t_{21}-1\}$	$f'(x)$	t_{27}	-1.99188858	-1.99437792		-2.00446146	-2.01122060	
$t_{21}-t_{26}/t_{27}$	x_{n+1}	t_{21}	-0.00234253	-0.00234318		-0.00045394	-0.00045658	

go back to iteration, if necessary.

$t_{25}/(1-c_0 t_{21})$		t_{28}	-1.19941644	-2.08740670
$1/(1+t_{21} t_{28})$		t_{29}	0.99719742	0.99904783
$t_{29} t_{28}-c_0$		t_{30}	0.00394502	0.01705437
$(k^2-1)t_{16}$	$\bar{\mu}_0$	t_{31}	0.0	0.0
$k^2(t_{17}+t_{30} t_{14})+t_{16} t_{29}$	$\bar{\mu}_1$	t_{32}	0.99719742	1.00561246
$k^2\{t_{18}+1+t_{30}(2(c_0 t_{13}-t_{14})+t_{30} t_{13})\}-t_{16} t_{29}^2$	$\bar{\mu}_2$	t_{33}	-0.98881461	-1.00931765
$t_{32}^2-t_{31} t_{33}$		t_{34}	0.99440269	1.01125642
$(\pm\sqrt{t_{34}}-t_{32})/t_{33}$	S_0	t_{35}	2.01695527	1.99265802
$k+t_{35}-1$	Q	t_{36}	0.01695527	-0.00734198
$N'\{t_1 t_{36}-(t_2^*)t_{21} t_{35}\}$	D_a	t_{37}	-0.00561266	-0.00153464
$N'\{t_3 t_{36}-(t_4^*)t_{21} t_{35}\}$	D_b	t_{38}	0.00472609	0.00401377
$c_0 t_9-t_{11}$		t_{39}	-0.075	0.10673406
$c\,t_{10}-t_{12}$		t_{40}	0.0	0.0
$N'\{t_{30} t_{35}(t_1-(t_2^*)t_{21})$		t_{41}	-0.00791218	0.01133003
$N'\{t_{30} t_{35}(t_3-(t_4^*)t_{21})\}$		t_{42}	0.00001864	-0.00941177
$t_{37} t_{39}+t_{41} t_9$	$\Delta\Lambda_{ya}$	t_{43}	-0.00007356	0.00007353
$t_{37} t_{40}+t_{41} t_{10}$	$\Delta\Lambda_{za}$	t_{44}	0.0	0.0
$t_{38} t_{39}+t_{42} t_9$	$\Delta\Lambda_{yb}$	t_{45}	-0.00035329	0.00023126
$t_{38} t_{40}+t_{42} t_{10}$	$\Delta\Lambda_{zb}$	t_{46}	0.0	0.0

$N(t_{10}t_{11}-t_9t_{12})$	t_{47}	0.0	0.0
$t_{47}/\sqrt{t_{16}}$	αE_x	0.0	0.0

$\varepsilon'_y = -0.0,3$

$\varepsilon'_z = 0.0$

Spherical aberration present in the system = $-0.0,3$

CHAPTER II.

APLANATIC OBJECTIVES

2.1 PARAXIAL EQUATIONS

Consider an optical system (Fig. 2.1) consisting of two reflecting surfaces of revolution which are arranged coaxially with an axial separation, t. For any paraxial ray (y,z,v,w) incident at such a reflecting surface, we have

$$y' = y \tag{2.1}$$

$$v' = \psi y + kv \tag{2.2}$$

where $k = \frac{N}{N'} = -1$, and $\psi = (1-k)c_0 = 2c_0$, are constants of the reflecting surface, and

$$y_+ = y' - tv' \tag{2.3}$$

$$v_+ = v' \tag{2.4}$$

Equations (2.1), (2.2) are referred to as the paraxial reflection equations of the surface, whereas equations (2.3), (2.4) are referred to as the paraxial transfer equations for the two surfaces.

Written in matrix form,

$$\left.\begin{aligned} \begin{bmatrix} y' \\ v' \end{bmatrix} &= \begin{bmatrix} 1 & 0 \\ \psi & k \end{bmatrix} \begin{bmatrix} y \\ v \end{bmatrix} = R \begin{bmatrix} y \\ v \end{bmatrix} \\ \begin{bmatrix} y_+ \\ v_+ \end{bmatrix} &= \begin{bmatrix} 1 & -t \\ 0 & 1 \end{bmatrix} \begin{bmatrix} y' \\ v' \end{bmatrix} = T \begin{bmatrix} y' \\ v' \end{bmatrix} \end{aligned}\right\} \tag{2.5}$$

Similarly, we can write

$$\left.\begin{aligned} \begin{bmatrix} z' \\ w' \end{bmatrix} &= \begin{bmatrix} 1 & 0 \\ \psi & k \end{bmatrix} \begin{bmatrix} z \\ w \end{bmatrix} = R \begin{bmatrix} z \\ w \end{bmatrix} \\ \begin{bmatrix} z_+ \\ w_+ \end{bmatrix} &= \begin{bmatrix} 1 & -t \\ 0 & 1 \end{bmatrix} \begin{bmatrix} z' \\ w' \end{bmatrix} = T \begin{bmatrix} z' \\ w' \end{bmatrix} \end{aligned}\right\} \tag{2.6}$$

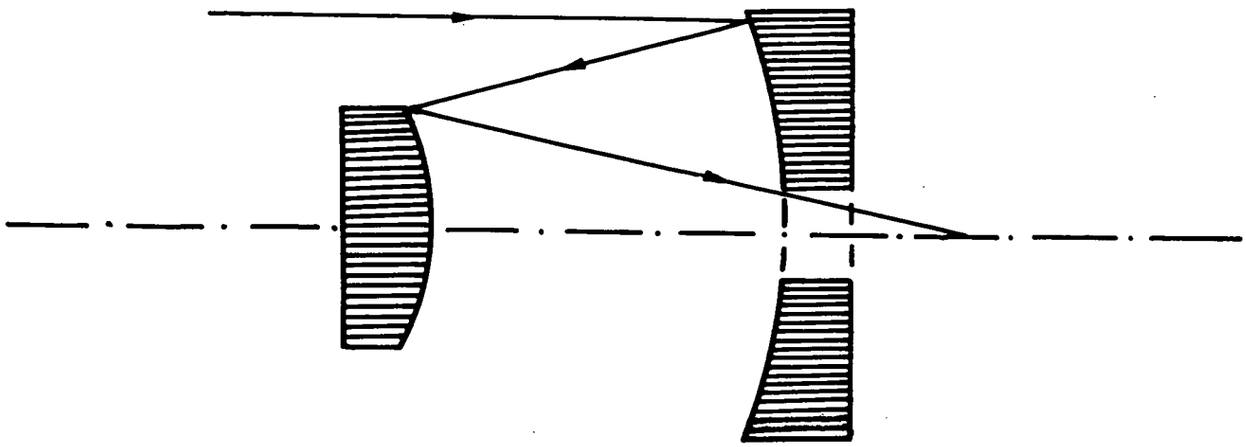

Fig 2.1

Optical diagram of the Ritchey – chretien mirror system

where primed symbols denote the coordinates of the ray after reflection and the subscript (+) denotes the following surface. R and T are known as the paraxial reflection matrix of the surface and paraxial transfer matrix of the two surfaces respectively.

The paraxial matrix of the whole system is then given by

$$P = \begin{bmatrix} A_2 & B_2 \\ C_2 & D_2 \end{bmatrix} = R_2 T_1 R_1 = \begin{bmatrix} 1 & 0 \\ \psi_2 & k_2 \end{bmatrix} \begin{bmatrix} 1 & -t \\ 0 & 1 \end{bmatrix} \begin{bmatrix} 1 & 0 \\ \psi_1 & k_1 \end{bmatrix}$$

$$= \begin{bmatrix} 1-2tc_{01} & t \\ 2c_{02}-2c_{01}-4tc_{01}c_{02} & 1+2tc_{02} \end{bmatrix} \qquad (2.7)$$

where c_{01}, c_{02} are the paraxial curvatures of the two mirrors.

2.2 PARAMETERS of the SYSTEM

Important quantities associated with a telescope objective are the diameter of the primary mirror, $2h_1$, the focal length of the system, f', and the f-numbers at different foci. In the development of the design, it is convenient to work with a unit power system. We introduce two new parameters R and x, where R is defined as the ratio of the f-number, υ_2, of the whole system to the f-number, υ_1, of the primary mirror, and x is the distance of the back focal plane from the vertex of the primary mirror.

Then, by definition,

$$\upsilon_1 = -\frac{f_1'}{2h_1} = -\frac{1}{4c_{01}h_1}$$

$$\upsilon_2 = \frac{f'}{2h_1} = \frac{1}{2h_1}$$

whence $$R = \frac{v_2}{v_1} = -2c_{01}$$

or $$c_{01} = -\frac{R}{2}$$

The back focal distance is given by

$$-t + x = l'_f = \frac{A_2}{C_2} = A_2$$

that is, $$-t + x = 1 - 2tc_{01} = 1 + tR$$

or $$t = \frac{x - 1}{R + 1}$$

Since the power, C_2, of the system is unity,

$$2c_{02} - 4tc_{01}c_{02} - 2c_{01} = 1$$

from which, we get

$$c_{02} = \frac{(1 - R^2)}{2(1 + Rx)}$$

Assembling these results, the paraxial arrangement of the whole system is given by

$$\left.\begin{aligned} R &= v_2/v_1 \\ c_{01} &= -R/2 \\ c_{02} &= (1-R^2)/2(1+Rx) \\ t &= (x-1)/(R+1) \end{aligned}\right\} \qquad (2.8)$$

If h_2 is the semi-aperture of the secondary mirror sufficient to transmit the full aperture axial pencil, then h_2 is given by

$$h_2 = (1 - 2tc_{01})h_1 = \frac{(1+Rx)h_1}{R + 1} \qquad (2.9)$$

This aperture has to be increased to about $(h_2 + tv_1)$ to transmit an unvignetted pencil at a field angle of $2v_1$.

2.3 THIRD-ORDER ABERRATION COEFFICIENTS

The third-order aberration polynomials of a system consisting of non-spherical surfaces of revolution may be written (Buchdahl, 1948)

$$\left.\begin{aligned} \varepsilon_{yk}' &= \sigma_1 \rho^4 \cos\theta + \sigma_2 \rho^2 \bar{H}(2+\cos 2\theta) + (3\sigma_3+\sigma_4)\rho \bar{H}^2 \cos\theta + \sigma_5 \bar{H}^3 \\ \varepsilon_{zk}' &= \sigma_1 \rho^3 \sin\theta + \sigma_2 \rho^2 \bar{H} \sin 2\theta + (\sigma_3+\sigma_4)\rho \bar{H}^2 \cos\theta \end{aligned}\right\} \qquad (2.10)$$

where $(\rho y_{01}, \theta)$ are the polar coordinates of the intersection point of a ray in the first polar tangent plane relative to the corresponding intersection point of the principal ray and $(l_{01}, -\bar{H}l_{01}, 0)$ are the coordinates of the object point. For objects at infinity, $\bar{H}$ is given by the tangent of the semi-field angle. The coefficients σ_1 to σ_5 are the coefficients of the third order spherical aberration, circular coma, astigmatism, petzval curvature of field, and distortion, respectively, given by

$$\left.\begin{aligned} \sigma_1 &= \mu\Sigma(S_0 + T_0) \\ \sigma_2 &= \mu\Sigma(qS_0 + PT_0) \\ \sigma_3 &= \mu\Sigma(q^2 S_0 + P^2 T_0) \\ \sigma_4 &= \mu\Sigma\tilde{\omega} \\ \sigma_5 &= \mu\Sigma(q^3 S_0 + P^3 T_0 + q\tilde{\omega}) \end{aligned}\right\} \qquad (2.11)$$

and

$$\left.\begin{aligned} \mu &= 1/N_k' v_{0k}' \\ \tilde{\omega} &= \frac{(N'-N)c_0}{2NN'} = \frac{c_0(1-k)}{2N} \\ q &= i/i_0 \\ P &= y/y_0 \\ S_0 &= 0.5 N i_0^2 y_0 (1-k)(i_0'-v_0) \\ T_0 &= (N'-N)c_1 y_0^4 \end{aligned}\right\} \qquad (2.12)$$

It should be noted that the quantity S_0 is associated with the axial curvature (spherical form) of the surface, whereas the quantity T_0 is related to the asphericity of the surface.

In these equations, the quantities y_0, v_0, i_0, i_0', y, i are obtained by tracing through the system two formal paraxial rays called the a-ray (axial ray, distinguished by the suffix 0) and the b-ray (principal ray). The initial data for these two rays are

$$\left.\begin{aligned} y_{01} &= 1 & v_{01} &= 1/l_{01} \\ y_1 &= pv_1 & v_1 &= 1/(1-p/l_{01}) \end{aligned}\right\} \qquad (2.13)$$

where l_{01} is the distance of the object plane and p is the distance of the paraxial entrance pupil, both measured from the vertex of the first surface.

For the two-mirror telescope objective system, we have

$$\left.\begin{aligned} N_1 &= N_2' = 1 & N_1' &= N_2 = -1 \\ \mu &= 1 & l_{01} &= -\infty & p &= 0 \end{aligned}\right\} \qquad (2.14)$$

Equations (2.1) - (2.4), and (2.8) then give

$$\left.\begin{aligned} y_{01} &= 1 & v_{01} &= 0 & i_{01} &= -R/2 & i_{01}' &= R/2 \\ y_{02} &= \frac{(1+Rx)}{(1+R)} & v_{02} &= -R & i_{02} &= \frac{(1+R)}{2} & i_{02}' &= -\frac{(1+R)}{2} \\ y_1 &= 0 & v_1 &= 1 & i_1 &= -1 \\ y_2 &= \frac{(x-1)}{(R+1)} & v_2 &= -1 & i_2 &= \frac{(1+x)(1+R)}{2(1+Rx)} \end{aligned}\right\} \qquad (2.15)$$

Substituting these expressions in equations (2.12), we obtain

$$\left.\begin{aligned} q_1 &= 2/R & q_2 &= (1+x)/(1+Rx) \\ P_1 &= 0 & P_2 &= (x-1)/(1+Rx) \\ \omega_1 &= -R/2 & \omega_2 &= (R^2-1)/2(1+Rx) \\ S_{01} &= R^3/8 & S_{02} &= (1-R^2)(1+Rx)/8 \\ T_{01} &= -2c_{11} & T_{02} &= 2c_{12}(1+Rx)^4/(1+R)^4 \end{aligned}\right\} \qquad (2.16)$$

Combining equations (2.11), (2.16), the expressions for the third order aberration coefficients may be obtained.

The third order spherical aberration is given by

$$\begin{aligned} \sigma_1 &= S_{01} + T_{01} + S_{02} + T_{02} \\ &= \frac{R^3}{8} - 2c_{11} + \frac{(1-R^2)(1+Rx)}{8} + 2c_{12}\frac{(1+Rx)^4}{(1+R)^4} \end{aligned} \qquad (2.17)$$

Similarly, the third order circular coma coefficient is

$$\begin{aligned} \sigma_2 &= q_1 S_{01} + P_1 T_{01} + q_2 S_{02} + P_2 T_{02} \\ &= \frac{R^2}{4} + \frac{(1-R^2)(1+x)}{8} + \frac{2c_{12}(x-1)(1+Rx)^3}{(1+R)^4} \end{aligned} \qquad (2.18)$$

Continuing in this manner, we obtain

$$\sigma_3 = \frac{R}{2} + \frac{(1-R^2)(1+x)^2}{8(1+Rx)} + \frac{2c_{12}(x-1)^2(1+Rx)^2}{(1+R)^4} \qquad (2.19)$$

$$\begin{aligned} \sigma_4 &= c_{01} - c_{02} = -\frac{R}{2} + \frac{R^2-1}{2(1+Rx)} \\ &= \frac{R^2(1-x) - R - 1}{2(1+Rx)} \end{aligned} \qquad (2.20)$$

$$\sigma_5 = \frac{(1-R^2)(1+x)(x^2+2x-3)}{8(1+Rx)^2} + \frac{2c_{12}(1+Rx)(x-1)^3}{(1+R)} \qquad (2.21)$$

It should be noted that the third order aberration coefficients involve only the first of the extra axial curvatures.

2.4 THIRD ORDER APLANATISM

Noting again the closing remark of the last section, it is clear that equations (2.17), (2.18) allow us to choose c_{11}, c_{12} so that σ_1 and σ_2 are adjusted to zero or any desired small value. The condition that $\sigma_2 = 0$, for example, is, from equation (2.18),

$$c_{12} = \frac{(R^2x - R^2 - x - 1)(1 + R)^4}{16(x-1)(1+Rx)^3} \tag{2.22}$$

The condition that $\sigma_1 = 0$ as well, then, requires that

$$c_{11} = \frac{R^3(1-x) + 2(1+Rx)}{16(1-x)} \tag{2.23}$$

This means that with these values of the first extra-axial curvatures, the system is aplanatic to third order.

The third order residual aberrations, astigmatism, petzval curvature of field, and distortion of the aplanatic system are then obtained by substituting the expressions for c_{11}, c_{12} in equations (2.19), (2.20) and (2.21). We now have

$$\sigma_3 = \frac{(1+x+2R)}{4(1+Rx)} \tag{2.24}$$

$$\sigma_4 = \frac{R^2(1-x) - 1 - R}{2(1+Rx)} \tag{2.25}$$

$$\sigma_5 = \frac{(2-3R^2)x^2 + 2R^2x + R^2 - 2}{4(1+Rx)^2} \tag{2.26}$$

The variation of the residual aberrations, astigmatism, petzval curvature of field with respect to the parameters R and x are shown in Figures 2.2 a - d. The figures illustrate that both astigmatism and petzval curvature vary similarly with respect to R and x. The figures also illustrate that both the

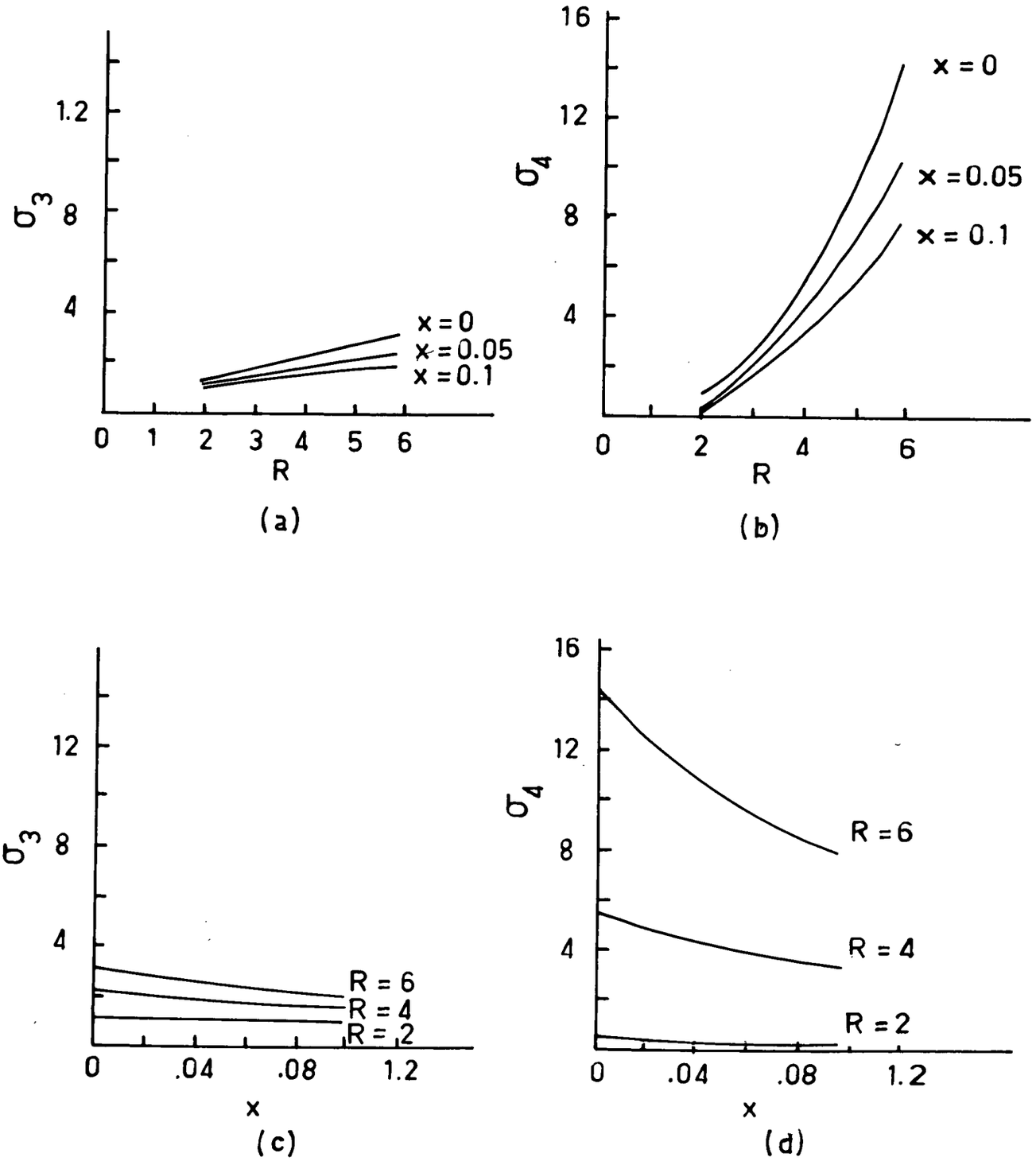

Fig 2.2 Variation of residuals σ_3, σ_4 with R and x.

residuals can be decreased by decreasing R and increasing x. The petzval curvature is more sensitive to R and x as compared to astigmatism. Hence a proper selection of the ratio of the f-numbers at the two foci, R and the back focal distance, x has to be made in order to keep the residual aberrations low. These values, however, are determined by considerations other than those concerning residual aberrations.

2.5 MEAN FOCAL SURFACE.

If the principal ray intersection in the paraxial image plane is taken as the reference point for measuring the aberrations, then the third order aberration polynomials (2.10) for this aplanatic system reduce to

$$\left.\begin{aligned} \varepsilon_{yk}' &= (3\sigma_3 + \sigma_4)\rho\bar{H}^2 \cos\theta \\ \varepsilon_{zk}' &= (\sigma_3 + \sigma_4)\rho\bar{H}^2 \sin\theta \end{aligned}\right\} \qquad (2.27)$$

At any other plane distant x' from the paraxial image plane, the aberration equations (2.27) become (Buchdahl, 1954)

$$\left.\begin{aligned} \varepsilon_{yk}' &= (3\sigma_3 + \sigma_4)\rho\bar{H}^2 \cos\theta + x'\rho\cos\theta \\ \varepsilon_{zk}' &= (\sigma_3 + \sigma_4)\rho\bar{H}^2 \sin\theta + x'\rho\sin\theta \end{aligned}\right\} \qquad (2.28)$$

The distances of the tangential focal line x_t' and the sagittal focal line x_s' measured from the paraxial image plane may be written as

$$\left.\begin{aligned} x_t' &= -(3\sigma_3 + \sigma_4)\bar{H}^2 \\ x_s' &= -(\sigma_3 + \sigma_4)\bar{H}^2 \end{aligned}\right\} \qquad (2.29)$$

In the presence of astigmatism and petzval curvature, the best image is formed on the mean focal surface which is half way between the tangential and sagittal surfaces. Hence the distance, x_m', of the mean focal surface from the paraxial image plane is

$$x_m' = -(2\sigma_3 + \sigma_4)\bar{H}^2 \qquad (2.30)$$

Therefore, the best image will be formed on a curved surface whose profile is given by equation (2.30), where $\bar{H}$ is the same as y, the image height. For this focal surface, the aberration equations (2.28) reduce to

$$\left.\begin{aligned} \varepsilon_{yk}' &= \sigma_3 \rho \bar{H}^2 \cos\theta \\ \varepsilon_{zk}' &= -\sigma_3 \rho \bar{H}^2 \sin\theta \end{aligned}\right\} \qquad (2.31)$$

The image of a star in this mean focal surface is a circle of diameter $2\sqrt{\varepsilon_{yk}'^2 + \varepsilon_{zk}'^2}$ which is equal to $2\sigma_3 \rho \bar{H}^2$. Since the focal length is unity, the angular diameter of the blur circle will be

$$2\sigma_3 \rho \bar{H}^2 / f' = 2\sigma_3 \rho \bar{H}^2$$

If we specify the image quality in terms of the angular diameter of the blur spot, then, if the blur circle diameter for acceptable definition is limited to d seconds of arc, then the maximum semi-field of the objective, $\bar{H}$, measured in radians, is

$$\bar{H} = \sqrt{\upsilon_2 d / (\sigma_3 \times 206265)}$$

or, more conveniently, if $\bar{H}$ is expressed in minutes of arc, we have

$$\bar{H} = \sqrt{57.3\, \upsilon_2 d / \sigma_3} \qquad (2.32)$$

2.6 NUMERICAL EXAMPLE.

We will now consider a numerical example, the purpose of which is to make use of the equations of the previous sections in the development of an actual telescope objective system. The writer understands that the proposed Anglo-Australian 150-inch telescope is to be a Ritchey-Chretien system, with the following specifications:

$\upsilon_1 = 10/3$	$\upsilon_2 = 8$
$f' = 1200$ inches	$x' = 66$ inches
$2h_1 = 150$ inches	$d = 0.5$ seconds

It will be of interest then to consider the design of an objective of this type. Reducing the system to unit focal length, we have

$$\upsilon_1 = 10/3 \qquad \upsilon_2 = 8$$

$$f' = 1 \qquad x' = 0.055$$

$$2h_1 = 0.125$$

(1) Using equations (2.8), the paraxial arrangement of the objective is

$$R = 2.4$$

$$c_{01} = -1.200000$$

$$c_{02} = -2.1024735$$

$$t = -0.27794118$$

(2) Using equations (2.22), (2.23), the values of the first extra-axial curvatures which will give third order aplanatism ($\sigma_1 = 0$, $\sigma_2 = 0$) are found to be

$$q_1 = 1.0137355$$

$$q_2 = 39.592933$$

(3) Having obtained the aplanatic system, the next step is to calculate the coefficients of third order residual astigmatism, petzval curvature, and distortion. Equations (2.24) - (2.26) give for these

$$\sigma_3 = 1.2930654$$

$$\sigma_4 = 0.90247351$$

$$\sigma_5 = 0.8481537$$

From equation (2.30), we obtain the profile of the mean focal surface as

$$X = -3.4886043\ \bar{H}^2$$

from which it follows that the axial curvature of this surface is

$$c_{0m} = -6.9772086$$

Equation (2.32) gives the maximum semi-field for which the angular diameter of the blur circle does not exceed 0.5 seconds of arc as

$$\bar{H}_{max} = 13.3 \text{ minutes}$$

The spot diagram programme is now used to analyse the correction state of the third order aplanatic system. The image spread is compared with a 0.5 seconds of arc diameter circle. About 200 points are obtained to produce the spot diagram. The spot diagrams are obtained (i) for the axial object point ($v = 0$), (ii) for an extra-axial object point corresponding to a semi-field angle of 6.5 minutes ($v = 6.5$), and (iii) for an object point given by $v = 13$ minutes. Figures 2.3 a - c illustrate the appearance of the image for the above three cases. Figure 2.3a illustrates that the third order aplanat objective system suffers from a higher order spherical aberration equivalent to 0.16 seconds of arc in diameter. This is well within the tolerance of the 0.5 seconds of arc diameter. The spot diagrams for the extra-axial object points show that the system suffers from aberrations other than the third order astigmatism and higher order spherical aberration. For the semi-field angle of 13 minutes, the image spread is equal to 0.64 seconds of arc. This clearly illustrates that the performance of the system is not determined by third order aberrations only. For the tolerance of 0.5 seconds of arc image spread, the field coverage of the third order aplanat is about 9.5 minutes only. The third order analysis of the two-mirror system is therefore inadequate. If the quality of the extra-axial images is to be improved, it is clear that higher order aberrations must be considered. Just what higher order aberrations are involved needs to be investigated.

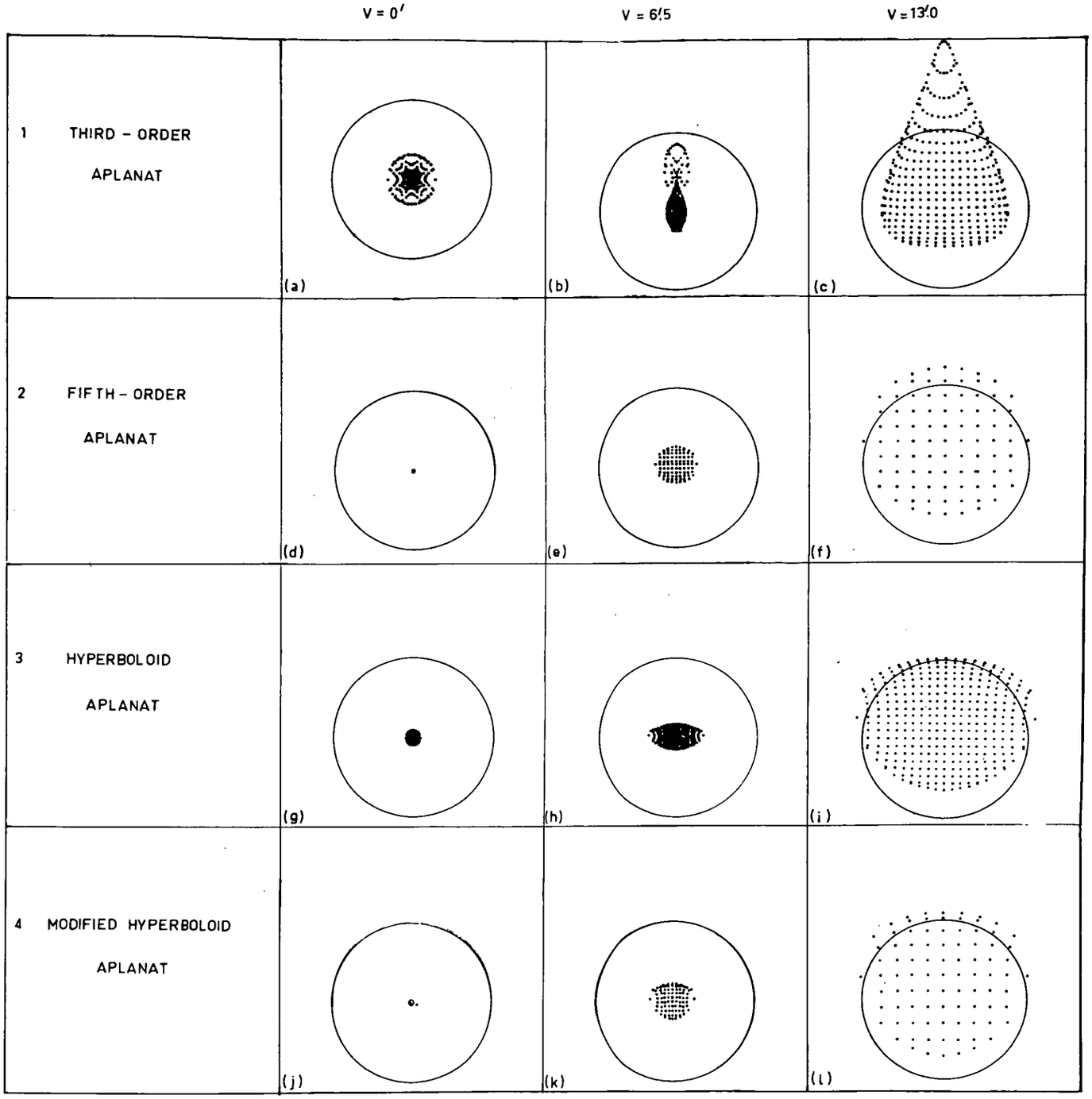

Fig 2.3 SPOT DIAGRAMS FOR APLANATIC SYSTEMS

(The circles correspond to 0.5″)

2.7 THE EFFECT of FIFTH ORDER COEFFICIENTS.

As the angular field of the telescope objectives under consideration is very small, it will probably be sufficient to consider those fifth order aberrations which are independent of $\bar{H}$ or are linear in $\bar{H}$. Hence we begin with an investigation of the fifth order spherical aberration and coma. This requires explicit expressions for the coefficients μ_1, μ_2, μ_3. Equations (68.7), (68.8) of Buchdahl (1954) may be used in deriving expressions for these. The full contribution to the coefficient of fifth order spherical aberration is given by

$$S_{1p} = 3\sigma_{1i}\{\frac{1}{8}(i_0^2+i_0'^2+v_0'^2+v_0^2)+(q'A-\bar{A})-\frac{1}{2}v_{01}^2\}$$
$$+\{\bar{c}_2 y_0^6+\frac{3}{4}\bar{c}_1 y_0^3\{y_0(i_0'-i_0'v_0-i_0v_0)+\frac{4A}{Ni_0}\}\} \quad (2.33)$$

The contribution $\bar{S}_{1p}$ to the first of the coefficients governing effective fifth order circular coma is given by

$$\bar{S}_{1p} = qS_{1p} - \{\bar{A}_q - q(\bar{A}+'A_q) + q^2\,'A\}\sigma_{1i}$$
$$+(P-q)\{y_0\breve{S}_{1p}+\bar{c}_1 y_0^4\{(\bar{A}-2'A_q)+(2P-q)\,'A\}\} \quad (2.34)$$

where, σ_{1i} is the surface contribution to σ_1, and an antiprime indicates division by N_1, the refractive index of the medium in which the object lies, and

$$A_j = \sum_{i=1}^{j-1}\sigma_{1i} \qquad \bar{A}_j = \sum_{i=1}^{j-1}\sigma_{2i}$$

$$\bar{c}_n = (N'-N)c_n \qquad 'A_q = \bar{A} - \frac{1}{2}(v_0^2-v_{0i}^2)$$

$$\bar{A}_q = \{q(q\,'A - \frac{1}{2}N_1(v_0^2-v_{01}^2)\} + P^2\bar{c}_1 y_0^4$$

$$\breve{S}_{1p} = \bar{c}_2 y_0^6 + \frac{1}{4}\bar{c}_1\{2(i_0'-v_0)i_0' + c_0 y_0(i_0-3v_0)\}y_0^3$$

In the equation for $\bar{A}_2$, $^{\circ}A$ is the spherical part of A and all the quantities on the right hand side except $^{\circ}A$ are meant for the previous surface. It follows from these definitions that

$$A_1 = \bar{A}_1 = {}^{\circ}A_1 = {}^{\circ}\bar{A}_1 = {}^{\circ}A_{q1} = {}^{\circ}\bar{A}_{q1} = 0$$

We now apply these considerations to the objective developed in the preceding sections. Using equations (2.21), (2.22), we obtain

$$\left.\begin{aligned}
&\breve{S}_{1\,p1} = -2c_{21} - \frac{c_{11}R(R-c_{01})}{4} \\
&A_2 = \sigma_{11} \qquad \bar{A}_2 = \frac{R^2}{4} \qquad {}^{\circ}A_2 = A_2 = \sigma_{11} \\
&{}^{\circ}\bar{A}_2 = \bar{A}_2 = \frac{R^2}{4} \qquad {}^{\circ}A_{q2} = -\frac{R^2}{4} \qquad {}^{\circ}\bar{A}_{q2} = -\frac{q_1R^2}{4} \\
&\breve{S}_{1\,p2} = 2c_{22}y_{02}{}^6 + \frac{q_2}{2}\left\{\frac{1-R^2}{2} + \frac{y_{02}c_{02}(1+7R)}{2}\right\} y_{02}{}^8
\end{aligned}\right\} \qquad (2.35)$$

Combining equations (2.35), (2.33), (2.34), we get

$$\left.\begin{aligned}
S_{1\,p1} &= \frac{9R^2\sigma_{11}}{16} - \frac{3}{8}R^2c_{11} - 2c_{21} \\
S_{1\,p2} &= 3\sigma_{12}\left\{\frac{(1+R)^2}{16} + \frac{1-R^2}{8} + q_2\sigma_{11}\right\} \\
&\quad + \frac{3}{2}c_{12}y_{02}{}^3\left\{\frac{y_{02}(1+R)^2}{4} - \frac{8\sigma_{11}}{1+R}\right\} + 2c_{22}y_{02}{}^6
\end{aligned}\right\} \qquad (2.36)$$

$$\left.\begin{aligned}
\bar{S}_{1\,p1} &= \frac{R}{8}\{9\sigma_{11} - 2c_{11} - 4c_{01}c_{11}\} \\
\bar{S}_{1\,p2} &= 2P_2y_{02}{}^6c_{22} + 3q_2\sigma_{12}\left\{\frac{(1+R)^2}{16} + \frac{1-R^2}{8} + q_2\sigma_{11}\right\} \\
&\quad + \frac{3}{2}q_2c_{12}y_{02}{}^3\left\{\frac{y_{02}(1+R)^2}{4} - \frac{8\sigma_{11}}{1+R}\right\} \\
&\quad + \left(\frac{R}{2} - q_2{}^2\sigma_{11}\right)\sigma_{12} \\
&\quad + \frac{y_{02}{}^6c_{12}}{4}\{1 - R^2 + y_{02}c_{02}(1+7R)\}(P_2-q_2) \\
&\quad + 2c_{12}(P_2-q_2)y_{02}{}^4\left\{\frac{3R^2}{4} + (2P_2-q_2)\sigma_{11}\right\}
\end{aligned}\right\} \qquad (2.37)$$

The fifth order spherical aberration coefficient, μ_1, is then given by

$$\begin{aligned}\mu_1 &= S_{1\,p1} + S_{1\,p2} \\ &= \mu_1^{(3)} - 2c_{21} + 2c_{22}y_{02}{}^6 \end{aligned} \tag{2.38}$$

where $\mu_1^{(3)}$ is the fifth order spherical aberration coefficient of the aplanat system at the stage in which $c_{21} = 0 = c_{22}$, and is given by

$$\begin{aligned}\mu_1^{(3)} = 3\sigma_{12}\{&\frac{(1+R)^2}{16} + \frac{1-R^2}{8} + q_2\sigma_{11}\} \\ &+ \frac{3}{2}c_{12}y_{02}{}^3\{\frac{y_{02}(1+R)^2}{4} - \frac{8\sigma_{11}}{1+R}\} \\ &+ \frac{3R^2}{16}\{\frac{3R^3}{8} - 8c_{11}\}\end{aligned} \tag{2.39}$$

If the third order spherical aberration and coma coefficients are zero, then μ_2, μ_3 are given by

$$\left.\begin{aligned}\mu_2 &= 3(\bar{S}_{1\,p2} + \bar{S}_{2\,p2}) = \mu_2^{(3)} + 6P_2c_{22}y_{02}{}^6 \\ \mu_3 &= \frac{2}{3}\mu_2\end{aligned}\right\} \tag{2.40}$$

where $\mu_2^{(3)}$ is the fifth order coma of the aplanat system at the stage in which $c_{21} = 0 = c_{22}$, given by

$$\begin{aligned}\mu_2^{(3)} = 3\{&\frac{9R^4}{64} - \frac{c_0c_{11}}{2} - \frac{5}{2}Rc_{11} + q_2\{\mu_1^{(3)} - \frac{9R^5}{128} + \frac{3}{2}R^2c_{11}\} \\ &+ (\frac{R}{2} - q_2{}^2\sigma_{11})\sigma_{12} + \frac{c_{12}y_{02}{}^4}{4}\{1 - R^2 + y_{02}c_{02}(1+7R)\}(P_2 - q_2) \\ &+ 2c_{12}(P_2 - q_2)y_{02}{}^4\{\frac{3R^2}{4} + (2P_2 - q_2)\sigma_{11}\}\}\end{aligned} \tag{2.41}$$

where

$$\left.\begin{aligned}y_{02} &= \frac{(1+Rx)}{(1+R)} \qquad q_2 = \frac{(x+1)}{(1+Rx)} \qquad P_2 = \frac{(x-1)}{(1+Rx)} \\ \sigma_{11} &= \frac{R^3}{8} - 2c_{11} \qquad \sigma_{12} = 2c_{12}y_{02}{}^4 - \frac{(R+1)(R^2-1)y_{02}}{8}\end{aligned}\right\} \tag{2.42}$$

Returning now to the numerical example, the values of the coefficients, μ_1, μ_2, μ_3 of the objective, obtained by using equations (2.38), (2.40) are

$$\mu_1 = 0.35731 \qquad \mu_2 = -6.4764 \qquad \mu_3 = -4.3176$$

If we include the effect of the fifth order aberration coefficients μ_1, μ_2, μ_3 in the computation of the aberrations, then the aberration displacements in the mean focal surface are given, by extension of equations (2.31), as

$$\begin{aligned} \varepsilon'_{yk} &= \sigma_3 \rho \bar{H}^2 \cos\theta + \mu_1 \rho^5 \cos\theta + (\mu_2 + \mu_3 \cos 2\theta)\rho^4 \bar{H} \\ \varepsilon'_{zk} &= -\sigma_3 \rho \bar{H}^2 \sin\theta + \mu_1 \rho^5 \sin\theta + \mu_3 \sin 2\theta \rho^4 \bar{H} \end{aligned} \qquad (2.43)$$

Using these equations, the predicted intersection points in the mean focal surface of the rays coming from an object point corresponding to a semifield angle of 13 minutes were computed for the maximum aperture zone of the objective. Figures (2.4, a - c) show the effect on the shape of the predicted intersection locus of (i) σ_3, (ii) σ_3 and μ_1, and (iii) σ_3, μ_1, μ_2 and μ_3 respectively.

Using the ray trace programme to obtain the true intersection locus for this zone, Figure 2.4d is obtained. The agreement between the shapes of the predicted intersection locus in Figure 2.4c and the actual intersection locus in Figure 2.4d confirms the expectation that the principal effect of fifth order coefficients is confined to that of μ_1, μ_2 and μ_3. Hence it should be possible to improve the quality of the image by the adjustment of these fifth order coefficients.

2.8 FIFTH ORDER APLANATISM

If we solve equations (2.38), (2.40), for those values of c_{21}, c_{22} which will make $\mu_1 = \mu_2 = 0$, the objective then becomes aplanatic to the fifth order. Proceeding in this way, we obtain

$$c_{21} = \frac{1}{2}\left\{\mu_1^{(3)} - \frac{\mu_2^{(3)}}{3P_2}\right\} = -1.1143405$$

$$c_{22} = -\mu_2^{(3)} / 6P_2 y_{02}^6 = -949.27$$

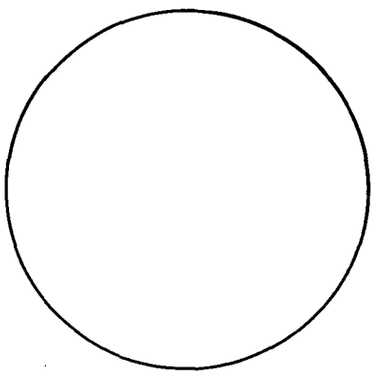

(a)
effect of σ_3

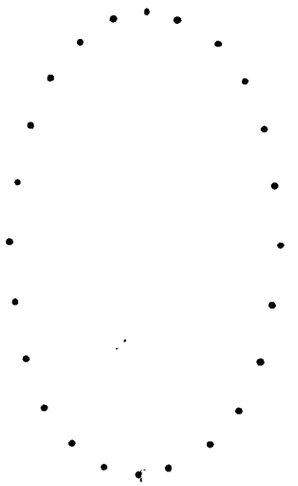

(b)
effect of σ_3 and μ_1

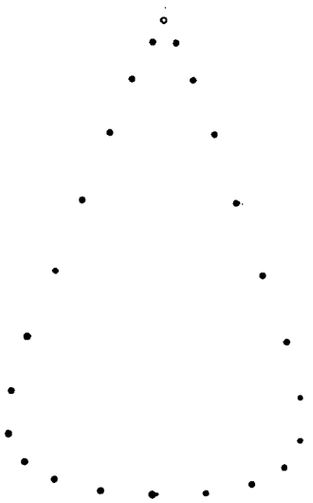

(c)
effect of σ_3, μ_1, μ_2, and μ_3
(predicted locus)

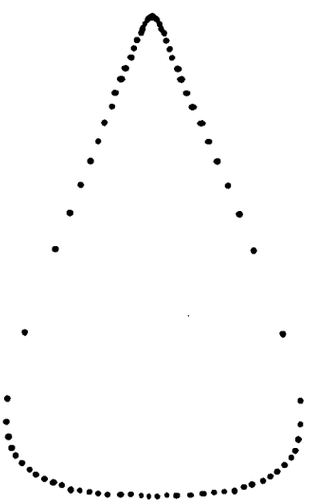

(d)
actual locus

Fig 2.4

The performance of this fifth order aplanatic system is now submitted to analysis by ray tracing. Spot diagrams for (i) $v = 0$, (ii) $v = 6.5$ minutes, and (iii) $v = 13$ minutes are shown in Figures (2.3d-f) and comparison of these with the corresponding third order aplanat diagrams in Figures (2.3a-c) show that a great improvement has been achieved by the reduction of μ_1 and μ_2 to zero. The system still has spherical aberration equivalent to 0.004 seconds of arc, but this is negligible compared with the tolerance of 0.5 seconds. The spot diagram plotted for the maximum semi-field angle of 13 minutes shows that the image spread is within the 0.5 seconds of arc tolerance and indicates that the coma present in the system is negligible. The field coverage of the system is therefore limited by astigmatism only, unlike the third order aplanatic system where the field coverage is limited by astigmatism, spherical aberration, and coma. The last traces of spherical aberration and coma may be eliminated by correcting the seventh order coefficients τ_1, τ_2, τ_3 with the help of the extra axial curvatures c_{3_1}, c_{3_2}, but it is questionable whether this would have any practical significance.

2.9 HYPERBOLOID APLANAT

It has been customary to consider the Ritchey-Chretien objective as consisting of two hyperboloids. An hyperboloid is defined by its paraxial curvature c_0 and its eccentricity e. Once these are given, all the extra axial curvatures are determined (equation (1.11) of Chapter 1). It becomes of interest, then, to examine the connection between a system of two hyperboloids and the fifth order aplanatic system that we have developed. Now, considering a two-mirror objective consisting of two hyperboloids which have the same paraxial curvatures c_{0_1}, c_{0_2} and the same extra-axial curvatures c_{1_1}, c_{1_2} as the third order aplanat of section 2.6, we obtain

$$e_1 = \left[-\frac{2c_{01}}{c_{01}^3} \right]^{\frac{1}{2}} = 1.083192$$

$$e_2 = \left[-\frac{2c_{02}}{c_{02}^3} \right]^{\frac{1}{2}} = 2.9189593$$

The curvature coefficients of these two hyperboloids, obtained by using equations (1.11), are then

$c_{01} = -1.2$	$c_{02} = -2.1024735$
$q_1 = 1.0137355$	$q_2 = 39.592933$
$c_{21} = -1.2845745$	$c_{22} = -1118.3972$
$c_{31} = 1.8086371$	$c_{32} = 35102.009$
.....	.....

It is very interesting to note that the second extra-axial curvature coefficients c_{21}, c_{22} of these hyperboloids are not far removed from the values obtained for the fifth order aplanatic system. The adoption of hyperboloid form for each mirror, then, ensures that the coefficients μ_1, μ_2, μ_3 will have values close to those desired for best fifth order correction.

Figures (2.3,g-i), which give the spot diagrams for this system, show considerable improvement in its performance as compared to the third order aplanatic system. Still, the system has spherical aberration equivalent to 0.045 seconds of arc in diameter. The image spread for the object point, given by $v = 13$ minutes, is 0.535 seconds. The spot diagrams for extra-axial object points indicate that the shape of the image is mostly dependent on spherical aberration and astigmatism, with little coma dependence. The hyperboloid aplanatic system is much superior in performance to the third order aplanatic system and inferior, but close, to the fifth-order aplanatic system. The

residual spherical aberration of this system may be reduced further by correcting spherical aberration to fifth order at the maximum aperture. The same type of correction may be applied to coma, but, because of the small angular fields considered, this analysis for coma is scarcely necessary.

We call the hyperboloid objective which is corrected for spherical aberration to fifth order, the modified hyperboloid aplanat. The general equations to obtain such a system are given first, so that they may be used for systems having different values of the parameters, and then the equations are used to get such a system for the numerical example. Replacing c_{11}, c_{12}, c_{21}, c_{22} in equations (2.17), (2.38) by their respective expressions from equations (1.11), we get

$$\sigma_1 = \frac{R^3 - (R^2-1)(1+Rx)}{8} + e_1^2 c_{01}^3 - y_{02}^4 e_2^2 c_{02}^3 \qquad (2.44$$

$$\mu_1 = \frac{9R^5}{128} + 3\sigma_{12}\left\{\frac{(1+R)^2}{16} + \frac{1-R^2}{8} + \frac{q_2 R^3}{8}\right\} + \frac{3}{4}\left\{R^2 + 4q_2\sigma_{12}\right\}c_{01}^3 e_1^2$$
$$- \frac{3}{4}\, y_{02}^3 c_{02}^3 e_2^2 \left\{\frac{y_{02}(1+R)^2}{4} - \frac{R^3}{1+R}\right\}$$
$$+ \frac{6 y_{02}^3 c_{01}^3 c_{02}^3 e_2^2 e_1^2}{(1+R)}$$
$$- \frac{3}{4}\, c_{01}^5 e_1^4 + \frac{3}{4}\, y_{02}^6 c_{02}^5 e_2^4 \qquad (2.45)$$

The eccentricity of the secondary mirror, e_2, remains the same as previously obtained, and e_1 will be obtained from the condition

$$\sigma_1 \rho^3 + \mu_1 \rho^5 = 0 \qquad (2.46)$$

which provides spherical aberration correction to fifth order.

Returning now to the numerical example, the eccentricity and the extra-axial curvatures for the primary mirror are calculated using equations (2.44) - (2.46). In this way we obtain

$$e_1 = 1.0830655 \qquad c_{11} = 1.0134987 \qquad c_{21} = -1.2839744 \qquad c_{31} = 1.8073699$$

The spot diagrams, Figures (2.4, j-1), show the improvement in the image quality following this adjustment. Spherical aberration is reduced to one-third. The image spread for the object point at v = 13 minutes is equal to 0.5 seconds, which is the specified tolerance. The image quality, still, is not as good as that obtained with the fifth order aplanatic system.

2.10 SPECIFICATIONS

The focal length of the aplanatic system is now raised to the desired focal length of 1200 inches. For this focal length the paraxial arrangement is computed. The profile equations for the mirrors of the four aplanatic systems are obtained. Tables I and II give for the four aplanatic systems the departure of the mirrors from their respective polar tangent spheres. The semi-aperture of the secondary mirror sufficient to transmit an unvignetted pencil, and the size of the photographic plate required for a given field size is shown in Figure (2.5). The requirements for the 1200 inch focal length objective system are given below.

Paraxial Arrangement

	1	2
c_0	-0.001 inch^{-1}	-.00175206 inch^{-1}
r_0	-1000 inch	-570.75671 inch
t'	-333.52942 inch	
l_f'	66 inch	

Profile Equations of the Mirrors

Primary Mirror

1. Third order aplanat

$$x = -5\times10^{-4}y^2 + 2.166312\times10^{-11}y^4 + 8.416312\times10^{-17}y^6 + 3.390396\times10^{-23}y^8$$

2. Fifth order aplanat

$$x = -5\times10^{-4}y^2 + 2.166312\times10^{-11}y^4 + 9.525045\times10^{-18}y^6 - 5.006387\times10^{-23}y^8$$

3. Hyperboloid aplanat

$$x = -5\times10^{-4}y^2 + 2.166312\times10^{-11}y^4 - 1.877158\times10^{-18}y^6 + 2.033249\times10^{-25}y^8$$

4. Modified hyperboloid aplanat

$$x = -5\times10^{-4}y^2 + 2.162886\times10^{-11}y^4 - 1.871222\times10^{-18}y^6 + 2.023621\times10^{-25}y^8$$

Secondary Mirror

1. Third order aplanat

$$x = -8.760307\times10^{-4}y^2 + 5.055852\times10^{-9}y^4 + 1.655192\times10^{-14}y^6 - 1.2384\times10^{-19}y^8$$

2. Fifth order aplanat

$$x = -8.760307\times10^{-4}y^2 + 5.055852\times10^{-9}y^4 - 4.702980\times10^{-14}y^6 - 3.434153\times10^{-19}y^8$$

3. Hyperboloid aplanat

$$x = -8.760307\times10^{-4}y^2 + 5.055852\times10^{-9}y^4 - 5.835787\times10^{-14}y^6 + 8.420048\times10^{-19}y^8$$

4. Modified hyperboloid aplanat

$$x = -8.760307\times10^{-4}y^2 + 5.055852\times10^{-9}y^4 - 5.835787\times10^{-14}y^6 + 8.420048\times10^{-19}y^8$$

Photographic Plate

Vertex radius of curvature = -171.98857 inches

Profile equation $x = -2.90717 \times 10^{-3}y^2$

TABLE I. PRIMARY MIRROR

Semi-aperture Y in inches	Departure from the polar tangent sphere, dx, in wavelengths (λ = 0.00002165 inches) 3rd order aplanat	5th order aplanat	7th order aplanat	hyperboloid aplanat	modified hyperboloid aplanat
75.0	-215.551	-214.934	-214.937	-214.843	-214.793
67.5	-141.272	-140.944	-140.946	-140.896	-140.863
60.0	-88.111	-87.950	-87.950	-87.926	-87.905
52.5	-51.606	-51.533	-51.533	-51.522	-51.510
45.0	-27.835	-27.806	-27.806	-27.802	-27.796
37.5	-13.415	-13.406	-13.406	-13.404	-13.401
30.0	-5.492	-5.490	-5.490	-5.489	-5.488
22.5	-1.737	-1.737	-1.737	-1.737	- 1.736
15.0	-.343	-.343	-.343	-.343	-.343

TABLE II. SECONDARY MIRROR

Semi-aperture Y in inches	Departure from the polar tangent sphere, dx, in wavelengths (λ = 0.00002165 inches) 3rd order aplanat	5th order aplanat	7th order aplanat	hyperboloid aplanat	modified byperboloid aplanat
27.87228	-160.057	-158.676	-158.691	-158.451	-158.451
25.085052	-104.966	-104.233	-104.239	-104.111	-104.111
22.297824	-65.504	-65.142	-65.145	-65.081	-65.081
19.510596	-38.383	-38.221	-38.222	-38.194	-38.194
16.723368	-20.712	-20.648	-20.648	-20.637	-20.637
13.93614	-9.986	-9.964	-9.964	-9.961	-9.961
11.148912	-4.089	-4.084	-4.084	-4.083	-4.083
8.361684	-1.294	-1.293	-1.293	-1.292	-1.292
5.574456	-.256	-.255	-.255	-.255	-.255
2.787228	-.016	-.016	-.016	-.016	-.016

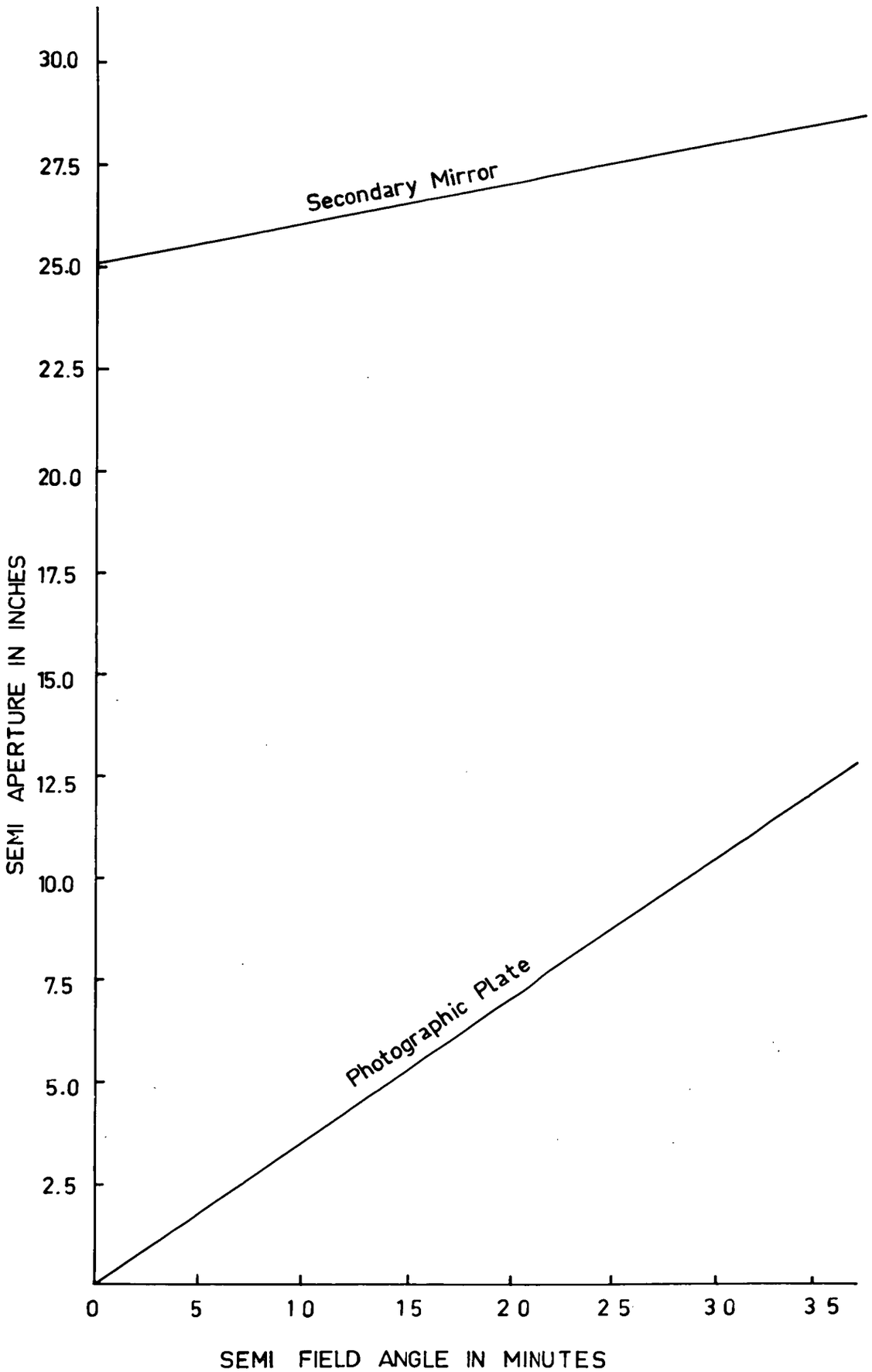
30.0
27.5
25.0
22.5
20.0
17.5
15.0
12.5
10.0
7.5
5.0
2.5
SEMI APERTURE IN INCHES
Secondary Mirror
Photographic Plate
0
5
10
15
20
25
30
35
SEMI FIELD ANGLE IN MINUTES

Fig 2.5

2.11 CONCLUSIONS

A comparative study of the performance of the four aplanatic systems reveal that the fifth order aplanat, modified hyperboloid aplanat, hyperboloid aplanat, and third order aplanat are in that order of merit as regards performance. The fifth order aplanatic system is almost free from spherical aberration and coma. However, the last traces of these two aberrations may be eliminated by correcting the seventh order spherical aberration and circular coma with the help of the third of the extra-axial curvatures of the mirrors. The profiles of the mirrors obtained on this basis indicate that they can scarcely be distinguished from the mirrors of the fifth order aplanatic system. We can, therefore, confidently state that the analysis of the mirrors to obtain images aplanatic to seventh or higher order is not of practical significance, even though, theoretically, it may appear encouraging.

For all practical purposes, where the limitation is put on the image spread only, it appears from the above analysis that the best solution for the two-mirror system may be approximated closely by two hyperboloids. This is rather accidental, and is due to the fact that when such an approximation is made, the higher order extra-axial curvatures of the mirrors are approximately those of the mirrors of the fifth order aplanatic system. The performance of the hyperboloid system may be improved further by the introduction of a small amount of third order spherical aberration to balance the higher order residuals. But it should be noted that the quality of the image obtained with the hyperboloid systems is not as good as that of the fifth order aplanatic system. Inspection of Tables I and II shows that the differences in profile of the mirrors of any of the four aplanats studied amount to about a wavelength at the edges of the mirrors.

CHAPTER III

SECONDARY FOCUS CORRECTORS.

3.1 INTRODUCTION

It was shown in the previous chapter that the focus of the Ritchey-Chretien mirror system is free from spherical aberration and coma, but has considerable astigmatism and petzval curvature of field. The image spread due to these two aberrations is proportional to the square of the angular size of the field. These aberrations must be corrected or reduced if it is desired to increase the size of the field. For this purpose, certain corrector systems have been proposed for addition to the objective near the secondary focus. Some of these consist of lens systems with spherical surfaces (Wynne, 1965, 1968; Rosin, 1966), while others include an aspheric plate (Gascoigne, 1965; Schulte, 1966). The field size is also limited by the availability of large photographic plates. This limitation is particularly important in systems having long focal lengths. The usual practice among astronomers is to regard a total angular field of one degree as the general aim. Some basic considerations which govern the design of the field correctors will be discussed. The advantages and disadvantages in using the Ritchey-Chretien mirror constants as free parameters whilst designing the corrector system are also investigated. One example of each of the two types of correctors will be considered. This chapter is devoted to study the design principles along with the merits and demerits of a corrector system consisting of an aspheric plate and field flattening lens. All the monochromatic aberrations are corrected for the e-line and the system is achromatised for the h- and C-lines, whereas the spot diagrams are given for the spectral range 365 nm - 706 nm, where necessary.

3.2 ASPHERIC PLATE and FIELD FLATTENER.

A negative lens (Piazzi-Smyth field lens), placed a short distance away from the focal plane, may be used to correct the petzval curvature of field of the aplanatic system. The size of the field for good imagery is then limited by astigmatism only. This residual astigmatism may be eliminated (Gascoigne, 1965) by introducing an aspheric plate at a suitable distance in front of the focal plane. The selection of this distance involves a compromise between the asphericity of the plate and the aberrations introduced by the plate. This is discussed in the succeeding sections. The presence of the field flattener introduces some transverse colour. We shall, then, choose the axial power of the aspheric plate to correct the transverse colour introduced by this negative lens. The astigmatism is then corrected by a proper selection of the asphericity of the plate.

The Ritchey-Chretien aplanatic system with corrector is shown in Figure (3.1). Surfaces 4 and 6 are plane surfaces. The curvatures of surfaces 3 and 5 are to be chosen to correct petzval curvature and colour simultaneously. All the parameters of the corrector which are not directly involved in the correction of transverse colour, field curvature and astigmatism will be chosen arbitrarily and within reasonable limits. The petzval curvature coefficient, σ_4, of the whole system per unit focal length (Fig. 3.1) is given by

$$\sigma_4 = \frac{R^2(1-x) - 1 - R}{2(1+Rx)} + \frac{1 - k_3}{2} c_{03} + \frac{1 - k_5}{2} c_{05} \qquad (3.1)$$

The paraxial transverse colour, tch', present in the system is measured by the difference in the paraxial heights of the principal ray intersection points for the h- and C-lines in the paraxial image plane for e-line and is written as

$$tch' = h'_{hk} = h'_{Ck} = l'_{ke}(v'_{kh} - v'_{kC}) + y'_{kC} - y'_{kh} \qquad (3.2)$$

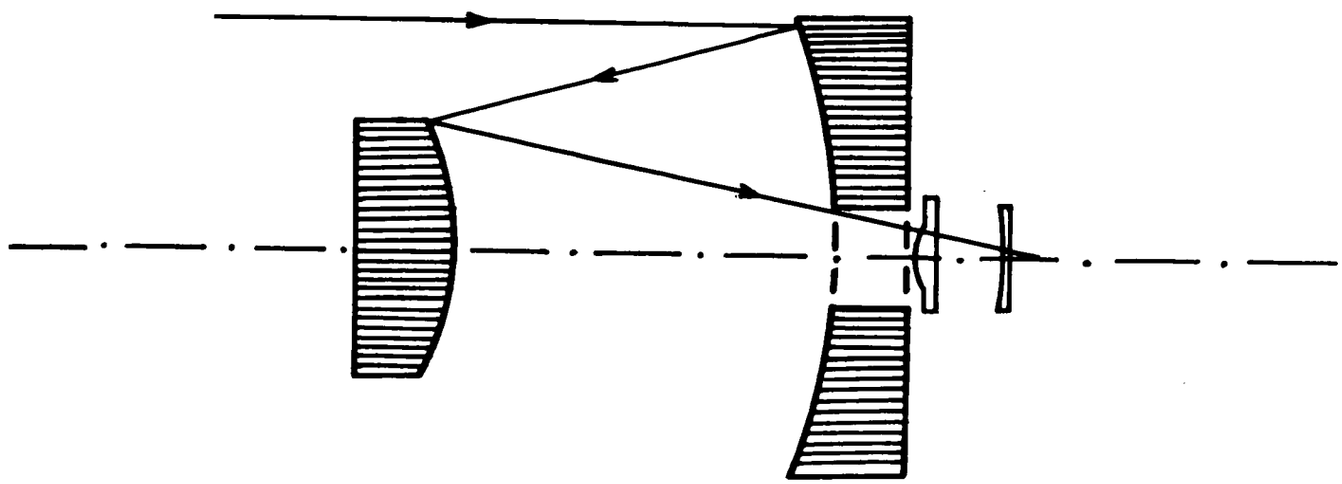

Fig 3.1

Ritchey – chretien mirror system with the corrector

The expressions for $1'_{0ke}$, v'_{kh} , v'_{kC}, y'_{kC}, y'_{kh} in equation (3.2) may be obtained by tracing the following rays through the whole system; (i) a-ray for the e-line with initial coordinates $y_{01} = 1$, $v_{01} = 1/1_{01} = 0$, which provides us with the expression for $1'_{0ke}$; (ii) the b-ray for C-line with initial coordinates $y_1 = p/(1-p/1_{01}) = 0$, $v_1 = 1/(1-p/1_{01}) = 1$. This provides us with the expressions for v'_{kC} and y'_{kC}; (iii) the b-ray for the h-line with initial coordinates same as in (ii) which provides us with the expressions for v'_{kh} and y'_{kh}. Tracing these three rays through the whole system, we obtain

$$
\left.
\begin{aligned}
1'_{0ke} &= y'_{0k}/v'_{0k} \\
y'_{kh} &= a_{1h} - k_{5h}d'_5 v_3 - \{a_{2h} + (k_{4h} - 1)k_{5h}d'_5 y_3\}c_{03} - a_{1h}d'_5(1-k_{5h})c_{05} \\
&\qquad + a_{2h}d'_5(1-k_{5h})c_{03}c_{05} \\
v'_{kh} &= v_3 + (k_{4h}-1)y_3 c_{03} + a_{1h}(k_{6h}-1)c_{05} - a_{2h}(k_{6h}-1)c_{03}c_{05} \\
y'_{kC} &= a_{1C} - k_{5C}d'_5 v_3 - \{a_{2C} + (k_{4C}-1)k_{5C}d'_5 y_3\}c_{03} - a_{1C}d'_5(1-k_{5C})c_{05} \\
&\qquad + a_{2C}d'_5(1-k_{5C})c_{03}c_{05} \\
v'_{kC} &= v_3 + (k_{4C}-1)y_3 c_{03} + a_{1C}(k_{6C}-1)c_{05} - a_{2C}(k_{6C}-1)c_{03}c_{05}
\end{aligned}
\right\} \qquad (3.3)
$$

where

$$
\begin{aligned}
y'_{0k} &= a_{1e} - k_{5e}d'_5 v_{03} - \{a_{2e} + (k_{4e}-1)k_{5e}d'_5 y_{03}\}c_{03} - a_{1e}d'_5(1-k_{5e})c_{05} \\
&\qquad + a_{2e}d'_5(1-k_{5e})c_{03}c_{05} \\
v'_{0k} &= v_{03} + (k_{4e}-1)y_{03}c_{03} + a_{1e}(k_{6e}-1)c_{05} - a_{2e}(k_{6e}-1)c_{03}c_{05}
\end{aligned}
$$

and

$$
\begin{aligned}
a_{1e} &= y_{03} - k_{3e}d'_3 v_{03} - d'_4 v_{05} \\
a_{1h} &= y_3 - k_{3h}d'_3 v_3 - d'_4 v_3 \\
a_{1C} &= y_3 - k_{3C}d'_3 v_3 - d'_4 v_3
\end{aligned}
$$

$$a_{2e} = (1-k_{3e})d_3'y_{03} + (k_{4e}-1)d_4'y_{03}$$

$$a_{2h} = (1-k_{3h})d_3'y_3 + (k_{4h}-1)d_4'y_3 \qquad (3.4)$$

$$a_{2C} = (1-k_{3C})d_3'y_3 + (k_{4C}-1)d_4'y_3$$

$v_{03} = 1$ (power of the aplanatic system considered being unity)

$v_3 = (R+x)/(1+Rx)$

$$y_{03} = \frac{1 + Rx}{1 + R} - d_2'$$

$$y_3 = \frac{x - 1}{R + 1} - \frac{(R + x)}{(1 + Rx)}\ d_2'$$

and the letters e, h, C in the subscript of any quantity indicates that the quantity is meant for that line. Once the air separations and thicknesses are prescribed and the material for the plate and field flattener are chosen, then the coefficient σ_4 and the transverse colour, tch', will be purely functions of c_{03} and c_{05}. Hence, for any required residual values for the petzval curvature and transverse colour (usually zero residuals will be prescribed initially), the paraxial curvatures of surfaces 3 and 5 may be found by solving equations (3.1) and (3.2). We will then be left with astigmatism only.

The coefficient of the third order astigmatism, σ_3, for the whole system per unit focal length is given by

$$\sigma_3 = \frac{(1+x+2R)}{4(1+Rx)} + \sum_{i=3}^{6} q_i^2 S_{0i} + P_3^2\ T_{03} \qquad (3.5)$$

The values of q_i and P_3 may be obtained by tracing the a- and b-rays for the e-line through the whole system. S_{0i} values may be computed from equation (2.12). For any given σ_3 residual value, T_{03} may be obtained from equation (3.5) and then the values of the first of the extra-axial curvatures of the plate (surface 3) may be obtained from the equation

$$\sigma_{i\,3} = T_{03}/(N_3' - N_3)y_{03}^4 \tag{3.6}$$

The unknown residual aberrations per unit focal length of this new objective system are then given by

$$\begin{aligned}
\sigma_1 &= \sum_{i=3}^{6} S_{0i} + T_{03} \\
\sigma_2 &= \sum_{i=3}^{6} q_i S_{0i} + P_3 T_{03} \\
\sigma_3 &= \sum_{i=3}^{6} q_i^3 S_{0i} + P_3^3 T_{03} + \sum_{i=3}^{6} q_i \sigma_{4i} + \frac{(2-3R^2)x^2 + 2R^2 x + R^2 - 2}{4(1 + Rx)^2}
\end{aligned} \tag{3.7}$$

We will now use these equations in the case of the numerical example of Chapter II to add a corrector system to the fifth order aplanat. Choosing quartz as the material to be used for the plate and the field flattener, on account of its transparency, then

$$N_{4e} = N_{6e} = 1.46013;\ N_{4C} = N_{6C} = 1.45642;$$

$$N_{4h} = N_{6h} = 1.47021$$

Placing the plate a short distance behind the primary mirror and the field flattener sufficiently in front of the paraxial focal plane to afford the necessary clearance, we have

$$d_2' = 0.28746866 \qquad d_3' = 0.00125 \qquad d_4' = 0.04104251 \qquad d_5' = 0.0004$$

We shall, however, study the effect of the variation of the distance of the plate, d_2', on the aberrations and on the asphericity of the plate later. For $\sigma_4 = 0$, equation (3.1) gives the relation between c_{03} and c_{05} as

$$c_{05} = -5.7276361 - c_{03} \tag{3.8}$$

Substituting the prescribed values in equations (3.4) and then combining these computed values with equations (3.3), we obtain

$$\left.\begin{aligned} l'_{oke} &= \frac{(-0.00000011\ c_{03}^3 - 0.00088256\ c_{03} + 0.00330253)}{(0.00040338\ c_{03}^2 + 0.02158922\ c_{03} + 0.99058112)} \\ v'_{kC} &= -0.00786793\ c_{03}^2 - 0.00358913\ c_{03} + 4.7626856 \\ y'_{kC} &= 0.00000216\ c_{03}^2 + 0.01723935\ c_{03} - 0.99356192 \\ v'_{kh} &= -0.00834894\ c_{03}^2 - 0.00509929\ c_{03} + 4.84101085 \\ y'_{kh} &= 0.00000227\ c_{03}^2 + 0.01775717\ c_{03} - 0.9935535 \end{aligned}\right\} \quad (3.9)$$

Now for $t_{ph}' = 0$, we obtain from equation (3.2)

$$0.00000854\ c_{03}^4 + 0.21343327\ c_{03}^3 - 11.443951\ c_{03}^2 - 587.23858\ c_{03} + 250.33079 = 0.0 \quad (3.10)$$

Solving equation (3.10) by Newton's method, we obtain

$$c_{03} = 0.42282805$$

and then from equation (3.8)

$$c_{05} = -6.1504642$$

As the paraxial arrangement of the whole system is now known, we trace the two paraxial a- and b-rays through the whole system and compute the values of q_1, S_{01} and P_3. Substituting these values in equation (3.5) and for $\sigma_3 = 0$, we get

$$T_{03} = -0.00322228$$

Then, from equation (3.6), c_{13} is determined as

$$c_{13} = -1637.9$$

The residual aberrations of the whole system are then computed from equations (3.7). The corrector system specifications and the third order aberrations of the objective are given by

$d_2' = 0.28746826$ $d_3' = 0.00125$ $d_4' = 0.04104251$ $d_5' = 0.0004$

$c_{03} = 0.42282805$ $c_{04} = 0.0$ $c_{05} = -6.150464\overline{2}$ $c_{06} = 0.0$

$c_{13} = -1637.9$

$\sigma_1 = -0.0027223$ $\sigma_2 = 0.065291$

$\sigma_3 = 0.0$ $\sigma_4 = 0.0$

$\sigma_5 = 29.13966$

The performance of the fifth order aplanat with the corrector system may then be assessed from the spot diagrams which are shown in Figures (3.2, a-o). These indicate that the addition of the corrector to the fifth order aplanatic system has not as yet improved either the quality of the image or the size of the field. The reason for this is that the corrector system, while correcting the astigmatism and the field curvature, introduces considerable spherical aberration and coma. The spot diagram for V = 0 shows that the corrector introduces spherical aberration equivalent to about 0.288 seconds. The image spread for the object point given by V = 10 minutes amounts to about 0.65 seconds and the shape of the image is comatic. The spherical aberration is continuing its domination in shaping the image. In fact, the general situation would be improved if this corrector were added to the third order aplanatic system, as the fifth order residual aberrations of such a system compensate partially the third order aberrations of the corrector system. But it was shown in the previous chapter that the residual aberrations of the third order aplanat produced poor imagery for off-axial object points. Hence the possibility of the addition of the corrector to the third order aplanatic system is ruled out. This shows that this corrector system in its present arrangement may not be a useful solution for the elimination of astigmatism and field curvature. However, it is worth trying to reduce the aberrations of the plate, if possible, by an alteration of the plate's position before coming to any conclusions.

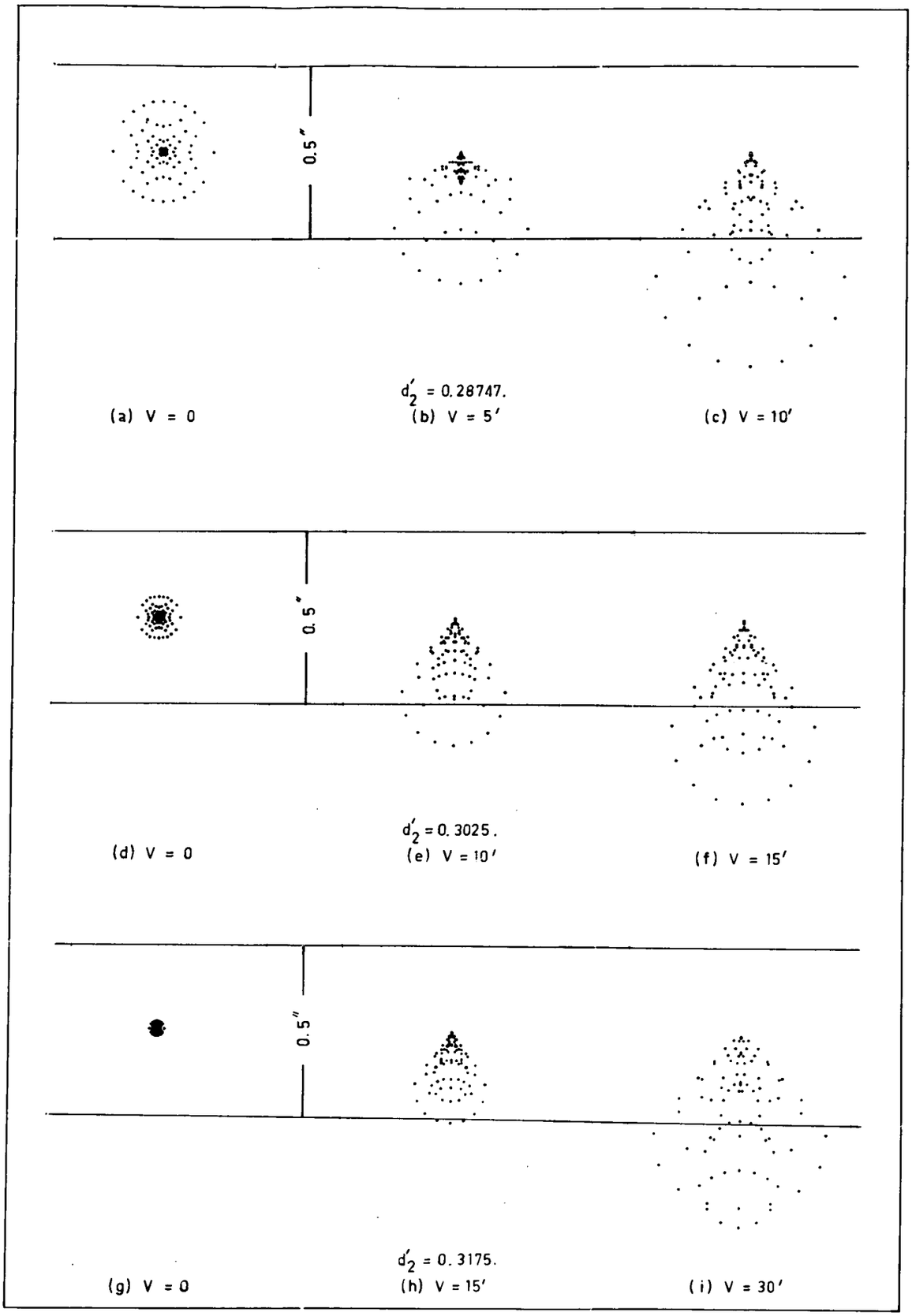

Fig 3.2

SPOT DIAGRAMS FOR THE RITCHEY – CHRETIEN SYSTEM WITH THE CORRECTOR

3.3 EFFECT of the DISTANCE of the PLATE

The effects of changes in the distance of the plate from the vertex of the secondary mirror, d_2', on the aberrations introduced by the plate and on its asphericity are now investigated. Corresponding to an increase or decrease in d_2', the distance between the plate and the field flattener, d_4', has also to be adjusted accordingly. The distance, d_2', is changed twice and the whole procedure of section (3.2) is repeated to obtain two more corrector system arrangements for the correction of colour, field curvature and astigmatism. The second and third arrangements for the corrector along with the third order aberrations for the objective system are:

(2) $d_2' = 0.3025$ $d_3' = 0.00125$ $d_4' = 0.02604251$ $d_5' = 0.0004$

$c_{03} = 0.65794614$ $c_{04} = 0.0$ $c_{05} = -6.3855823$ $c_{06} = 0.0$

$c_{13} = -3485.4486$

$\sigma_1 = -0.00111$ $\sigma_2 = 0.042181$

$\sigma_3 = 0.0$ $\sigma_4 = 0.0$

$\sigma_5 = 44.165$

(3) $d_2' = 0.3175$ $d_3' = 0.00125$ $d_4' = 0.01104251$ $d_5' = 0.0004$

$c_{03} = 1.5111767$ $c_{04} = 0.0$ $c_{05} = -7.2388128$ $c_{06} = 0.0$

$c_{13} = -12080.171$

$\sigma_1 = -0.00035382$ $\sigma_2 = 0.020686$

$\sigma_3 = 0.0$ $\sigma_4 = 0.0$

$\sigma_5 = 85.544$

These results are plotted in Figure (3.3).

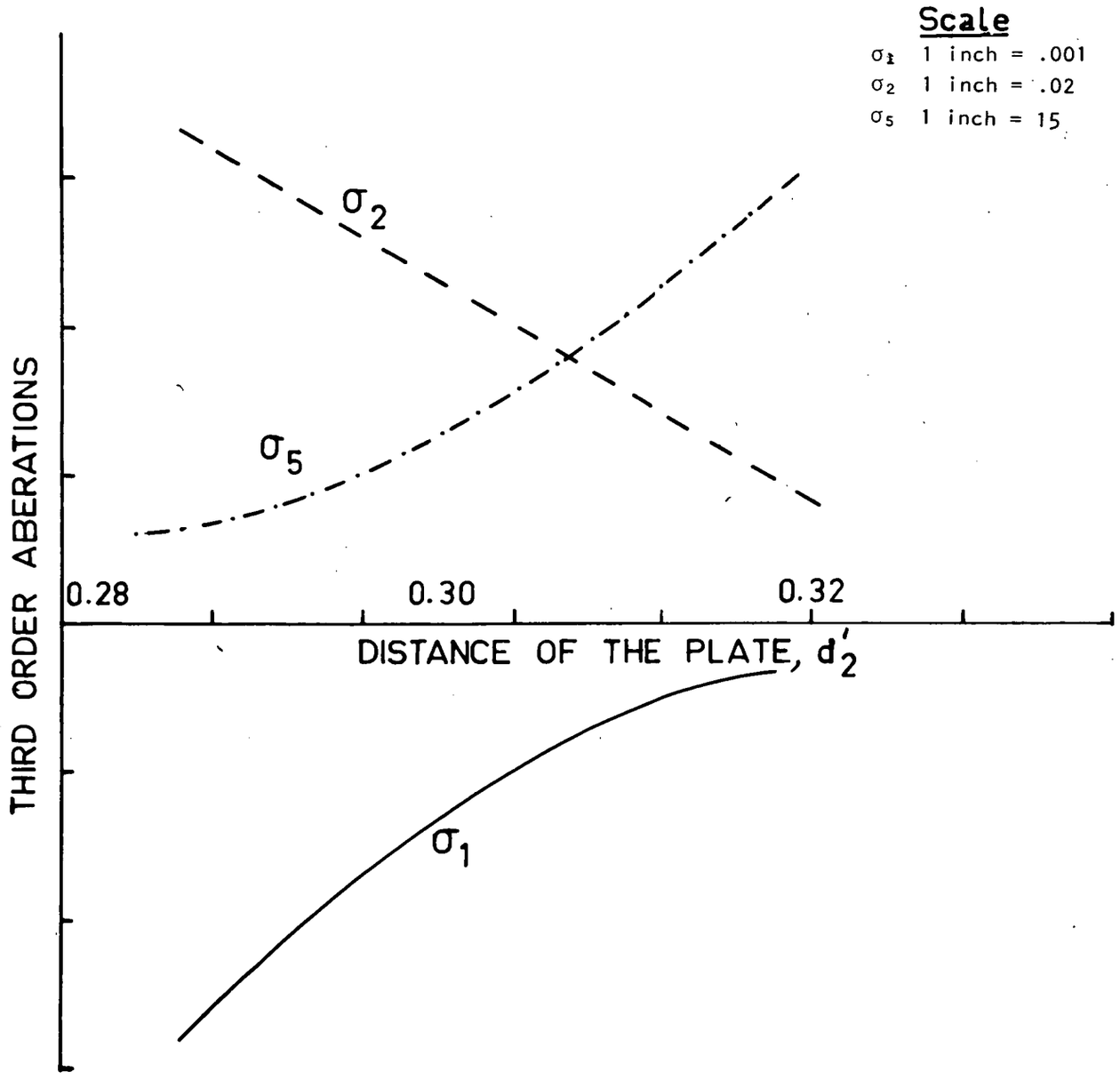

Fig 3.3

Variation of aberration with distance of the plate, d'_2

These two corrector systems are again added to the fifth order aplanatic system and the spot diagrams, obtained in these cases are shown in Figures (3.2,d-i). For the second arrangement, the spot diagram for V = 0 indicates that the spherical aberration is reduced to 0.123 seconds of arc. This is further reduced to 0.041 seconds for the third arrangement. The spot diagrams for the extra-axial object points illustrate that there is considerable reduction in coma. As a result of these reductions, the field size for the prescribed tolerance (0.5 seconds of arc), also increases. For the second arrangement, the semi-field covered by the system for the same tolerance will be about 14 minutes. This shows that the sizes of the field covered by the fifth order aplanatic system and the fifth order aplanatic system with corrector are almost the same. But it should be remembered that the fifth order aplanatic system produces very good images on a curved surface, whereas the fifth order aplanat with the corrector system produces comatic images of about the same size on a plane surface. In this way, the two systems are not comparable.

In the third arrangement at a semi-field angle of 30 minutes, the image spread amounts to about 0.543 seconds and the corresponding spot diagram illustrates that the shape of the image is not only governed by the effect of coma but also by higher order astigmatism.

A comparison of the values of the first of the extra-axial curvatures of the plate for the three corrector arrangements indicates that the asphericity of the plate increases rapidly as the distance between the plate and the back focus decreases. This is shown clearly in Figures (3.4), which give the departure of the surface from its polar tangent sphere for different semi-apertures for the three corrector arrangements. The asphericity of the surface for the second and third arrangements is about twice and seven times that of the plate for the first arrangement respectively. For a semi-aperture of 7.5 inches,

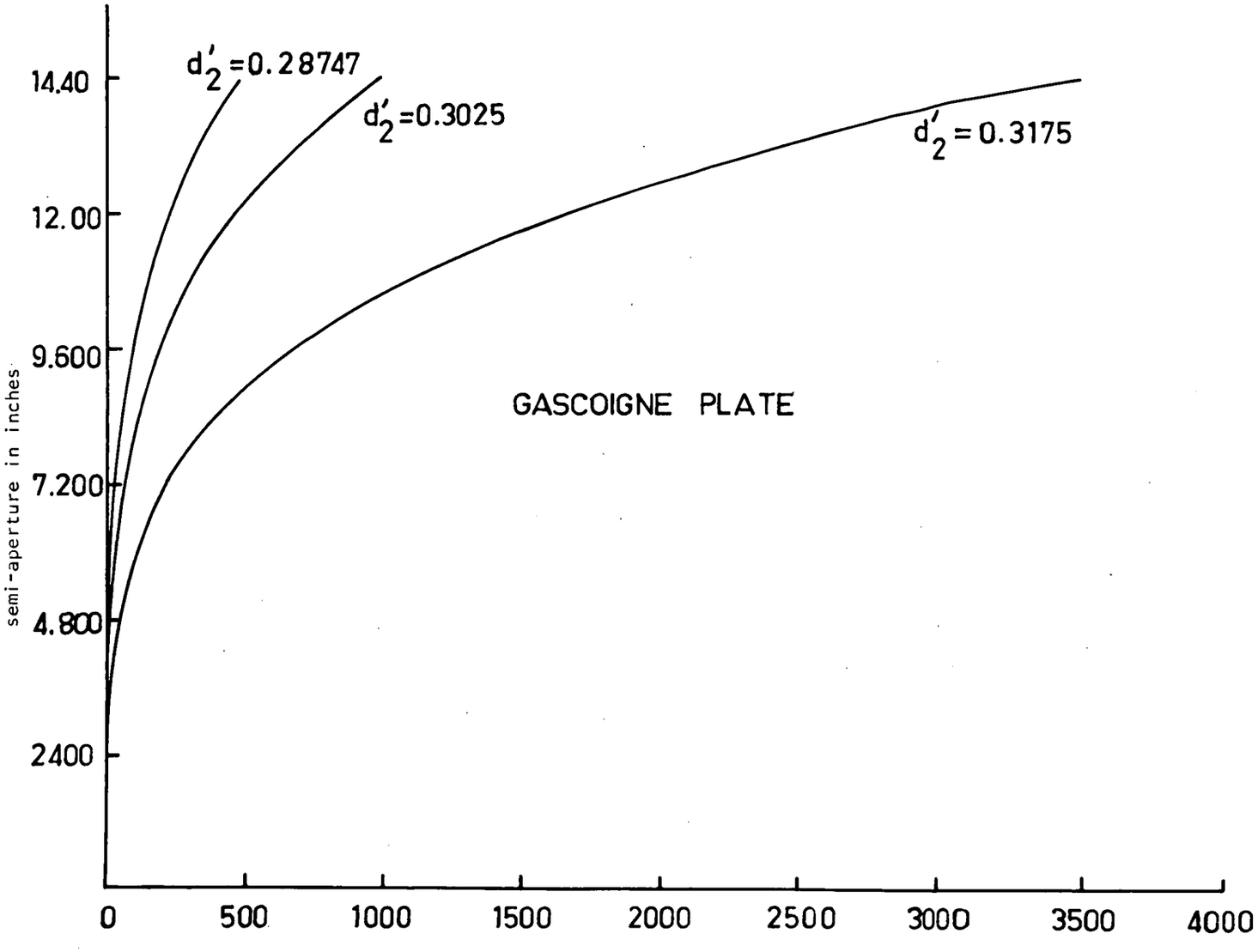

Variation of asphericity of the plate with distance, d'_2

Fig 3.4

the departure of the surface from its polar tangent sphere for the three arrangements is (i) 38λ, (ii) 78λ, (iii) 260λ respectively, λ being equal to 0.00002165 inches.

The effects of the change in the distance of the plate, d_2', on the aberrations introduced by the corrector for (i) $\rho = 0.0625$, $\bar{H} = 0.00435$; (ii) $\rho = 0.0625$, $\bar{H} = 0.0087$ are shown in Figures (3.5 a-b). These figures illustrate that both the third order spherical aberration and coma reduce considerably as the plate approaches the focus. The spherical aberration introduced by the plate for the third arrangement of the corrector amounts to only one-thirteenth of the prescribed tolerance and the coma spread amounts to less than half the tolerance for a semi-field angle of 15 minutes, which increases to about the tolerance value of 0.5 seconds of arc for the semi-field of 30 minutes. Of the fifth order aberrations, spherical aberration and circular coma are negligible. The fifth order cubic astigmatism is reasonably stable with a change in the distance of the plate. Cubic coma and linear astigmatism increase considerably when the distance between the plate and the back focus decreases. For the semi-field of 15 minutes, the contribution of these aberrations is insignificant. But the increase in the contribution of these aberrations becomes pronounced when the field is doubled. This is due to the fact that the cubic coma and linear astigmatism are respectively proportional to the third and fourth powers of the field size. The fifth order cubic astigmatism, being opposite in sign compensates partially the linear astigmatism. As compared to the large reduction obtained in the third order spherical aberration and coma, the increase in the fifth order aberrations is not discouraging. However, the fifth order residual astigmatism may be balanced by introducing a small third order residual astigmatism. This, however, does not reduce the image spread much as the advantage gained by this compensation

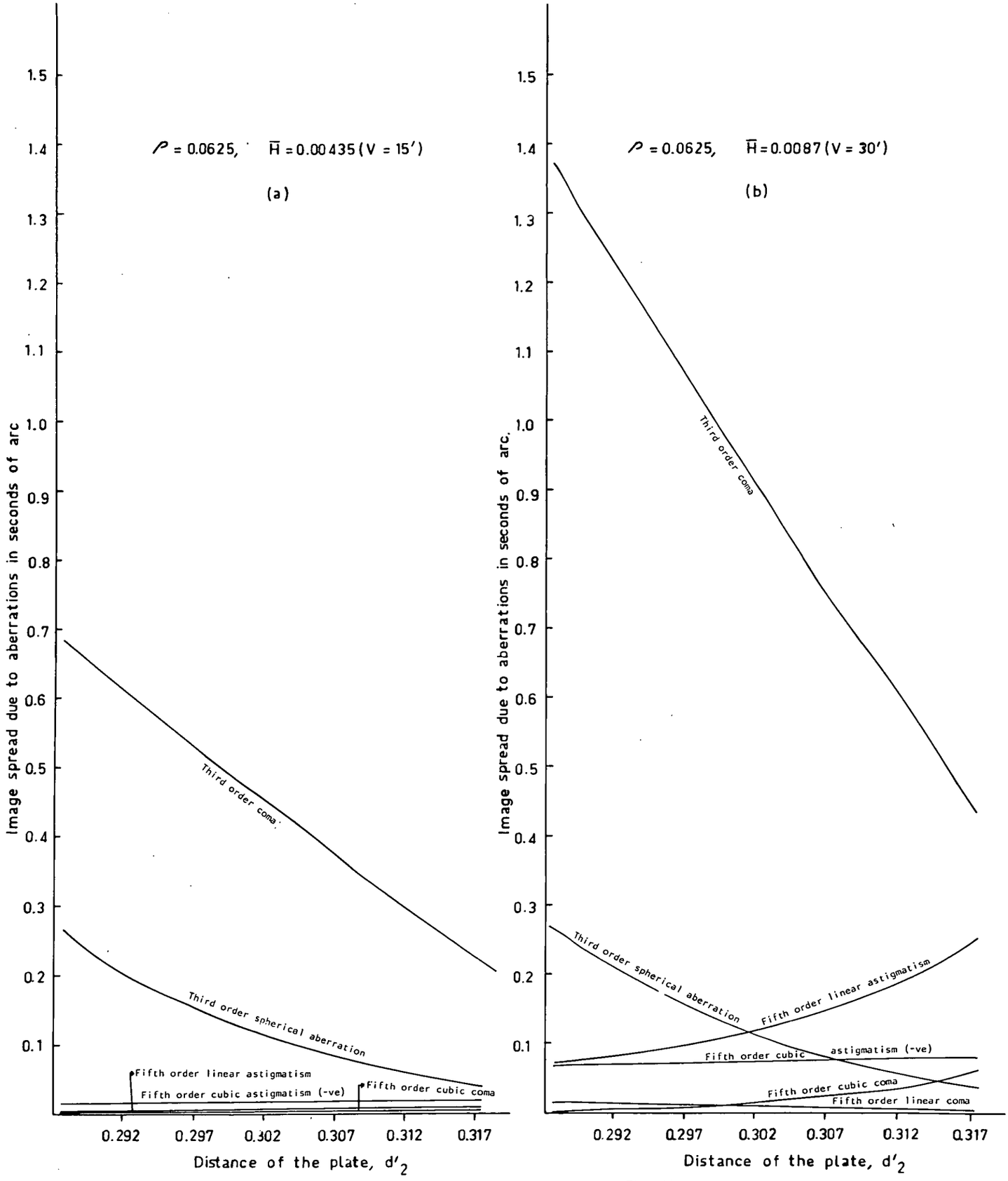

VARIATION OF ABERRATION WITH, d'_2

Fig 3.5

is offset partially by the increase in the third order coma and fifth order cubic coma. With the astigmatism balanced, we will be left with almost comatic imagery. Hence, it should be noticed that the selection of the distance of the plate, d_2', depends mostly on the limitation put to the asphericity of the plate than on the higher order aberrations. It appears from the above analysis that this type of corrector system may not be very useful unless astronomers are not concerned about the type of energy distribution within the prescribed circle (0.5").

The requirements for the third corrector arrangement which is to be used with the 1200- inch focal length Ritchey-Chretien telescope objective are computed and are given below. All the parameters are expressed in inch units.

Paraxial Arrangement

$d_2' = 381.0$

	3	4	5	6
c_0	0.00125931	0.0	-0.00603234	0.0
r_0	794.08565	∞	-165.77315	∞
d'	1.5	13.251012	0.48	

Profile equation: Aspheric Plate

$$x = 6.2965696 \times 10^{-4} y^2 - 1.7474603 \times 10^{-8} y^4 - 2.7714455 \times 10^{-12} y^6 + 1.1535565 \times 10^{-16} y^8$$

TABLE I.

ASPHERIC PLATE

Y	dx
12.0	1674.08
10.8	1098.368
9.6	685.702
8.4	401.942
7.2	216.955
6.0	104.625
4.8	42.854
3.6	13.559
2.4	2.678
1.2	0.167

Y = semi-aperture

dx = departure of the aspheric surface from its polar tangent sphere in wavelengths (λ = 0.00002165)

CHAPTER IV

ANASTIGMAT OBJECTIVES

4.1 ANASTIGMATS.

It was shown in the previous chapter that a corrector system consisting of an aspheric plate and field flattening lens can be used to correct the astigmatism and the field curvature inherent in the two-mirror aplanatic objective. It was noticed that such a corrector system used with a pure aplanatic objective introduces considerable positive coma and spherical aberration which cause the image quality to deteriorate. It was also noted that for different corrector arrangements, these aberrations become smaller as the distance between the plate and the focus decreases, while the required asphericity of the plate and the higher order aberrations increase. Gascoigne (1965) has stated that the telescope objective may be corrected for third-order spherical aberration, coma and astigmatism simultaneously by allowing the Ritchey-Chretien mirror constants to be free parameters, and on this basis Schulte (1966) developed the optical design of a 152 centimetre objective with very encouraging results. The asphericities of the mirrors and the plate may be chosen to correct simultaneously spherical aberration, coma, and astigmatism, while the paraxial set up of the corrector makes the system free from transverse colour and petzval curvature. The resultant system is called an anastigmatic objective. Accordingly, we may now develop anastigmatic objectives, corresponding to the different aplanatic objectives of Chapter II. It should be noted that the two-mirror objective without the corrector no longer gives aplanatic images at the secondary focus. The development of the anastigmatic objective is considered for only one specified paraxial arrangement of the correcting system, and as the asphericity of the plate and the higher order aberrations are quite small for the first corrector arrangement, we select this paraxial arrangement for the anastigmat.

4.2 THIRD-ORDER ANASTIGMAT.

Once the air separations, thicknesses, and material for the field flattener and plate are chosen, the axial curvatures of surfaces 3 and 5 (Fig. 3.1) may be found by employing the procedure of section (3.2) for colour and petzval sum correction. We will then find the first of the extra-axial curvatures c_1 of the mirrors and plate to correct third-order spherical aberration, coma and astigmatism. The third-order aberration coefficients σ_1, σ_2, σ_3 per unit focal length are given by

$$\sigma_1 = \sum_{i=1}^{6} S_{0i} + \sum_{i=1}^{3} T_{0i} \tag{4.1}$$

$$\sigma_2 = \sum_{i=1}^{6} q_i S_{0i} + \sum_{i=1}^{3} P_i T_{0i} \tag{4.2}$$

$$\sigma_3 = \sum_{i=1}^{6} q_i^2 S_{0i} + \sum_{i=1}^{3} P_i^2 T_{0i} \tag{4.3}$$

Solving equations (4.1) - (4.3) for T_{01}, T_{02}, T_{03} and substituting $P = 0$, we obtain

$$T_{01} = R_1 - \frac{R_3 - P_3 R_2}{P_2^2 - P_2 P_3} - \frac{R_3 - P_2 R_2}{P_3^2 - P_2 P_3}$$

$$T_{02} = \frac{R_3 - P_3 R_2}{P_2^2 - P_2 P_3} \tag{4.4}$$

$$T_{03} = \frac{R_3 - P_2 R_2}{P_3^2 - P_2 P_3}$$

where,
$$R_1 = \sigma_1 - \sum_{i=1}^{6} S_{0i}$$
$$R_2 = \sigma_2 - \sum_{i=1}^{6} q_i S_{0i} \qquad (4.5)$$
$$R_3 = \sigma_3 - \sum_{i=1}^{6} q_i^2 S_{0i}$$

The first of the extra-axial curvatures are then given by

$$c_{1i} = T_{0i}/(N_i' - N_i)y_{0i}^4 \qquad (4.6)$$

Once the paraxial arrangement of the system is known, we can compute q_i, S_{0i}, P_2, P_3 as mentioned earlier. Then finding the extra-axial curvatures for any given residual values of σ_1, σ_2, σ_3 is a simple procedure.

Returning now to the numerical example, if the first corrector arrangement is chosen to combine with the aplanatic system, from section (3.2) we have

	1	2	3	4	5	6
c_0	-1.2	-2.1024735	0.4228280 5	0.0	-6.1504642	0.0
d'	-0.27794118	0.28746866	0.00125	0.04104251	0.0004	0.0

quartz being the material chosen for the plate and the field flattener. The trace of a- and b-rays provides us with

$$\sum_{i=1}^{6} S_{0i} = 1.05496071 \qquad \sum_{i=1}^{6} q_i S_{0i} = 0.81367824$$
$$\sum_{i=1}^{6} q_i^2 S_{0i} = 0.58805695$$

$$P_2 = -0.83480568 \qquad P_3 = -19.822585$$

For $\sigma_1 = 0 = \sigma_2 = \sigma_3$, equations (4.4) and (4.5) then give

$$T_{01} = -2.10623698 \qquad T_{02} = 1.05464334 \qquad T_{03} = -0.00336711$$

We then obtain from equation (4.6) the values for the extra-axial curvatures as

$$c_{11} = 1.0531184\text{9} \qquad c_{12} = 42.914665 \qquad c_{13} = -1711.5171$$

The third-order anastigmat is now submitted to analysis by ray tracing. The spot diagrams (Figs. 4.1 a-d) are obtained for (i) V = 0, (ii) V = 10 minutes, (iii) V = 20 minutes, and (iv) V = 30 minutes. The spot diagram corresponding to V = 0 indicates that the system suffers from higher order spherical aberration equivalent to 0.267 seconds. The system covers about 30 minutes semi-field for the 0.5 seconds image spread tolerance. But the image shape is typically comatic, modified somewhat by spherical aberration.

Figures (4.2a), (4.2b) represent respectively the actual intersection loci for the zones corresponding to the maximum aperture and 0.707 times the maximum aperture, whereas Figures (4.2c), (4.2d) represent the corresponding predicted loci. The predicted locus is obtained by taking the aberration coefficients μ_1, μ_2, μ_3 into consideration. A comparison of the predicted and the actual loci for the two zones illustrates that such poor image quality for the third-order anastigmat is mostly due to the presence of the fifth-order spherical aberration and linear coma in the objective. Considerable reduction in the image spread should therefore be possible if the coefficients μ_1, μ_2, μ_3 are either corrected or reduced, and the next step in the process of improving the image quality will obviously be to reduce the effect of μ_1, μ_2, μ_3.

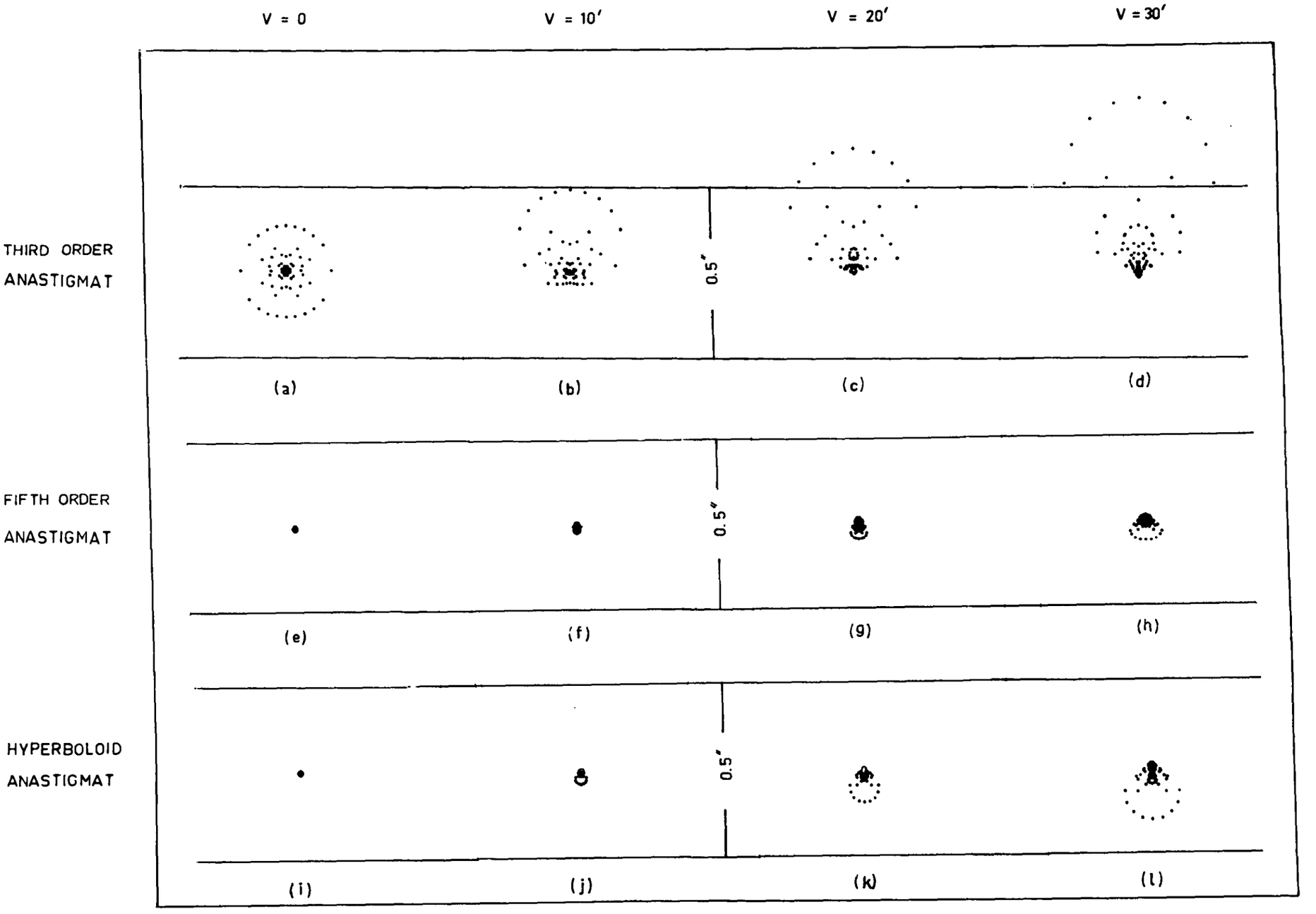

Fig 4.1

SPOT DIAGRAMS FOR CASSEGRAIN TYPE ANASTIGMAT

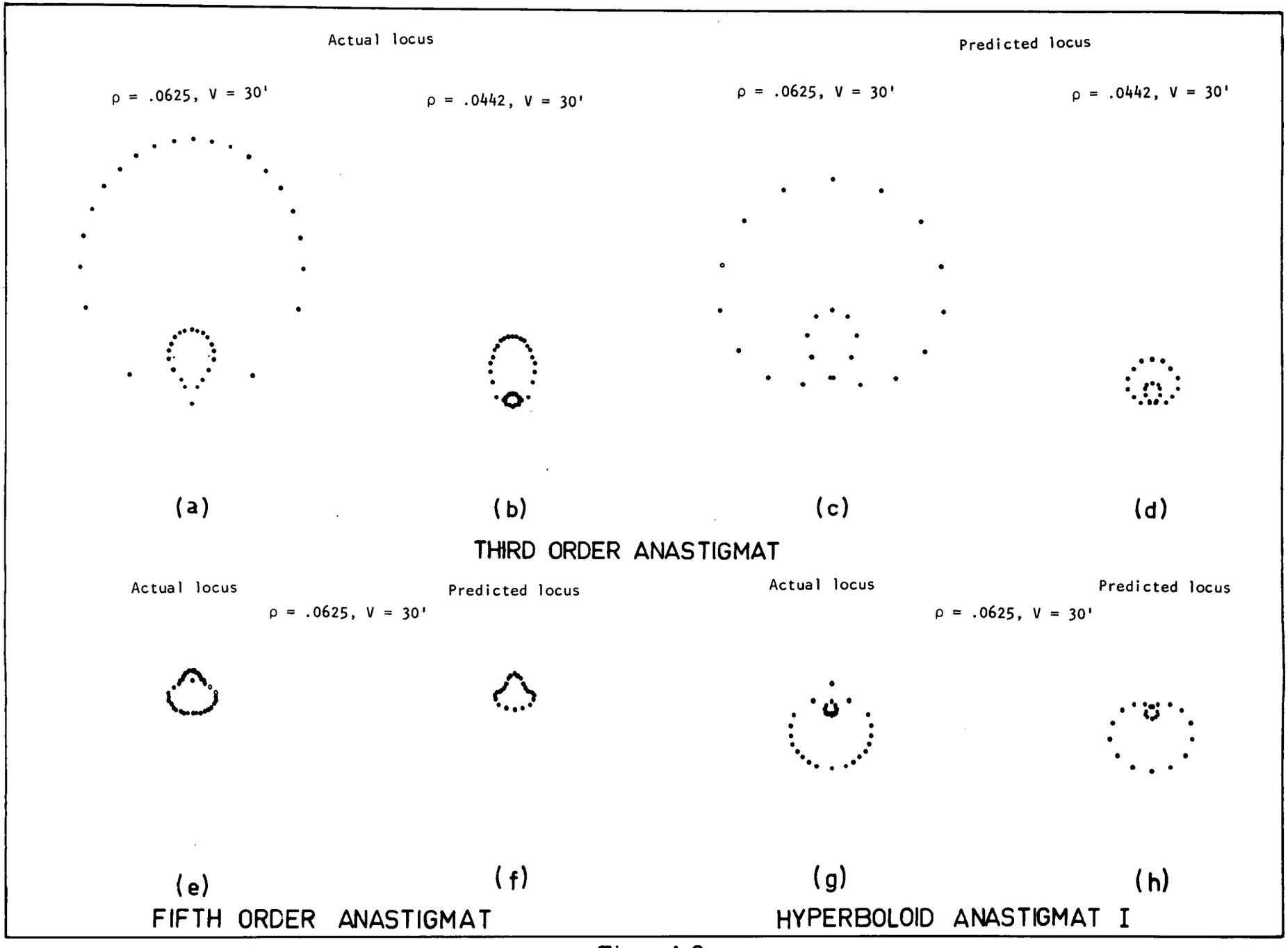

Fig 4.2

PREDICTED AND ACTUAL LOCI FOR ANASTIGMATS

4.3 FIFTH-ORDER ANASTIGMAT.

Based on the last comment of the previous section we will now attempt to reduce the effect of the coefficients μ_1, μ_2, μ_3 by the use of the second of the extra-axial curvatures of the mirrors c_{21}, c_{22}. As the third-order aberrations of the two mirrors are still small, we can use equations (2.38), (2.40) of Chapter II to find c_{21}, c_{22} which provide μ_1, μ_2, μ_3 correction. It is sufficient if we make $\mu_1 = 0$ and leave a small negative residual for μ_2 and μ_3 for the mirrors as the other members of the anastigmat objective contribute negligible spherical aberration and very small positive fifth-order linear coma. Returning now to the numerical example, for $\mu_1 = 0$, $\mu_2 = -0.27$, and substituting the new values of c_{11}, c_{12} in equations (2.39), (2.41), and then from equations (2.38), (2.40), we obtain the values of c_{21}, c_{22} as

$$c_{21} = -1.0911112 \qquad c_{22} = -1037.0176$$

With these values of the extra-axial curvatures, the fifth-order anastigmat objective provides images free from spherical aberration up to fifth-order, circular coma up to fifth-order, third-order astigmatism and petzval curvature, and presumably colour.

The spot diagrams for (i) V = 0, (ii) V = 10 minutes, (iii) V = 20 minutes, and (iv) V = 30 minutes are obtained for the fifth-order anastigmat and are shown in Figures 4.1 e-h. The spot diagrams show remarkable improvement in the image quality. The image spread for axial and extra-axial object points is negligible as compared to the prescribed tolerance. Even at V = 30 minutes, the image spread amounts to 0.075 seconds only. The actual locus of the intersection points for the maximum aperture zone for V = 30 minutes, (Fig. 4.2e) and the predicted locus, obtained on the basis of fifth-order aberrations, (Fig.4.2f),

illustrate that this small image spread is mostly due to the fifth-order linear and cubic astigmatism with a small amount of cubic coma. The image spread can be reduced still further to an insignificant size by balancing the present residual aberrations with small residual third-order astigmatism and fifth-order linear coma. This kind of analysis is made while considering the mirrors as hyperboloids in the next section.

4.4 HYPERBOLOID ANASTIGMATS.

While considering the development of the hyperboloid aplanat objective, it was noticed that the fifth-order spherical aberration and linear coma reduce considerably in magnitude when the mirrors are considered as hyperboloids and the modified hyperboloid aplanat objective, for which spherical aberration is corrected to fifth-order, improves the image quality further. We will therefore consider firstly the development of an hyperboloid anastigmat I objective, which is corrected for spherical aberration to fifth-order, whereas coma and astigmatism are corrected to third-order. The secondary mirror of this objective will have the same axial and the first extra-axial curvatures as that of the third-order anastigmat and, being an hyperboloid, defines the other curvature coefficients. We can use equations (2.44), (2.45), (2.46) of Chapter II to find the eccentricity of the primary mirror, which provides spherical aberration correction to fifth-order for the hyperboloid mirrors only, but, as the other members of the anastigmat contribute negligible fifth-order spherical aberration, we obtain an anastigmat for which spherical aberration is corrected to fifth-order. Once the eccentricity is found and as the axial curvature is known, we can obtain from equation (1.11) of Chapter I all the other curvature coefficients for the primary mirror also. Proceeding in this way, we get for the numerical example,

$e_1 = 1.01386284$ $c_{1,1} = 1.0527954$ $c_{2,1} = -1.3854726$ $c_{3,1} = 2.0258599$

$e_2 = -2.1024735$ $c_{1,2} = 42.914665$ $c_{2,2} = -1313.9299$ $c_{3,2} = 44698.826$

The specifications for the other members of the anastigmat remain the same as that of the other anastigmats obtained before.

Figures (4.1i) - (4.1l), which give the spot diagrams for the hyperboloid anastigmat, show the improvement in the reduction of the image spread as compared with that of the third-order anastigmat. The image spread for the maximum field amounts to 0.16 seconds only. The spherical aberration present in the system is negligible as compared with the tolerance. The comatic shape of the image is modified by astigmatism. To confirm this view, and to know exactly what higher order aberrations are present, the actual locus of the intersection points for the maximum aperture zone (Fig. 4.2g) is obtained. The close resemblance of this locus with the predicted locus (Fig. 4.2h), obtained by the use of third- and fifth-order aberration coefficients, indicates that the image shape of the hyperboloid anastigmat I is mostly governed by the fifth-order linear and cubic coma and also by the linear and cubic astigmatism.

We shall now consider the development of the hyperboloid anastigmat II. The fifth-order spherical aberration, coma and linear astigmatism of this anastigmat are balanced by the introduction of corresponding residual third-order spherical aberration, coma and astigmatism. To study the effect of the change in the paraxial transverse colour on the monochromatic fifth-order aberrations which is necessary for prescribing residual monochromatic aberrations, while considering colour correction, a small residual value is introduced by changing arbitrarily the axial curvature of surface 3. It is later noticed that such a change does not affect the fifth-order aberrations

much. The balancing of the aberrations is made at the maximum aperture and at the edge of the field. The residual values for σ_1, σ_2, σ_3 required to balance the fifth-order aberrations are found from the equations

$$\begin{aligned} &\sigma_1 \rho^3 + \mu_1 \rho^5 = 0 \\ &2\sigma_2 \rho^2 \bar{H} + \mu_2 \rho^4 \bar{H} + \mu_7 \rho^2 \bar{H}^3 = 0 \\ &3\sigma_3 \rho \bar{H}^2 + \mu_{10} \rho \bar{H}^4 = 0 \end{aligned} \qquad (4.7)$$

Returning now to the numerical example, c_{03} is changed from 0.42282805 to 0.42614443 and, correspondingly, c_{05} is changed from -6.1504642 to -6.1537806 to retain field curvature correction. The a- and b-rays are then traced through the whole system and the values of

$$\sum S_{0i}, \quad \sum q_i S_{0i}, \quad \sum q_i^2 S_{0i}, \quad P_2 \text{ and } P_3$$

are computed. The third-order residuals σ_1, σ_2, σ_3 required to compensate the effect of the fifth-order coefficients μ_1, μ_2, μ_{10} are obtained from equations (4.7). Equations (4.4) - (4.6) then give

$$c_{11} = 1.05654525 \qquad c_{12} = 43.221034 \qquad c_{13} = -1722.08$$

The curvature coefficients of the mirrors are obtained as

$$\begin{aligned} c_{01} &= -1.2 & c_{11} &= 1.05654525 & c_{21} &= -1.39535983 & c_{31} &= 2.0475844 \\ c_{02} &= -2.1024735 & c_{12} &= 43.221034 & c_{22} &= -1332.7572 & c_{32} &= 45662.997 \end{aligned}$$

Figures (4.3 a-d) show the corresponding spot diagrams. The spot diagrams are also obtained for C, F, h lines and Figures (4.3 e-p) represent these spot diagrams. The spot diagrams for the e-line show considerable improvement in the image quality. There is some variation of distortion with wavelength. The system has some marginal transverse colour. The total image spread due to the whole spectrum, 656.3 nm - 400 nm, amounts to about 0.366 seconds of arc for the maximum field. The colour correction and a further improvement in the reduction of the

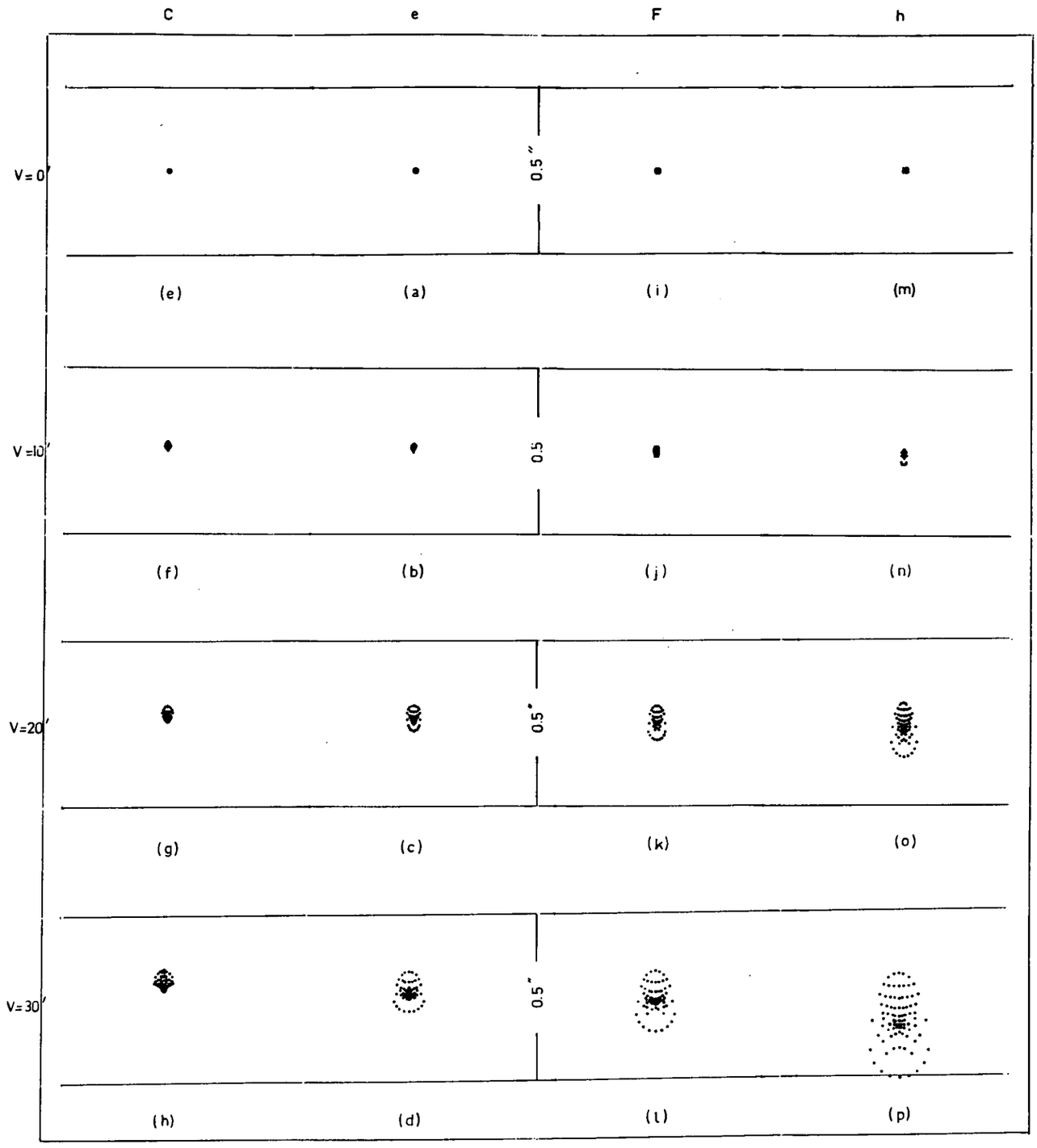

Fig 4.3

SPOT DIAGRAMS FOR THE HYPERBOLOID ANASTIGMAT II

image spread is considered, and the objective for which this is done will be called the hyperboloid anastigmat III, for which the process of development is given below.

For V = 30 minutes, it is found that the marginal transverse colour present in the system is

$$H'_{hk} - H'_{Ck} = 0.00000058$$

Therefore we prescribe the residual paraxial transverse colour as

$$h'_{hk} - h'_{Ck} = -0.00000058$$

which residual is supposed to give colour correction at the edge of the field. Therefore, the value of t'_{ch} in equation (3.2) becomes

$$t'_{ch} = -0.00000058/0.0087 = -0.00006666$$

This is required as the t'_{ch} of equation (3.2) corresponds to unit semi-field angle. With this residual lateral colour the axial curvatures of surfaces 3 and 5 are found from equations (3.1), (3.2), to obtain field curvature correction and lateral colour correction at the edge of the field, as

$$c_{03} = 0.53448654 \qquad c_{05} = -6.26212268$$

The σ_3 residual required for the system is computed from the equation

$$3\sigma_3\rho\bar{H}^2 + \mu_{1\,0}\rho\bar{H}^4 + (\mu_4+\mu_6)\rho^3\bar{H}^2 = 0 \qquad (4.8)$$

whereas the σ_1, σ_2 residuals required are found from equation (4.7), and with these residuals the extra-axial curvatures of the mirrors and the plate are determined by adopting a similar procedure used in the development of hyperboloid anastigmat II. Arranging the calculated values together, we have

c_{01} = -1.2 c_{11} = 1.0548921 c_{21} = -1.3909966 c_{31} = 2.0379879

c_{02} = -2.1024735 c_{12} = 43.074204 c_{22} = -1323.7173 c_{32} = 45199.198

c_{03} = 0.53448654 c_{13} = -1682.2546

c_{05} = -6.26212268

The spot diagrams for the hyperboloid anastigmat III (Figs. 4.4 a-p) show considerable improvement in the image quality and the colour is corrected fully at the edge of the field. There is small longitudinal colour present in the system. The image spread for the whole spectrum, 656.3 nm - 400.0 nm, up to the maximum field angle amounts to about 0.186 seconds only. This shows remarkable improvement in the image quality as compared with the hyperboloid anastigmat II. The spot diagrams illustrate that there is some variation of astigmatism and coma with wavelength. A small introduction of negative coma for e-line seems to be useful in reducing the image spread for the whole spectrum.

4.5 SPECIFICATIONS.

The specifications for the 1200-inch focal length fifth-order anastigmat II and the hyperboloid anastigmat III telescope objectives are given below. All the parameters are expressed in inch units. The symbols Y, dx represent respectively the semi-aperture and the departure of a surface from its polar tangent sphere.

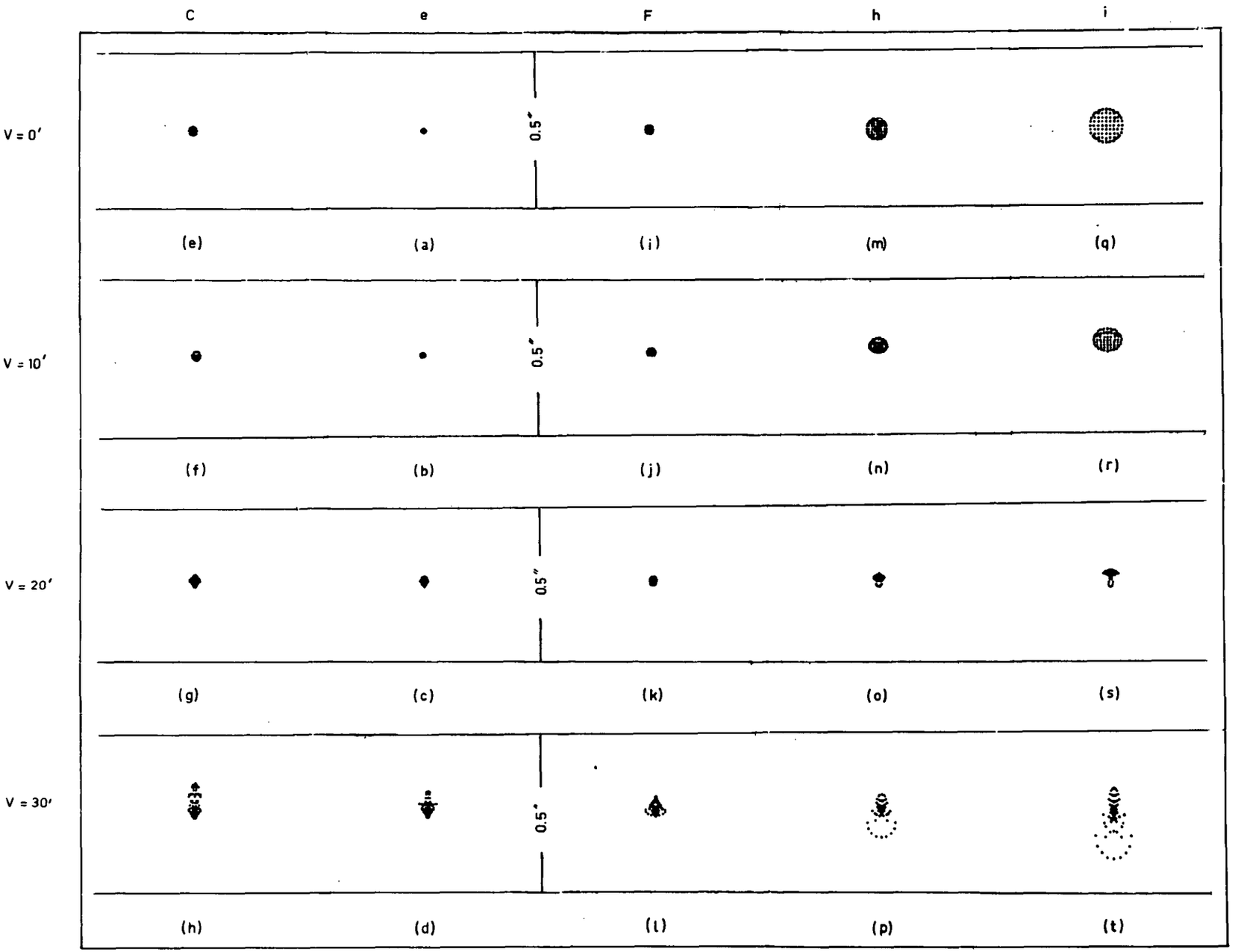

Fig 4.4

SPOT DIAGRAMS FOR THE HYPERBOLOID ANASTIGMAT III

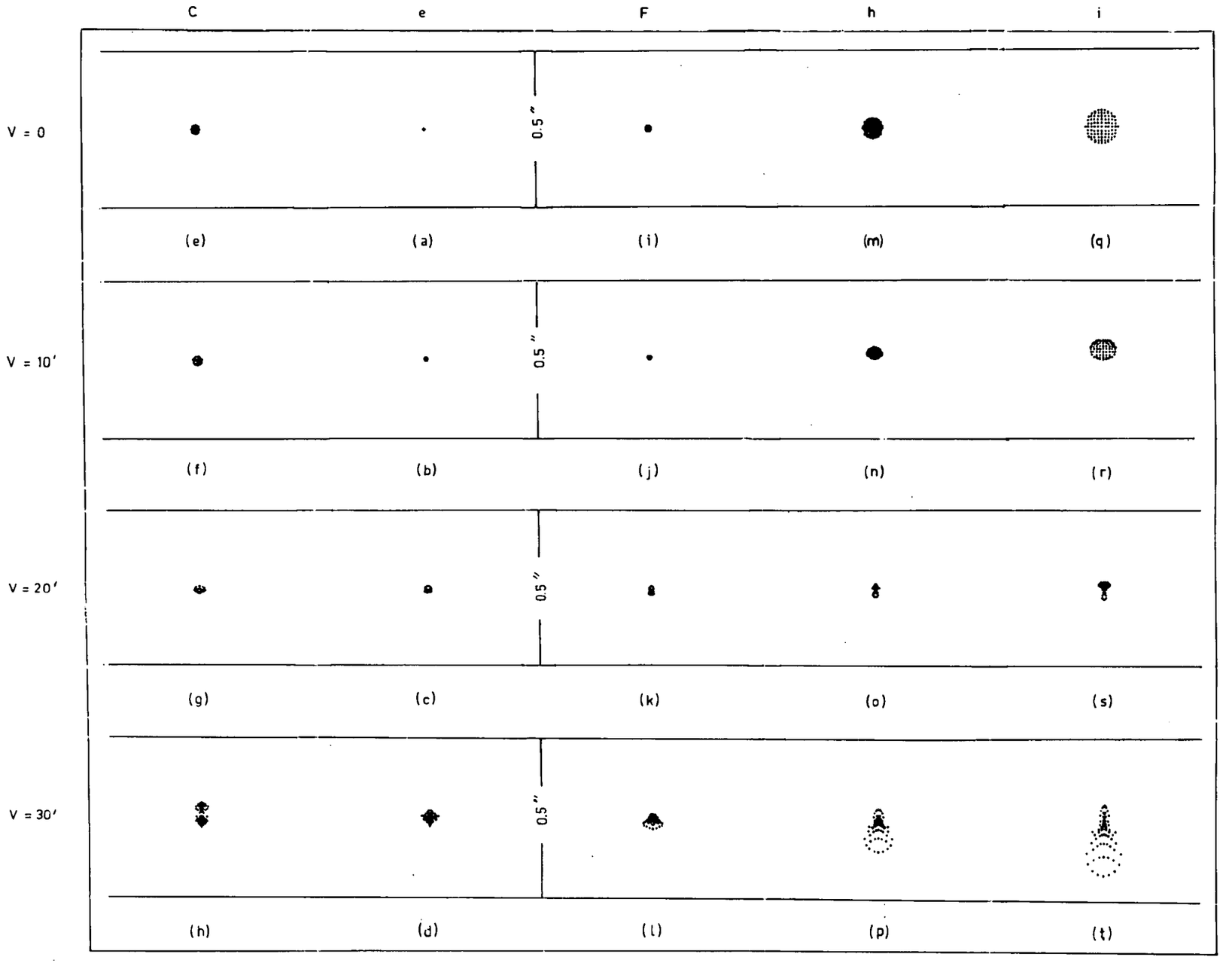

Fig 4.5
SPOT DIAGRAMS FOR THE FIFTH ORDER ANASTIGMAT II

TABLE 1. PARAXIAL ARRANGEMENT

	Surface number and type	Vertex radius of curvature	Distance to next surface	Clear aperture
1.	Aspheric (or hyperboloid)	-1000.0000	-333.52942	150
2.	Aspheric (or hyperboloid)	- 570.75671	344.96239	56
3.	Aspheric	2245.1454	1.5	24
4.	Spherical	∞	49.251012	
5.	Spherical	-191.62831	0.48	21
6.	Spherical	∞	3.3894 (back focal distance)	

2. Profile equations

Primary mirror

1. Fifth-order anastigmat II $x = -5 \times 10^{-4}y^2 + 2.7167436 \times 10^{-11}y^4 + 2.1871114 \times 10^{-17}y^6 - 4.2141178 \times 10^{-23}y^8$

2. Hyperboloid anastigmat III $x = -5 \times 10^{-4}y^2 + 2.7617488 \times 10^{-11}y^4 - 3.0508978 \times 10^{-18}y^6 + 4.2129047 \times 10^{-24}y^8$

Secondary mirror

1. Fifth-order anastigmat II $x = -8.760307 \times 10^{-4} y^2 + 5.5190452 \times 10^{-9} y^4 - 4.6804483 \times 10^{-14} y^6 - 3.7247501 \times 10^{-19} y^8$

2. Hyperboloid anastigmat III $x = -8.760307 \times 10^{-4} y^2 + 5.5595084 \times 10^{-9} y^4 - 7.0564047 \times 10^{-14} y^6 + 1.11954259 \times 10^{-18} y^8$

Aspheric plate

1. Fifth-order anastigmat II $x = 2.2270272 \times 10^{-4} y^2 - 2.4397226 \times 10^{-7} y^4 - 4.8401781 \times 10^{-14} y^6 + 7.9533087 \times 10^{-17} y^8$

2. Hyperboloid anastigmat III $x = 2.2270272 \times 10^{-4} y^2 - 2.4337069 \times 10^{-7} y^4 - 4.828244 \times 10^{-14} y^6 + 7.9141357 \times 10^{-17} y^8$

3. Departures of the Surfaces from their Polar tangent spheres.

TABLE 2. PRIMARY MIRROR

Y	Fifth-order anastigmat II dx	Hyperboloid anastigmat III dx
75.0	-223.080	-223 .535
67.5	-146.276	-146.600
60.0	-91.271	-91.487
52.5	-53.477	-53.611
45.0	-28.854	-28.929
37.5	-13.910	-13.948
30.0	-5.695	-5.712
22.5	-1.802	-1.807
15.0	-0.356	-0.357

TABLE 3. SECONDARY MIRROR

Y	Fifth-order anastigmat II dx	Hyperboloid anastigmat III dx
28.0	-174.749	-175.395
25.2	-114.782	-115.265
22.4	-71.729	-72.065
19.6	-42.083	-42.298
16.8	-22.733	-22.857
14.0	-10.970	-11.034
11.2	-4.496	-4.523
8.4	-1.423	-1.432
5.6	-0.281	-0.283

TABLE 4. ASPHERIC PLATE

Y	Fifth-order anastigmat II dx	Hyperboloid anastigmat III dx
12.0	233.688	233.112
10.8	153.322	152.944
9.6	95.718	95.482
8.4	55.108	55.970
7.2	30.286	30.211
6.0	14.605	14.569
4.8	5.982	5.968
3.6	1.893	1.888
2.4	0.374	0.375

4.6 CONCLUSIONS.

The spot diagrams, which are obtained for the fifth-order anastigmat, when the colour correction is made for the maximum field, are shown in Figures (4.5 a-p). These figures show that, as compared with the hyperboloid anastigmat III, there is considerable improvement in the image quality as far as the e-line is concerned, but this improvement is not much for the spectral range considered, as the image spread has reduced to 0.136 seconds only. This shows that the mirrors of the anastigmatic system may be approximated as hyperboloids, as there is not much disadvantage incurred by such an approximation, which is evident from the spot diagrams. The objective system, when the corrector system is removed, covers a total field of 8 or 10 minutes approximately, depending on whether plane plates or bent plates will be used. The general situation regarding these aberrations improves if the plate is taken nearer to the focus, at the cost of increasing the asphericity of the plate. It seems that this kind of anastigmatic arrangement is mostly suitable in systems where maximum field coverage is required while using correctors, otherwise, it may not be an advisable solution.

An inspection of Tables I and II shows that the difference in profile of the mirrors of the two anastigmats amounts to less than a wavelength at the edges of the mirrors, indicating that the hyperboloid mirrors are not far removed from the aspheric mirrors of revolution.

CHAPTER V.

SPHERICAL LENS SECONDARY FOCUS CORRECTORS

5.1 INTRODUCTION.

In the previous two chapters, the usefulness of secondary focus correctors consisting of aspherical surfaces of revolution was discussed. It was noticed there that such systems require slight departure from the aplanatic condition of the R.C* system to balance the small spherical aberration and coma introduced by the corrector. This Chapter is particularly devoted to bringing out the principles of the correctors consisting of spherical surfaces only. Rosin (1966) has suggested a corrector system, which he used for an f/4 primary and f/10 system with an aperture of 105 inches, consisting of purely spherical surfaces. He uses either the concentric or the aplanatic principle in determining the curvature of any surface. This being the case, such a corrector does not suffer from either spherical aberration or linear coma as can be seen later. Therefore, such a corrector system, if added to the Ritchey-Chretien system, does not alter the aplanatic property at the cassegrain focus. Such a corrector system uses the glass constants as the parameters to correct field curvature and either longitudinal colour or transverse colour and all the remaining quantities except two, associated with the corrector will be determined to satisfy the aplanatic and concentric relations whilst correcting astigmatism. As the corrector employs glass constants also as parameters, different combinations of glasses are unavoidable.

As will be seen later, the aplanatic surfaces contribute zero spherical aberration, coma and astigmatism (third-order), whereas the contribution from the concentric surfaces to spherical aberration, coma and paraxial longitudinal colour

* Ritchey-Chretien

are zero. The aplanatic condition at any surface requires that $i'_{0j} - v_{0j} = 0$, whilst the concentric condition requires $i_{0j} = 0$. This later condition results in the relation $i_j y_{0j} = -1/N_j$, which can be derived easily from the consideration of the relation between the paraxial coefficients. The contribution of such surfaces to third-order aberration coefficients, $\sigma_1 - \sigma_4$, may be obtained by using equations (2.11) - (2.12) of Chapter II as follows.

(1) Aplanatic surface

$$\left.\begin{aligned}
\sigma_{1j} &= S_{0j} = \frac{1}{2} N_j y_{0j} i_{0j}^2 (1-k_j)(i'_{0j}-v_{0j}) = 0 \\
\sigma_{2j} &= q_j S_{0j} = \frac{1}{2} N_j y_{0j} i_j i_{0j} (1-k_j)(i'_{0j}-v_{0j}) = 0 \\
\sigma_{3j} &= \frac{1}{2} N_j y_{0j} i_j^2 (1-k_j)(i'_{0j}-v_{0j}) = 0 \\
\sigma_{4j} &= \frac{(1-k_j)c_{0j}}{2N_j}
\end{aligned}\right\} \qquad (5.1)$$

(2) Concentric surface

$$\left.\begin{aligned}
\sigma_{1j} &= \frac{1}{2} N_j y_{0j} i_{0j}^2 (1-k_j)(i'_{0j}-v_{0j}) = 0 \\
\sigma_{2j} &= \frac{1}{2} N_j y_{0j} i_j i_{0j} (1-k_j)(i'_{0j}-v_{0j}) = 0 \\
\sigma_{3j} &= \frac{1}{2} N_j y_{0j} i_j^2 (1-k_j)(i'_{0j}-v_{0j}) = -\frac{1}{2} \frac{c_{0j}(1-k_j)}{N_j} \\
\sigma_{4j} &= \frac{(1-k_j)c_{0j}}{2N_j}
\end{aligned}\right\} \qquad (5.2)$$

The expressions for σ_3, σ_4 indicate that for a concentric surface the astigmatic coefficient is equal and opposite to the petzval curvature coefficient of that surface. A close inspection of the expressions for σ_3 indicates that a concentric glass lens always contributes positive astigmatism, whereas a concentric air lens contributes negative astigmatism unless the axial separation of the two such surfaces is negative, which has no physical significance.

5.2 RITCHEY-CHRETIEN SYSTEM WITH ROSIN CORRECTOR.

The Ritchey-Chretien system along with the Rosin corrector is shown in Figure (5.1). It was noticed in Chapter II that the Ritchey-Chretien system suffers from positive astigmatism. It therefore follows from the concluding remark of the previous section that we should employ a concentric air-lens to correct the positive astigmatism of the Ritchey-Chretien system. The bounding surfaces of the two lenses may be chosen as aplanatic and different materials will be used for the two lenses so that the refractive indices and the V-numbers will be the parameters used to correct the petzval sum of the Ritchey-Chretien system and either the longitudinal colour or the transverse colour of the whole system. The resultant system will therefore have surfaces 3 and 6 as aplanatic and surfaces 4 and 5 as concentric. The following relations may be obtained by imposing the aplanatic conditions at surfaces 3 and 6 and concentric conditions at surfaces 4 and 5. The power of the Ritchey-Chretien system is considered as unity.

$$
\left.
\begin{aligned}
c_{03}\, y_{03} &= \frac{1 + k_3}{k_3} \\
v_{04} &= \frac{1}{k_3} \\
c_{04} y_{04} &= 1/k_3 \\
v_{05} &= 1/k_3 \\
c_{05} y_{05} &= 1/k_3 \\
v_{06} &= 1/k_3 \\
c_{06} y_{06} &= (1+k_6)/k_3 k_6 \\
v_{07} &= 1/k_3 k_6 = N_6/N_6
\end{aligned}
\right\} \qquad (5.3)
$$

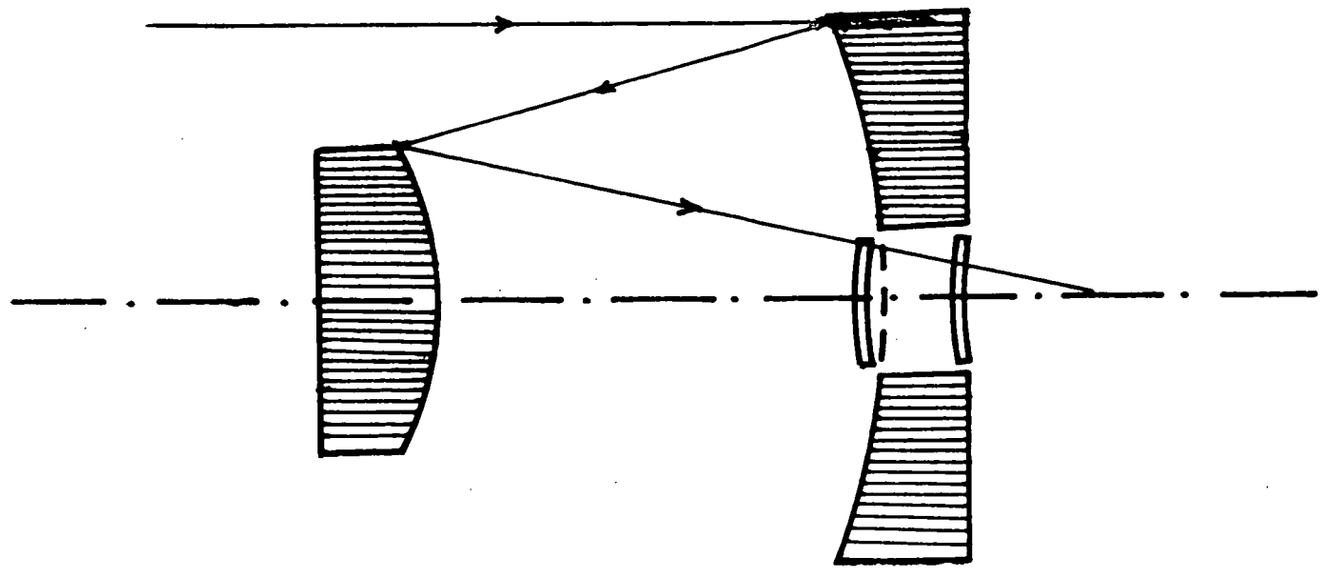

Fig 5.1

RITCHEY CHRETIEN SYSTEM WITH ROSIN CORRECTOR.

The expressions for v_{07} indicates that the focal length of the whole system changes from unity to the N_6/N_4 value.

The expressions for the third-order aberration coefficients $\sigma_1 - \sigma_4$ and for the paraxial colour may be derived as follows. The terms containing R and x refer to the mirror system.

$$\left.\begin{aligned}
\sigma_1 &= 0 \\
\sigma_2 &= 0 \\
\sigma_3 &= \frac{1}{N_k' v_{0k}'}\left\{\frac{(1+x+2R)}{4(1+Rx)} + \frac{c_{04}(k_4-1)}{2N_4} + \frac{c_{05}(k_5-1)}{2N_5}\right\} \\
&= \frac{N_6}{N_4}\left\{\frac{1+x+2R}{4(1+Rx)} + \frac{c_{04}(k_4-1)}{2N_4} + \frac{c_{05}(k_5-1)}{2N_5}\right\} \\
\sigma_4 &= \frac{1}{N_k' v_{0k}'}\left\{\frac{R^2(1-x)-1-R}{2(1+Rx)} + \frac{(c_{03}-c_{04})(N_4-1)}{2N_4} + \frac{(c_{05}-c_{06})(N_6-1)}{2N_6}\right\} \\
&= \frac{N_6}{N_4}\left\{\frac{R^2(1-x)-1-R}{2(1+Rx)} + \frac{(c_{03}-c_{04})(N_4-1)}{2N_4} + \frac{(c_{05}-c_{06})(N_6-1)}{2N_6}\right\}
\end{aligned}\right\} \qquad (5.4)$$

$$\left.\begin{aligned}
l_{ch}' &= \frac{1}{N_k' v_{0k}'^2}\left\{(y_{04}i_{04}-k_3 y_{03}i_{03})(N_x-N_y)_a + (y_{06}i_{06}-k_3 y_{05}i_{05})(N_x-N_y)_b\right\} \\
&= \frac{N_6^2}{N_4^2}\left\{(N_y-N_x)_a\, y_{03} + \frac{(k_3 y_{03}-d_3'-d_4'-d_5')(N_x-N_y)_b}{k_3^2 k_6}\right\} \\
t_{ch}' &= \frac{1}{v_{0k}'}\left\{(y_{03}i_3'-y_{04}i_4')(N_x-N_y)_a + (y_{05}i_5'-y_{06}i_6)(N_x-N_y)_b\right\} \\
&= \frac{N_6}{N_4}\left\{(y_{03}i_3' + \frac{1}{N_4})(N_x-N_y)_a - (\frac{1}{N_6} + y_{06}i_6)(N_x-N_y)_b\right\}
\end{aligned}\right\} \qquad (5.5)$$

where the subscripts $_x$, $_y$ indicate the two lines for which colour correction is required, and the subscripts $_a$ and $_b$ denote the front lens and the back lens respectively. The expressions for l_{ch}', t_{ch}' are obtained on the basis of chromatic coefficients (Cruickshank, 1968).

5.3 CORRECTION PROCEDURE.

The equations of the previous sections show that there are two possible ways of reaching an anastigmatic solution. One way is to assume the thickness of the lenses, the distance of the corrector from the focal plane and the refractive index of the front lens; and then determine the air separation between the two lenses and the refractive index of the back component along with the curvatures to obtain the required correction state while satisfying the aplanatic and concentric conditions. The second approach will be to assume the refractive indices, distance of the corrector from the focal plane, and thickness of the front lens as known quantities and then find the curvatures and separation of the two lenses and the thickness of the back component to obtain again the required correction state while satisfying the aplanatic and concentric principles. The latter approach is followed here, as the former procedure is more theoretical and the analysis is not very favourable because of the limited number of glasses available. Using equations (5.3) - (5.4), the explicit expressions for the different quantities are derived and are assembled as shown below. The values of d_2', d_3', N_4, N_6 are assumed to have been specified.

$$
\begin{aligned}
y_{03} &= y_{02} - d_2' = (1+Rx)/(1+R) - d_2' \\
c_{03} &= (1+k_3)/k_3 y_{03} \\
c_{04} &= 1/(k_3 y_{03} - d_3') \\
c_{05} &= \frac{2N_5}{(N_5-1)} \left\{ \frac{N_4 c_3}{N_5} - \frac{(1+x+2R)}{4(1+Rx)} - \frac{c_{04}(k_4-1)}{2N_4} \right\} \\
c_{06} &= \frac{2N_6}{(N_6-1)} \left\{ \frac{R^2(1-x)-1-R}{2(1+Rx)} + \frac{(c_{03}-c_{04})(N_4-1)}{2N_4} + \frac{c_{05}(N_6-1)}{2N_6} - \frac{N_4}{N_6} c_4 \right\} \\
d_4' &= \frac{(k_3 c_{05} y_{03} - c_{05} d_3' - 1)}{c_{05}} \\
d_5' &= \frac{k_3 k_6 c_{06} y_{03} - k_6 c_{06}(d_3'+d_4') - (1+k_6)}{k_3 c_{06}}
\end{aligned}
\qquad (5.6)
$$

where R, x have the same meaning as before, and σ_3, σ_4 are the residuals of the whole system, and will usually be zero or very small.

We are now left with colour correction. As the paraxial set up of the whole system is known, we shall trace two formal paraxial a- and b-rays through the whole system for the e-line (base line) and determine the unknown quantities in equations (5.5). The equations (5.5) will then become functions of $(N_x-N_y)_a$ and $(N_x-N_y)_b$ only. A proper choice of these two quantities is made depending on whether longitudinal colour correction or transverse colour correction is required. When one of these corrections is made, then the residual value of the other colour may be obtained from its own expression. As the refractive indices for the glasses are assumed to be known, it is necessary to search for the isoindex glasses in the glass catalogue for colour correction.

5.4 NUMERICAL EXAMPLE.

The principles outlined in the previous sections are now utilised in developing a doublet corrector system of the Rosin type to correct σ_3, σ_4 of the Ritchey-Chretien telescope objective system developed earlier. The distance of the corrector, d_2', is chosen arbitrarily and the front lens of the corrector lies just before the vertex of the primary mirror. However, the variation of the higher order aberrations with d_2' is studied by changing d_2' once. Initially, K3 518 590 and SK 16 620 603 are chosen as the materials for the front lens and the back lens respectively. The initial prescription for d_2', d_3', N_4, N_6 is

$$d_2' = 0.27325251 \qquad d_3' = 0.0008 \qquad N_4 = 1.52032 \qquad N_6 = 1.62286 \qquad \sigma_3 = \sigma_4 = 0.0$$

Using equations (5.6), we obtain

$c_{03} = 42.224436$ $c_{04} = 26.000643$ $c_{05} = 29.923601$ $c_{06} = 49.093165$

$d_4' = 0.00504215$ $d_5' = 0.00049744$

This corrector is added to the Ritchey-Chretien system and the third- and fifth-order aberration coefficients for the whole system are computed and are shown in Table I. With the same pair of glasses, the distance d_2' is now changed to 0.285 and the paraxial set up for the corrector is

$c_{03} = 52.571099$ $c_{04} = 32.537676$ $c_{05} = 35.752772$ $c_{06} = 58.31944$

$d_2' = 0.285$ $d_3' = 0.0008$ $d_4' = 0.00276374$ $d_5' = 0.00025704$

The third- and fifth-order aberration coefficients for the two-mirror system with this corrector added to it are again computed and are shown in Table I. An inspection of Table I indicates that the fifth-order linear astigmatism, cubic coma and distortion increase considerably, whereas the fifth-order cubic astigmatism is reasonably stable. It is to be noted that for this increase in d_2', both longitudinal and transverse colour also increase. An increase in d_2' decreases the diameter of the lenses. It is therefore more advantageous to select the first position of the corrector for further analysis.

To balance the fifth-order astigmatism it is necessary to introduce a small residual third-order astigmatism. The residual value for σ_3 is prescribed as 0.21234, which is supposed to balance the fifth-order linear astigmatism at the edge of the aperture for a semi-field of 20 minutes. The new set up for the corrector with this σ_3 residual value is obtained as

$c_{03} = 42.224436$ $c_{04} = 26.000643$ $c_{05} = 28.886353$ $c_{06} = 48.055916$

$d_2' = 0.27325251$ $d_3' = 0.0008$ $d_4' = 0.00384316$ $d_5' = 0.00098685$

TABLE I. ABERRATION COEFFICIENTS

	d'	0.27325251	0.285
Third-order aberration coefficients	σ_1	0.0	0.0
	σ_2	0.0	0.0
	σ_3	0.0	0.0
	σ_4	0.0	0.0
	σ_5	123.85	148.17
Fifth-order aberration coefficients	μ_1	0.0	0.0
	μ_2	0.0	0.0
	μ_3	0.0	0.0
	μ_4	-10.326	-10.12
	μ_5	-7.6161	-7.4097
	μ_6	-2.7098	-2.7099
	μ_7	309.43	351.58
	μ_8	155.81	176.89
	μ_9	153.63	174.7
	μ_{10}	-16242	-22891
	μ_{11}	-4438.1	-6184.8
	μ_{12}	182400	3102900

The colour of the system is found by using equations (5.5), and it is noticed that there is considerable change in colour when the residual value for σ_3 is changed. However, with the present set up, the longitudinal and the transverse colour are both found to be within the tolerance limits up to a field angle of 40 minutes for the wavelength range C - F. The system is now submitted to analysis by spot diagrams. Figures (5.2 a,b,c) show the spot diagrams for the e-line. The image spread up to a total field of 40 minutes amounts to about 0.115 seconds only. This image spread is found to have increased to about 0.89 seconds for the wavelength range C - F, and as a consequence of this, the spot diagrams are not plotted for the other wavelengths. This glass selection is therefore rejected and then proceeded to find isoindex glasses.

As SK 15 623 581 is nearly an isoindex glass to SK 16, this material is now chosen for the back lens and the combination has reduced longitudinal colour considerably, whereas the transverse colour has worsened the situation. A few more different combinations (restricting ourselves to highly transparent glasses) were tried and ultimately it was decided to leave some longitudinal colour and decrease transverse colour considerably. For this purpose, K 10 501 564 and SK 16 620 603 are found to be suitable materials for the front and back component lenses respectively. The paraxial set up for the corrector is found to be

$d_2' = 0.27325251$ $\quad d_3' = 0.0009$ $\quad d_4' = 0.00332564$ $\quad d_5' = 0.00108736$

$c_{03} = 41.942479$ $\quad c_{04} = 25.773153$ $\quad c_{05} = 28.189325$ $\quad c_{06} = 47.000128$

This set up makes the system suffer from some transverse colour and considerable longitudinal colour.

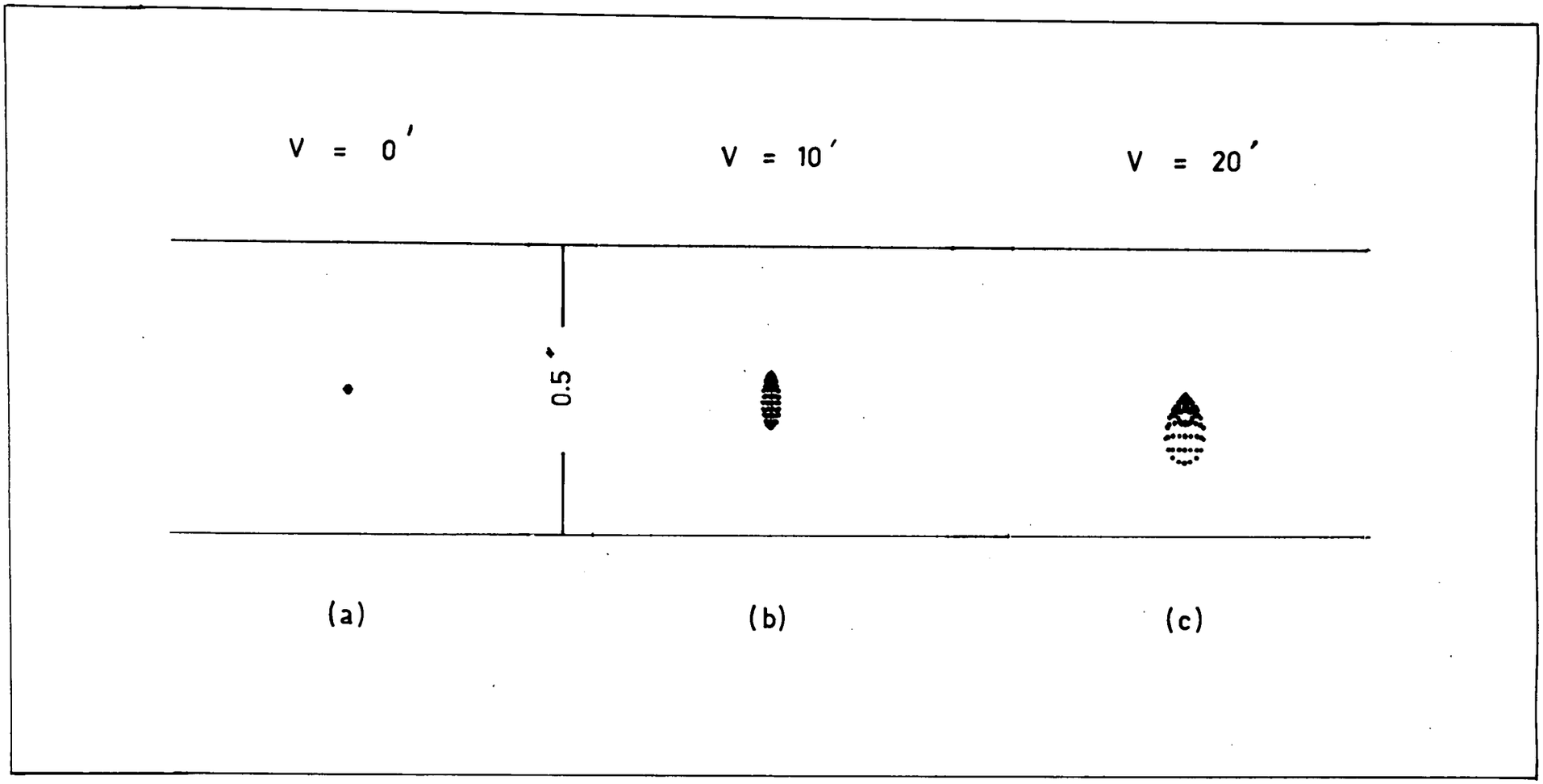

Fig 5.2

SPOT DIAGRAMS FOR RITCHEY – CHRETIEN SYSTEM WITH ROSIN CORRECTOR (initial correction)

This final corrector system is added to the Ritchey-Chretien system and the combined system is submitted to analysis by ray tracing. Figures (5.3 a-i) show the spot diagrams for the C, e, F lines for (i) V = 0, (ii) V = 10 minutes, (iii) V = 20 minutes. The image spread for the e-line amounts to about 0.136 seconds only up to a total field angle of 40 minutes, whereas this increases to about 0.77 seconds of arc for the wavelength range C - F, which is about one and a half times the prescribed tolerance. A study of the different combinations of glasses has revealed that with the present set up of the Ritchey-Chretien system, about this much image spread appears to be inevitable.

5.5 SPECIFICATIONS

The specifications of the corrector system which is to be added to the 1200 inch focal length telescope objective are computed and are given in Table II. All the parameters are expressed in inch units. Distance of the corrector from the vertex of the secondary mirror = 327.903.

5.6 CONCLUSIONS

The analysis given in the previous sections illustrates that the limitation in the use of the Rosin corrector is mainly confined to colour. With this type of corrector system, one could achieve the best monochromatic aberration correction, whereas the colour correction appears to be rather difficult. In fact, with such a corrector system, the useful field for a given spectral range is mainly limited by the image spread produced by other lines rather than the e-line. This type of corrector system also introduces considerable distortion. If the longitudinal colour is fully corrected, it

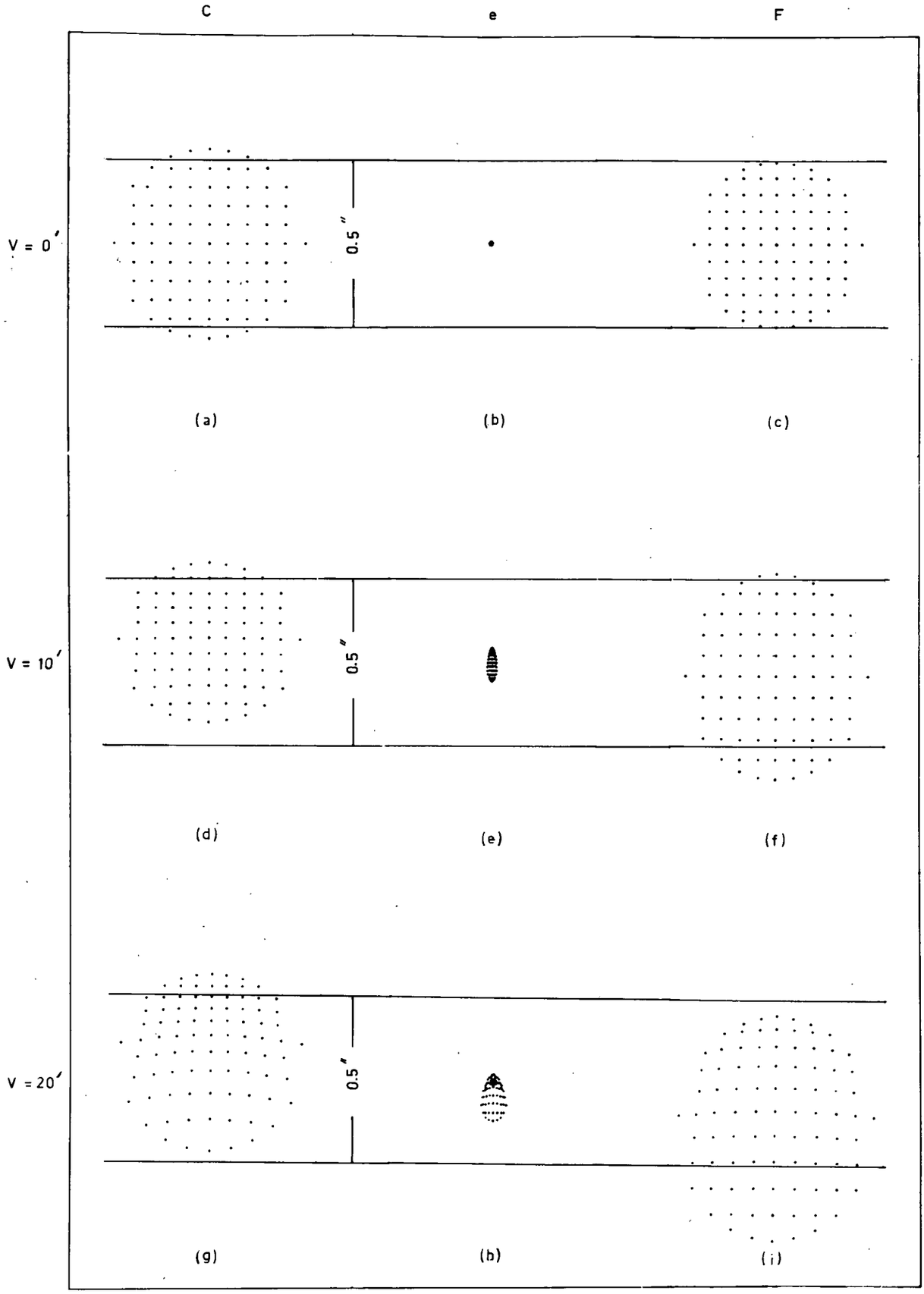

Fig 5.3

SPOT DIAGRAMS FOR RITCHEY CHRETIEN SYSTEM WITH ROSIN CORRECTOR

TABLE II

Surface number	radius of curvature	distance to next surface	material	clear aperture
3	28,610608	1.08		
			K10 501 564	21.0
4	46.560094	3.990768		
			SK16 620 603	21.0
5	42.569313	1.304832		
6	25,531848			

appears that there will not be much variation in the image shape with wavelength. Such a corrector system finds maximum utility where a narrow range of the spectrum is considered. The Gascoigne plate with the field flattening lens appears to have more useful application in improving the size of the field for a wide range of the spectrum. The advantage of the Rosin corrector is that it does not alter the Ritchey-Chretien configuration of the mirrors. Except for the best correction and the considerable increase in field size (a full one-degree field can be obtained without exceeding even 0.25 seconds of arc) for the e-line, this kind of corrector seems to have limited use.

CHAPTER VI

PRIME FOCUS CORRECTORS

6.1 INTRODUCTION.

The image formed at the primary focus of the Ritchey-Chretien telescope objective system suffers from spherical aberration, coma, field curvature and astigmatism. If the primary focus is to be used, prime focus correctors are therefore required. Prime focus correctors consisting of spherical surfaces (Wynne, 1965, 1968; Ross, 1935; Rosin, 1966), and aspheric surfaces of revolution (Meinel, 1953; Gascoigne, 1965, Kohler, 1966; Schulte, 1966) are proposed. Gascoigne has suggested a single plate corrector for the correction of third-order spherical aberration and coma. With this single plate corrector, the size of the useful field obtained may not be considerable. Meinel has suggested that the field aberrations of a parabolic mirror may be corrected by using three air spaced aspheric plates which are placed nearer to the focal plane. Following this earlier suggestion by Meinel, field correctors of this type for the primary mirror of a Ritchey-Chretien system were investigated by Schulte (1966) and Kohler (1966). Kohler has used one more spherical lens to correct the field curvature of the primary mirror. This chapter is particularly devoted to the investigation of the usefulness of field correctors for the primary focus involving aspheric surfaces. The design principles underlying the development of single plate and three plates correctors will be discussed.

6.2 PRIME FOCUS ABERRATIONS.

When deriving the expressions for the third-order aberration coefficients for the two-mirror objective system, the direct summation property of the aberration coefficients is used. It is therefore easy to obtain the expressions

for the third-order aberration coefficients for the primary mirror directly from equations (2.17)- (2.21) of Chapter II. In this way, we get

$$\left.\begin{aligned} \sigma_1 &= \frac{R^3}{8} - 2c_{11} \\ \sigma_2 &= \frac{R^2}{4} \\ \sigma_3 &= \frac{R}{2} \\ \sigma_4 &= -\frac{R}{2} \end{aligned}\right\} \qquad (6.1)$$

If we work with the unit power primary mirror and use the expression for c_{11} from equation (2.23), equations (6.1) then become

$$\left.\begin{aligned} \sigma_1 &= \frac{1}{R^3}\left\{\frac{R^3}{8} - 2c_{11}\right\} = -\frac{1+Rx}{4R^3(1-x)} \\ \sigma_2 &= \frac{1}{R^2} \cdot \frac{R^2}{4} = 0.25 \\ \sigma_3 &= \frac{1}{R} \cdot \frac{R}{2} = 0.5 \\ \sigma_4 &= -\frac{1}{R} \cdot \frac{R}{2} = -0.5 \end{aligned}\right\} \qquad (6.2)$$

Equations (6.2) show that for the unit power primary mirror the coefficients $\sigma_2 - \sigma_4$ are independent of R and x.

Returning now to the numerical example, where R = 2.4 and x = 0.055, we obtain the aberration coefficients $\sigma_1 - \sigma_4$ as

$$\sigma_1 = -0.0216631 \qquad \sigma_2 = 0.25 \qquad \sigma_3 = 0.5 \qquad \sigma_4 = -0.5 \qquad (6.3)$$

These figures for the aberration coefficients indicate that the prime focus suffers very seriously from all the monochromatic aberrations. The coefficient σ_1 itself produces a very large image spread, showing that prime focus correctors are required even to obtain axially stigmatic imagery.

6.3 SINGLE PLATE CORRECTORS.

Gascoigne has suggested that a single aspheric plate inserted at a suitable distance before the focal plane is capable of correcting coma and spherical aberration of the mirror. This therefore necessitates that the distance d_1' of the plate from the vertex of the mirror and the asphericity of the plate are to be chosen to correct spherical aberration and coma simultaneously. The asphericity imposed on the plate for this correction necessarily introduces considerable astigmatism as can be seen later. The size of the useful field is therefore limited by astigmatism and petzval curvature. The effect of the petzval curvature on the image spread may be eliminated by using the mean focal surface, which requires bent photographic plates. This also reduces the effect of astigmatism to some extent. Any small amount of colour introduced by the asphericity of the plate may be reduced by a proper choice of the axial power for the plate.

Figure (6.1) shows the optical arrangement of the primary mirror with the corrector plate. We shall make initially two approximations while deriving the expressions for the third-order aberration coefficients, $\sigma_1 - \sigma_4$, namely that the paraxial power of the plate is zero and the thickness of the plate is negligible. Because of these approximations, the contributions due to the sphericity of the bounding surfaces of the plate to the aberration coefficients $\sigma_1 - \sigma_4$ are zero. Tracing the a-ray ($y_{01} = 1$, $v_{01} = 1/l_{01}$) and the b-ray ($y_1 = p/(1-p/l_{01})$, $v_1 = 1/(1-p/l_{01})$) through the system shown in Figure (6.1), we get

$$\left.\begin{aligned} y_{02} &= y_{01} - d_1' v_{02} = 1 + d_1' \\ y_2 &= y_1 - d_1' v_2 = d_1' \\ P_2 &= d_1'/(1+d_1') \end{aligned}\right\} \qquad (6.4)$$

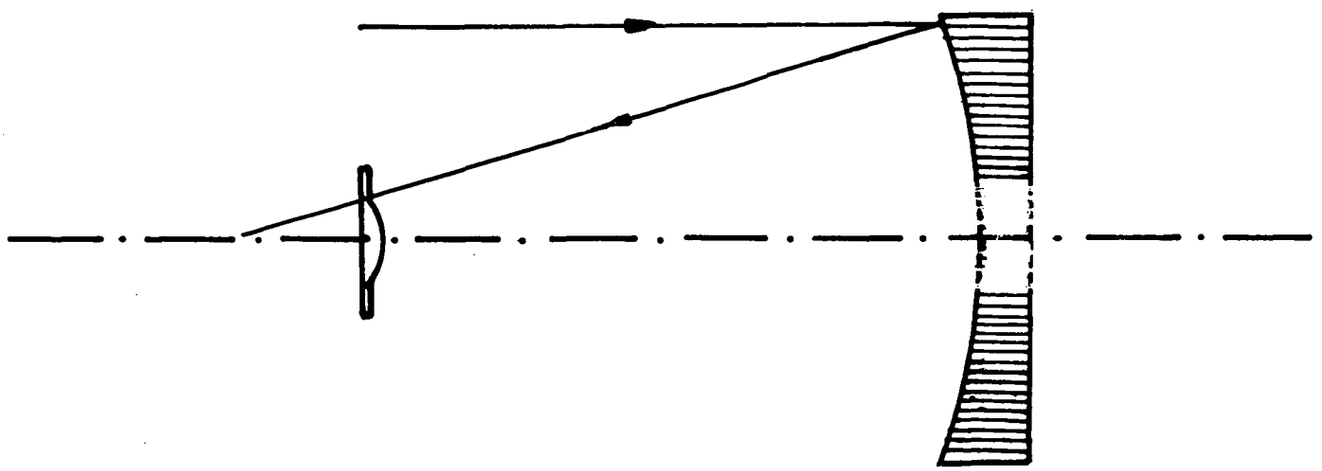

Fig 6.1

Primary mirror with single plate corrector

Substituting these expressions in the expressions for $\sigma_1 - \sigma_4$ of Chapter II, equations (2.11), (2.12), we get

$$\sigma_1 = -\frac{(1+Rx)}{4R^3(1-x)} + (N-1)c_{12}y_{02}^4 = -\frac{(1+Rx)}{4R^3(1-x)} + (N-1)c_{12}(1+d_1')^4 \qquad (6.5)$$

$$\sigma_2 = \frac{1}{4} + \frac{d_1'}{(1+d_1')}\ (N-1)c_{12}(1+d_1')^4 = \frac{1}{4} + (N-1)c_{12}d_1'(1+d_1')^3 \qquad (6.6)$$

$$\sigma_3 = \frac{1}{4} + \frac{d_1'^2}{(1+d_1')^2}\ (N-1)c_{12}(1+d_1')^4 = \frac{1}{2} + (N-1)c_{12}d_1'^2(1+d_1')^2 \qquad (6.7)$$

$$\sigma_4 = -0.5 \qquad (6.8)$$

For any required σ_1, σ_2 residual values for the system, the expressions for c_{12} and d_1' may be obtained by solving equations (6.5) - (6.6) as

$$\left.\begin{aligned} c_{12} &= \frac{1}{(N-1)}\ \frac{\left(\sigma_1 - \sigma_2 + \frac{1+Rx}{4R^3(1-x)} + \frac{1}{4}\right)^4}{\left(\sigma_1 + \frac{1+Rx}{4R^3(1-x)}\right)^3} \\ d_1' &= \frac{\sigma_2 - \frac{1}{4}}{\sigma_1 - \sigma_2 + \frac{1+Rx}{4R^3(1-x)} + \frac{1}{4}} \end{aligned}\right\} \qquad (6.9)$$

where, N is the refractive index of the material of the plate. The values of c_{12}, d_1' that will be obtained from equations (6.9) for any given σ_1, σ_2 residual values serve as an initial approximate solution, and any further improvement in the correction state of the spherical aberration and coma may be started from here, and the iterative process with the differential correction methods may be adopted to obtain the exact prescribed values for σ_1, σ_2. The further development of the correction state is given below in stages.

Stage (1): Initially σ_1 and σ_2 may be prescribed as zero. The initial starting solution may be obtained from equations (6.9). We shall then specify the actual paraxial curvature for the plate and the thickness of the plate. Changing c_{12} and d_1' by small quantities, one at a time, the derivatives $\partial\sigma_1/\partial c_{12}$, $\partial\sigma_2/\partial c_{12}$, $\partial\sigma_1/\partial d_1'$, and $\partial\sigma_2/\partial d_1'$ may be obtained. Then, using the equations given below and iterating the process, we can obtain the exact prescribed values for σ_1, σ_2.

$$\left.\begin{aligned} \frac{\partial\sigma_1}{\partial c_{12}} \cdot \Delta c_{12} + \frac{\partial\sigma_1}{\partial d_1'} \cdot \Delta d_1' &= (R_1 - \sigma_1) \\ \frac{\partial\sigma_2}{\partial c_{12}} \cdot \Delta c_{12} + \frac{\partial\sigma_2}{\partial d_1'} \cdot \Delta d_1' &= (R_2 - \sigma_2) \end{aligned}\right\} \qquad (6.10)$$

where R_1, R_2 are the residuals prescribed for σ_1, σ_2. We shall then compute the higher order aberrations for the system. We can choose the second of the extra-axial curvatures of the plate as a parameter to balance the seventh-order spherical aberration with fifth-order spherical aberration. We shall then choose a proper residual for σ_2 to balance the higher order coma effects, while prescribing σ_1 as zero. This type of correction makes spherical aberration zero up to seventh-order and higher order coma is balanced largely by third-order coma.

Stage (2): After the above correction, it is necessary to trace a few rays through the system in the C-, e- and h-lines to find the effect of the asphericity of the plate on the colour. The asphericity of the plate mainly effects the longitudinal colour whilst the effect on transverse colour is negligible. This present view is in contradiction to Wynne's statement (1968) where he reports that the asphericity of the plate introduces transverse colour. This present view of the author is supported later on when the actual

performance is shown by way of spot diagrams. The residual value to be prescribed for the paraxial longitudinal colour may be found from the traces. The approximate value of c_{0_2} which gives the necessary paraxial longitudinal colour may be obtained from the equation

$$c_{0_2} = - \frac{l'_{ch}}{(N_x - N_y)(1+d_1')^2} \qquad (6.11)$$

where l'_{ch} is the necessary longitudinal colour residual and N_x, N_y are the refractive indices of the lines for which colour correction is required. The above equation is obtained by using chromatic coefficients. Any further improvement in the colour correction may again be obtained by the iterative differential correction method, while tracing the paraxial a-rays in x, e, y-lines to determine the actual colour. This time c_{0_2} will be the parameter for such correction.

Stage (3): The introduction of the paraxial power to the plate slightly alters the monochromatic aberration correction. This therefore necessitates the repetition of the whole process of stage (1) and stage (2) to obtain the final correction.

Returning now to the numerical example considered earlier, we apply the above principles to obtain a single plate corrector which provides images at the prime focus free from colour, spherical aberration and coma. Quartz is the material chosen for the aspheric plate. As the process of development has been clearly described, the actual design of the corrector is given here, without detailing all the stages of the development. The set up for the unit power primary mirror is obtained as

$c_{0_1} = -0.5$	$c_{0_2} = 0.05$	$c_{0_3} = 0.0$
$d_1' = -0.92111176$	$d_2' = -0.0012$	
$c_{1_1} = 0.07333156$	$c_{1_2} = -1245.4205$	
$c_{2_1} = -0.01399463$	$c_{2_2} = 570489.74$	

The third-order aberration coefficients for the system are

$\sigma_1 = 0.0$ $\sigma_2 = -0.0081632$ $\sigma_3 = 3.5347$ $\sigma_4 = -0.5085$ $\sigma_5 = -35.398$

The whole system is now submitted to analysis by ray-tracing. The spot diagrams for the C-, e-, h-lines for (i) V = 0, (ii) V = 5 minutes are shown in Figures (6.2 a-f). The displacements are computed in the mean focal plane. It can be noticed from the spot diagrams that there is not much variation in the image spread with wavelength. The colour present in the system is negligible. For a semi-field angle of 5 minutes and for the spectral range, C - h, the image spread amounts to about 0.618 seconds. The size of the field increases to some extent, if the tolerance limit for the blur circle is increased. The usefulness of this corrector in improving the field size for good imagery is mainly limited by astigmatism only. As the size of the useful field obtained with this single plate corrector is small, this type of corrector finds limited applications. This type of corrector plate, as pointed out by Gascoigne, finds its use mostly in prime-focus spectroscopy, photometry and to some extent in astronomical work.

The following are the specifications of the corrector plate and the photographic plate when the power of the system is raised from unity to the actual power. All the dimensions are expressed in inch units.

Corrector Plate

Distance of the plate from the vertex of the primary mirror = -460.55588

Radius of curvatures of surfaces 1 and 2 are

$r_1 = 10000$

$r_2 = \infty$

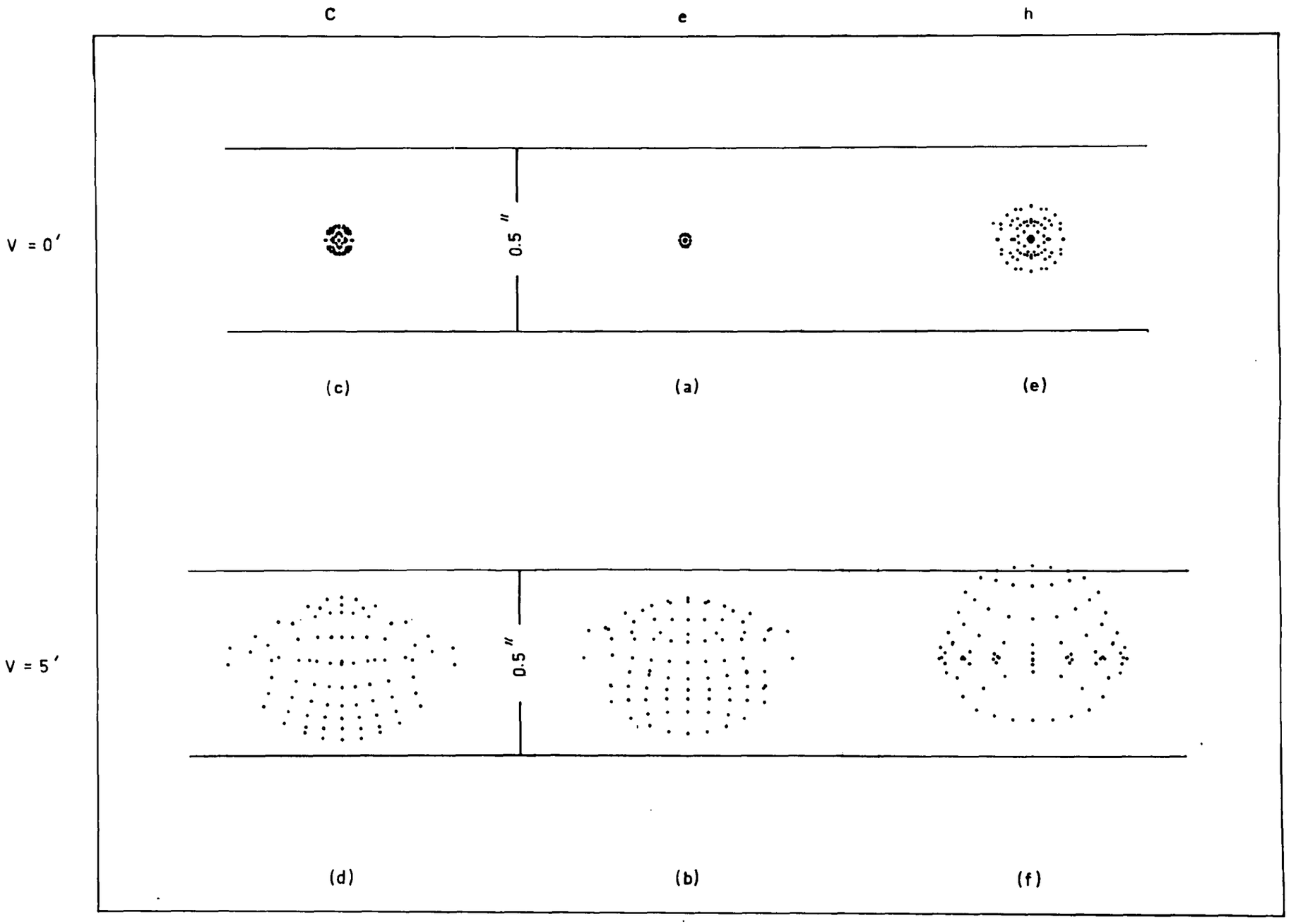

Fig 6.2

SPOT DIAGRAMS FOR PRIMARY MIRROR WITH SINGLE PLATE CORRECTOR

Thickness = 0.6

Diameter $\simeq$ 13.4

Profile equation is given by

$$x = 5 \times 10^{-6} y^2 - 2.4908409 \times 10^{-6} y^4 + 3.042587 \times 10^{-9} y^6 + 1.8955157 \times 10^{-15} y^8$$

Asphericity

Y	6.6	5.94	5.28	4.62	3.96	3.3	2.64	1.98	1.32
dx	496.054	328.936	207.294	122.516	66.601	32.310	13.298	4.224	0.837

Where, Y is the semi-aperture in inches, and dx is the departure from the polar tangent sphere in wavelengths (λ = .00002165 inches)

Photographic Plate

Vertex radius of curvature = -19.05328

Diameter $\simeq$ 1.6

6.4 THREE-PLATES CORRECTOR SYSTEM.

As the single plate corrector did not improve the field size considerably, it is desirable to proceed with the two or three plates corrector solutions to improve the size of the field further. Before proceeding with the design of a three-plates corrector system, a two-plates corrector system solution has been tried. With such a corrector, we will have six parameters to control the six required aberrations. These parameters are the air separations d_1', d_3' and the curvature coefficients c_{02}, c_{04}, c_{12}, c_{14}, and the third-order aberrations to be controlled are spherical aberration, longitudinal colour, transverse colour, field curvature, coma, and astigmatism. When the six parameters are used to control the six aberrations, the set up of the corrector has been found to have no physical significance due to the fact that one of the plates lies behind the focal plane. Therefore, it appears that a two-plates corrector

system does not provide a real physical solution to the problem. Due to this reason, a three-plates corrector system has been tried. In the case of the three-plates corrector, the paraxial curvatures will be chosen to control the longitudinal and transverse colour and field curvature, whereas the extra-axial curvature coefficients of the plates will be chosen to correct spherical aberration, coma and astigmatism, while the air separation and the axial thicknesses of the plates may be selected arbitrarily. As the higher order aberrations are not usually negligible with such correctors, the second of the extra-axial curvatures of the plates may be chosen to reduce the effect of these higher order aberrations. Figure (6.3) shows the optical arrangement of such a corrector system along with the primary mirror.

6.4.1 PARAXIAL ARRANGEMENT.

The initial solution for the paraxial arrangement of the corrector may be obtained by considering the plates as thin and assuming equal spacing between the plates. Using the thin lens equations (Cruickshank, 1968), we will obtain the paraxial equations as

$$v_{oa} = -1.0 \qquad v_a = -1.0$$

$$y_{oa} = 1 + d_1' \qquad y_a = d_1'$$

$$v_{ob} = -1.0 + y_{oa}\varphi_a$$

$$y_{ob} = y_{oa} - d_3' v_{ob}$$

$$v_{oc} = v_{ob} + y_{ob}\varphi_b$$

$$y_{oc} = y_{ob} - d_3' v_{oc}$$

$$v_b = -1.0 + y_a\varphi_a$$

$$y_b = y_a - d_3' v_b$$

$$v_c = v_b + y_b\varphi_b$$

$$y_c = y_b - d_3' v_c$$

where we have designated the plates by the symbols a, b, c.

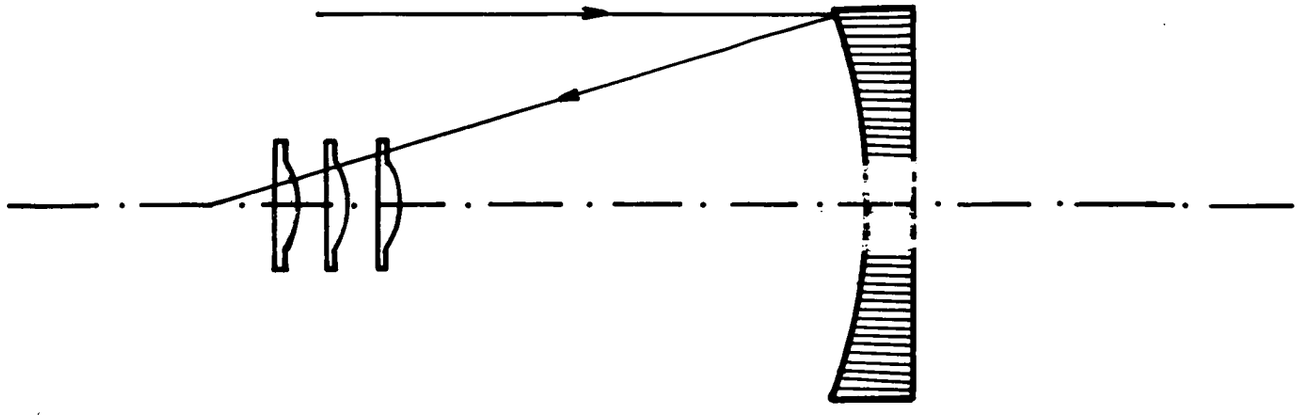

PRIMARY MIRROR WITH THREE PLATE CORRECTOR

Fig 6.3

The equations for the field curvature coefficient, σ_4, paraxial longitudinal and transverse colours may be written as

$$\sigma_4 = \frac{1}{N'_k v'_{ok}} \left\{ -0.5 + \frac{\varphi_a}{2N_a N'_a} + \frac{\varphi_b}{2N_b N'_b} + \frac{\varphi_c}{2N_c N'_c} \right\} \tag{6.13}$$

$$l'_{ch} = \frac{1}{v'^2_{ok}} \left\{ \frac{\varphi_a y^2_{oa}}{V_a} + \frac{\varphi_b y^2_{ob}}{V_b} + \frac{\varphi_c y^2_{oc}}{V_c} \right\} \tag{6.14}$$

$$t'_{ch} = \frac{1}{v'_{ok}} \left\{ \frac{\varphi_a y_{oa} y_a}{V_a} + \frac{\varphi_b y_{ob} y_b}{V_b} + \frac{\varphi_c y_{oc} y_c}{V_c} \right\} \tag{6.15}$$

We will choose the same material for all the three plates, and l'_{ch}, t'_{ch} may be prescribed as zero initially, and if any residual values are required, the spacing between the plates may be adjusted to achieve the actual colour prescribed. Equations (6.13) - (6.15) then become

$$\varphi_a + \varphi_b + \varphi_c = (N+R_4) \tag{6.16}$$

$$\varphi_a y^2_{oa} + \varphi_b y^2_{ob} + \varphi_c y^2_{oc} = 0 \tag{6.17}$$

$$\varphi_a y_{oa} y_a + \varphi_b y_{ob} y_b + \varphi_c y_{oc} y_c = 0 \tag{6.18}$$

where N is the refractive index of the material of the plate, and R_4 is given by

$$R_4 = 2N\sigma_4 \tag{6.19}$$

Equations (6.16) - (6.18) may be solved to obtain a very approximate solution for obtaining zero values for l'_{ch} and t'_{ch} and the actual value for σ_4. When the powers of the plates are determined, the axial curvatures may be computed from the equation

$$c_{oi} = (N-1)/\varphi_k \tag{6.10}$$

where $i = 2,4,6$ and $k = a,b,c$. With this as the initial solution, the actual values required for t'_{ch}, l'_{ch} may be obtained by further adjustment of the air spaces d'_3 , d'_5 by using differential correction method. This way, the whole paraxial set up can be determined.

6.4.2 THIRD-ORDER MONOCHROMATIC ABERRATIONS CORRECTION.

As the paraxial set up of the corrector is known, we will trace two formal paraxial rays, the a-ray ($y_{01} = 1$, $v_{01} = 1/l_{01}$) and the b-ray ($y_1 = p/(1-p/l_{01})$, $v_1 = 1/(1-p/l_{01})$) through the system to determine the values of s_0, P, q at every surface. Using equations (2.11), the third-order aberration coefficients σ_1, σ_2, σ_3 may be written as

$$\sigma_1 = \sum_{i=2}^{7} S_{0i} + \sum_{i=2}^{7} T_{0i} - \frac{1 + Rx}{4R^3(1-x)} \tag{6.21}$$

$$\sigma_2 = \sum_{i=2}^{7} q_i S_{0i} + \sum_{i=2}^{7} P_i T_{0i} + 0.25 \tag{6.22}$$

$$\sigma_3 = \sum_{i=2}^{7} q_i^2 S_{0i} + \sum_{i=2}^{7} P_i^2 T_{0i} + 0.5 \tag{6.23}$$

Solving equations (6.21) - (6.23) for T_{02}, T_{04}, T_{06}, which give simultaneously zero or any residual values of σ_1, σ_2, σ_3 for the whole system, we get

$$T_{02} = R_1 - \frac{(P_2R_2 + P_6R_2 - P_2P_6R_1 - R_3)}{(P_4 - P_2)(P_6 - P_4)} - \frac{(R_3 - P_4R_2 - P_2R_2 + P_4P_2R_1)}{(P_6 - P_4)(P_6 - P_2)} \tag{6.24}$$

$$T_{04} = \frac{P_2R_2 + P_6R_2 - P_2P_6R_1 - R_3}{(P_4 - P_2)(P_6 - P_4)} \tag{6.25}$$

$$T_{06} = \frac{(R_3 - P_4R_2 - P_2R_2 + P_4P_2R_1)}{(P_6 - P_4)(P_6 - P_2)} \tag{6.26}$$

where, $R_1 = \sigma_1 + \frac{1 + Rx}{4R^3(1-x)} - \sum_{i=2}^{7} S_{0i}$

$$R_2 = \sigma_2 - 0.25 - \sum_{i=2}^{7} q_i S_{0i} \tag{6.27}$$

$$R_3 = \sigma_3 - 0.5 - \sum_{i=2}^{7} q_i^2 S_{0i}$$

We will then find the first of the extra-axial curvature coefficients of the plates from the equation

$$q_i = \frac{T_{0i}}{(N-1)y_{0i}^4} \qquad (6.28)$$

With these values of the extra-axial curvatures, we will obtain the required correction state of the third-order aberrations.

6.4.3 HIGHER ORDER ABERRATIONS.

With this type of correction and also as the position of the plates is far removed from the entrance pupil (this is necessary to reduce the diameter of the plates), the system will suffer seriously from all the higher order aberrations. In order to reduce the effect of these higher order aberrations, a proper choice of the second of the extra-axial curvatures shall be made. However, as the fifth-order aberration coefficients are linearly related to the second of the extra-axial curvature coefficients, and also due to the fact that the introduction of the second of the extra-axial curvatures on a particular surface alters the aberration coefficients of that surface only, the labour reduces in the development of the design to some extent. If the aberrations are much beyond the tolerable limits, then, the introduction of third-order residuals for all or for some of the aberration coefficients may be inevitable. However, this decision will depend entirely on the actual values of the higher order aberration coefficients.

6.4.4 APPLICATION to NUMERICAL EXAMPLE.

The principles outlined in the previous sections are now illustrated by way of an example. Returning now to the numerical example considered earlier, we will develop a three-plates aspheric corrector suitable to the primary mirror of the telescope. We will select quartz as the material to be used for the plates.

In order to keep the diameter of the largest plate less than about 20 inches, we will choose d_1' as equal to -0.92. Using equations (6.12), (6.16 - 6.18), the initial paraxial set up is obtained as

$$c_{02} = -2.9246083 \quad c_{03} = 0.0 \quad c_{04} = 7.7993176 \quad c_{05} = 0.0$$
$$c_{06} = -8.0480082 \quad c_{07} = 0.0$$
$$d_1' = -0.92 \quad d_2' = -0.001 \quad d_3' = -0.026 \quad d_4' = -0.001$$
$$d_5' = -0.026 \quad d_6' = -0.001$$

With this arrangement, the actual values of σ_4 , l_{ch}', t_{ch}' are found to be

$$\sigma_4 = 0.0$$
$$l_{ch}' = 0.00003704$$
$$t_{ch}' = 0.00084739$$

where, the values for l_{ch}', t_{ch}' refer to the unit semi-aperture and semi-field. These values for l_{ch}', t_{ch}' may be reduced to negligible quantities by adjusting the air spaces d_3', d_6', using the differential correction method. After this adjustment, we obtain

$$c_{02} = -2.9246083 \quad c_{03} = 0.0 \quad c_{04} = 7.7993176 \quad c_{05} = 0.0$$
$$c_{06} = -8.0480082 \quad c_{07} = 0.0$$
$$d_1' = -0.92 \quad d_2' = -0.001 \quad d_3' = -0.02620383 \quad d_4' = -0.001$$
$$d_5' = -0.03491344 \quad d_6' = -0.001$$

Tracing the two formal paraxial rays with the initial coordinates $y_{01} = 1$, $v_{01} = 0$ for the a-ray, and $y_1 = 0$, $v_1 = 1$ for the b-ray, we will determine the values of q_1, S_{01}, P_1 at every surface. Employing the equations (6.24) - (6.28) we will determine the values of c_{12}, c_{14}, c_{16} of the plates which give $\sigma_1 = \sigma_2 = \sigma_3 = 0$. In this way, we get

$q_2 = -770.86889$

$q_4 = -5934.8109$

$q_6 = 46451.895$

The aberration coefficients for the whole system are

$\sigma_1 = \sigma_2 = \sigma_3 = \sigma_4 = 0.0, \quad \sigma_5 = 290.94$

$\mu_1 = 0.07164$	$\mu_2 = -2.491$	$\mu_3 = -1.6607$	$\mu_4 = 48.704$	$\mu_5 = 15.079$
$\mu_6 = 33.625$	$\mu_7 = -821.03$	$\mu_8 = -629.47$	$\mu_9 = -191.55$	$\mu_{10} = 35215$
$\mu_{11} = 2925.7$	$\mu_{12} = -158110$			
$\tau_1 = 0.24741$	$\tau_2 = -9.8183$	$\tau_3 = -6.854$	$\tau_4 = 299.75$	$\tau_5 = 97.428$
$\tau_6 = 216.47$	$\tau_7 = -5380.6$	$\tau_8 = -3563.4$	$\tau_9 = -1604$	$\tau_{10} = -136.47$
$\tau_{11} = 40764$	$\tau_{12} = 5893.9$	$\tau_{13} = 9412.7$	$\tau_{14} = 9097.5$	$\tau_{15} = 803730$
$\tau_{16} = 799780$	$\tau_{17} = 125380$	$\tau_{18} = -14805000$	$\tau_{19} = -593380$	$\tau_{20} = -70645000$

These figures indicate that the third-order correction of the aberrations increase the fifth-order aberrations to a very large extent. It is therefore necessary to choose the second of the extra-axial curvature coefficients to reduce the effect of these coefficients considerably. Changing the c_2 values of the plates from zero to some other values, and again computing the fifth-order aberration coefficients, we can obtain the derivatives of these coefficients with respect to c_{22}, c_{24}, c_{26} as

$\dot{\mu}_{12} = -0.0_6 12$	$\dot{\mu}_{22} = 0.0_5 519$	$\dot{\mu}_{32} = 0.0_5 279$	$\dot{\mu}_{42} = -0.0_4 9635$
$\dot{\mu}_{52} = -0.0_4 3212$	$\dot{\mu}_{62} = -0.0_4 6423$	$\dot{\mu}_{72} = 0.001108$	$\dot{\mu}_{82} = 0.00073867$
$\dot{\mu}_{92} = 0.00036933$	$\dot{\mu}_{102} = -0.01061791$	$\dot{\mu}_{112} = -0.00212362$	$\dot{\mu}_{14} = -0.0_8 74$
$\dot{\mu}_{24} = 0.0_6 41$	$\dot{\mu}_{34} = 0.0_6 27$	$\dot{\mu}_{44} = -0.0_4 1478$	$\dot{\mu}_{54} = -0.0_5 493$
$\dot{\mu}_{64} = -0.0_5 986$	$\dot{\mu}_{74} = 0.0_3 26896$	$\dot{\mu}_{84} = 0.0_3 17934$	$\dot{\mu}_{94} = 0.0_4 8967$
$\dot{\mu}_{104} = -0.00407815$	$\dot{\mu}_{114} = -0.00081572$	$\dot{\mu}_{16} = 0.0$	$\dot{\mu}_{26} = 0.0_8 23$
$\dot{\mu}_{36} = 0.0_8 16$	$\dot{\mu}_{46} = -0.0_6 2765$	$\dot{\mu}_{56} = -0.0_7 921$	$\dot{\mu}_{66} = -0.0_6 1843$
$\dot{\mu}_{76} = 0.0_4 164211$	$\dot{\mu}_{86} = 0.0_4 109475$	$\dot{\mu}_{96} = 0.0_5 54735$	$\dot{\mu}_{106} = -0.00081291$
$\dot{\mu}_{116} = -0.000162582$			

where, μ_{ij} is defined as the derivative of μ_i with respect to c_j, and i takes the values from 1 - 11 and j takes the values 2,4,6.

Using the derivatives of the fifth-order aberration coefficients, and taking into consideration the effects of seventh-order coefficients, along with the reduction of the image spread (irrespective of the type of energy distribution) as the main aim, the curvature coefficients c_{22}, c_{24}, c_{26} are prescribed as

$c_{22} = 635496$ $\quad c_{24} = -1200000$ $\quad c_{26} = 45234944$

This corrector is now added to the primary mirror and the aberration coefficients are obtained as

$\sigma_1 = \sigma_2 = \sigma_3 = \sigma_4 = 0.0$; $\quad \sigma_5 = 290.94$

$\mu_1 = 0.0082148$ $\quad \mu_2 = -0.21349$ $\quad \mu_3 = -0.14232$ $\quad \mu_4 = -6.4406$ $\quad \mu_5 = -3.3026$

$\mu_6 = -3.138$ $\quad \mu_7 = 246.16$ $\quad \mu_8 = 81.99$ $\quad \mu_9 = 164.17$ $\quad \mu_{10} = -526.7$

$\mu_{11} = -4222.5$ $\quad \mu_{12} = 242070$

$\tau_1 = 0.039493$ $\quad \tau_2 = -3.453$ $\quad \tau_3 = -2.0801$ $\quad \tau_4 = 146.34$ $\quad \tau_5 = 42.398$

$\tau_6 = 99.388$ $\quad \tau_7 = -2748.5$ $\quad \tau_8 = -1812.5$ $\quad \tau_9 = -722.65$ $\quad \tau_{10} = -137.41$

$\tau_{11} = 6636.6$ $\quad \tau_{12} = 31762$ $\quad \tau_{13} = -1067.4$ $\quad \tau_{14} = 17309$ $\quad \tau_{15} = -399550$

$\tau_{16} = -414410$ $\quad \tau_{17} = -69215$ $\quad \tau_{18} = 37574000$ $\quad \tau_{19} = 2920500$ $\quad \tau_{20} = -260410000$

The quality of the image at the prime focus is then analysed by means of the spot diagrams. Figures (6.4 a-d) show the spot diagrams for (i) V = 0, (ii) V = 10', (iii) V = 20', and (iv) V = 30'. The spot diagrams show that the quality of the image deteriorates very rapidly with the increase in field size. However, the image spread does not exceed 1 second of arc up to a total field of 50 minutes. An inspection of the aberration coefficients indicates that the deterioration of the image quality when the field is increased is mainly confined

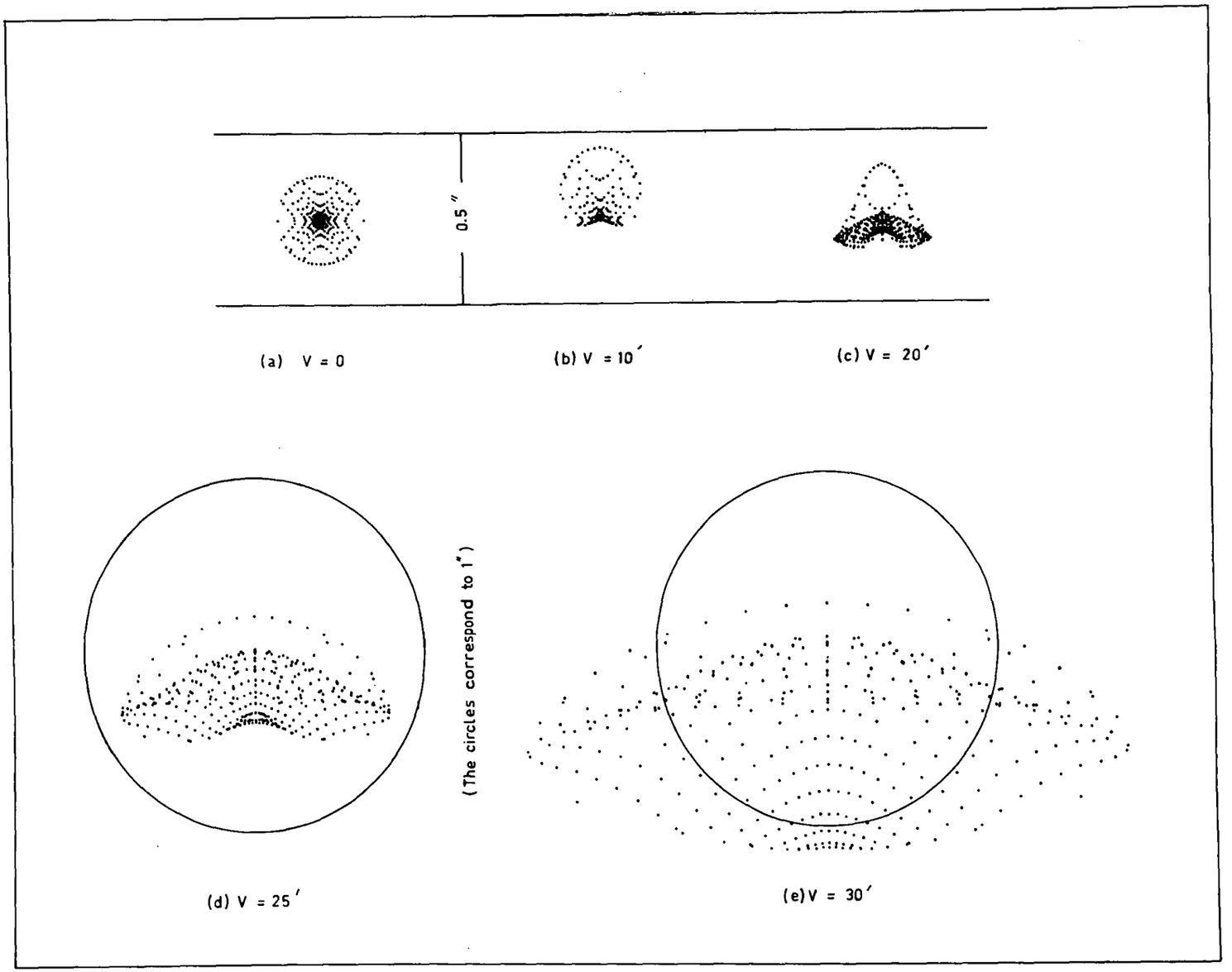

Fig 6.4

SPOT DIAGRAMS FOR PRIMARY MIRROR WITH THE THREE PLATE CORRECTOR IN PLACE.

to the fifth-order linear astigmatic coefficient μ_{11}. It is hardly possible to bring both the aberration coefficients μ_{10}, μ_{11} under control.

With the present set up, the system suffers from some higher order chromatic aberration. It is therefore required to prescribe proper residuals for the paraxial colours to balance the higher order chromatic effects for an appropriate aperture and field angle. A small positive residual value for σ_4 may be useful in balancing the effect of higher order astigmatic coefficients. These changes require the initial paraxial set up to be altered, which slightly alters the required asphericity of the plates, for the correction of monochromatic aberrations. The principles outlined earlier may be used to obtain a best three plates corrector system.

REFERENCES

Buchdahl, H.A. (1948) J.O.S.A. 38, 14-19

Buchdahl, H.A. (1954) "Optical Aberration Coefficients", Monograph, Oxford University Press

Chretien, H. (1922) Rev.d'Opt. 1, 13-22 and 49-64

Cruickshank, F.D. (1968) Lecture notes

Ford, P.W. (1966) J.O.S.A., 56, 209-212

Gascoigne, S.C.B. (1965) The Observatory 85, 79

Kohler, H. (1966) The Construction of Large Telescope (I.A.U. Symp. No. 27, 1965) London Academic Press, pp.9-21

Kohler, H. (1968) Appl. Opt. 7, 241-248

Meinel, A.B. (1953) Ap.J. 118, 335-344

Rosin, S. (1966) Appl. Opt. 5, 675

Ross, F.E. (1935) Ap.J. 81, 156-172

Schulte, D.H. (1963) Appl.Opt. 2, 141-151

Schulte, D.H. (1966) Appl.Opt. 5, 309-311

Schulte, D.H. (1966) Appl.Opt. 5, 313-317

Schwarzschild, K. (1905) Astr.Mitt.Königl.Sternwarte Göttingen

Wynne, C.G. (1965) Appl.Opt. 4, 1185-1192

Wynne, C.G. (1968) Ap.J. 152, 675-694